



Norwegian University of
Science and Technology

A Stochastic Capacity Expansion Model for the European Power System

Using a Distributed Progressive Hedging
Approach to Handle Long-Term Uncertainty

Mats Erik Mikkelsen

Aksel Reiten

Industrial Economics and Technology Management

Submission date: June 2018

Supervisor: Asgeir Tomasgard, IØT

Norwegian University of Science and Technology

Department of Industrial Economics and Technology Management

Problem Description

Ambitious CO₂-emission reduction targets, recent developments within renewable energy and changing dynamics of electricity demand frames the transition in the European power sector in the coming decades. The purpose of this thesis is to develop a model and solution method for solving the stochastic capacity expansion problem in the European power system. The problem at hand is concerned with simultaneously optimizing (1) strategic investments in generation, transmission and storage capacity and (2) operational dispatch to assess system performance and profitability of investments. Due to the long planning horizon being considered, dealing with uncertain input parameters becomes an integral part of the problem, which calls for tailored solution methods. An implementation of a distributed progressive hedging algorithm is therefore proposed.

Preface

This master's thesis concludes our Master of Science in Industrial Economics and Technology Management at the Norwegian University of Science and Technology, at the Department of Industrial Economics and Technology Management. The thesis is a continuation of our specialization project completed during the fall of 2017.

The choice of subject for this thesis was motivated partly by an aspiration to obtain a deeper understanding of energy system modelling, and partly by a wish to develop our skills within computer science. We would like to thank our supervisor, Professor Asgeir Tomasgard, for valuable guidance and insightful opinions during the course of the work with this thesis.

Trondheim, June 2018

Aksel Reiten

Aksel Reiten

Mats Erik Mikkelsen

Mats Erik Mikkelsen

Abstract

In an attempt to limit the adverse effects of human-generated greenhouse gas emissions, the EU has set ambitious targets to reduce its domestic CO₂-emissions by more than 80 percent from 1990 to 2050. The European power system has proven a significant potential for emission reductions, implying almost complete decarbonization of the sector in a time where both electricity demand and the share of intermittent, renewable power supply are expected to increase. To support policy makers in this transition, optimization based models are often used to study optimal capacity expansion pathways for the European power system. The task of modeling both technological details and economic behavior in a broad geographical and sectoral scope gives rise to substantial computational complexity, often resulting in the use of deterministic modeling approaches. Solutions from such approaches are, however, tailored to a particular realization of the future, neglecting the uncertain nature of many essential model inputs.

Several power system optimization models accounting for either long- or short-term uncertainty already exist, but models accounting for both have not been observed in the research literature. In this thesis, this gap is addressed by defining and formulating a mathematical model for the Long- and Short-term Stochastic Capacity Expansion Problem for Power Systems (LSSCEPPS). Central to the problem is the simultaneous co-optimization of long-term investment decisions and short-term operational decisions in the European power system over several decades, in the presence of stochastic long- and short-term input parameters. The primary objective is to find a sustainable, least-cost and robust development for the European power system while securing coverage of demand and complying with political regulations. To solve this problem, the EMPIRE model, a power system capacity expansion model developed at NTNU, is extended in this thesis to account for both long- and short-term uncertainty. This extension quickly results in intractable problem sizes for commercially available solvers, resulting in a need for improved solution methods.

In this thesis, a distributed progressive hedging algorithm is implemented to solve large instances of the EMPIRE model. The method decomposes the model by long-term scenario, iteratively solving decentralized subproblems in parallel. The performance of the algorithm is tested on a number of different problem instances under variation of both short- and long-term input data. It is demonstrated to be capable of solving instances of the EMPIRE model with more than 1.2 billion variables and 1.7 billion constraints, obtaining an optimality gap of 0.1 percent in 18 iterations after about 70 hours. The algorithm exhibits impressive convergence properties, generating tight gaps of less than 0.35 percent for all instances tested for in this thesis. It is further observed that the elapsed time required to solve instances with differing numbers of long-term scenarios remains roughly constant. This result illustrates the algorithm's profound scaling properties as long as sufficient computational resources are available, and implies that the convergence rate is mainly driven by the size and complexity of the short-term input data.

To verify the practical implications of including long-term uncertainty in power system

capacity expansion models, a thorough analysis of the techno-economic implications of introducing stochastic CO₂-emission restrictions is conducted. In a comparison of a long-term stochastic approach to a long-term deterministic approach, VSS-calculations display significant values of modeling both long- and short-term uncertainty compared to short-term uncertainty only, ranging from 7.9-11.6 percent for test instances with 8 or more long-term scenarios. Analyses further show that including fewer long-term scenarios results in a negligible VSS, indicating that a sufficient amount of long-term scenarios need to be assessed to capture the value of modeling long-term uncertainty.

The long-term stochastic approach is also proven to choose hedging strategies through increased investments in low-CO₂ power generation and infrastructure that increases the flexibility of the power system, such as transmission, storage and more flexible thermal generation. These strategies are shown to yield slightly higher investment costs upfront, but with the benefit of vast reductions in future expected operational costs, indicating that politicians can significantly reduce the expected costs of power system capacity expansion by eliminating uncertainty about future energy policy.

Sammendrag

Med formål om å begrense de negative effektene av menneskeskapt CO₂-utslipp, har EU satt ambisiøse mål for å redusere mengden CO₂-utslipp i Europa med mer enn 80 prosent i 2050 sammenlignet med nivået fra 1990. Det europeiske kraftsystemet har utvist betydelig potensial for utslippsreduksjoner, noe som betyr at en overgang til et kraftsystem med tilnærmet null utslipp er forventet i en tid der både strømforbruk og andelen uregulerbar, fornybar kraftforsyning trolig vil øke. Optimeringsmodeller blir ofte anvendt i analyser av optimal kapasitetsutvidelse i det Europeiske kraftsystemet, og kan benyttes som beslutningsstøtte til politikere i overgangen nevnt ovenfor. Det å matematisk modellere både teknologiske detaljer og økonomisk adferd i et bredt geografisk og industrielt omfang medfører betydelig kompleksitet, noe som ofte resulterer i bruk av deterministiske optimeringsmodeller. Løsningene slike modeller finner er imidlertid skreddersydd for en bestemt realisering av fremtiden, og overser dermed usikkerheten i mange viktige modellparametere.

Det finnes flere optimeringsmodeller for kraftsystemer som inkluderer enten lang- eller korttidsusikkerhet, men modeller som inkluderer usikkerhet langs begge disse tidsaksene har ikke blitt funnet i relevant forskningslitteratur. I denne oppgaven adresseres denne mangelen i litteraturen ved å definere og formulere en matematisk modell for det lang- og kortsiktig stokastiske kapasitetsutvidelsesproblemet for kraftsystemer (Long- and Short-term Stochastic Capacity Expansion Problem for Power Systems - LSSCEPPS). Sentralt for problemet er samtidig optimering av både langsiktige investeringsbeslutninger og kortsiktige operasjonelle beslutninger i det europeiske kraftsystemet over flere tiår, hvor usikkerhet er inkludert i både lang- og kortsiktige modellparametere. Formålet med å studere problemet er å finne en bærekraftig, kostnadseffektiv og robust utvikling for det europeiske kraftsystemet samtidig som kraftteterspørsel skal dekkes og politiske reguleringer skal overholdes. For å løse dette problemet har EMPIRE-modellen, en kapasitetsutvidelsesmodell for kraftsystemer utviklet ved NTNU, i denne oppgaven blitt utvidet til å inkludere usikkerhet i både lang- og kortsiktige modellparametere. En slik utvidelse resulterer ofte i at kommersielt tilgjengelige løsningsalgoritmer ikke klarer å håndtere realistiske problemstørrelser, hvilket resulterer i et behov for forbedrede løsningsmetoder.

I denne oppgaven implementeres en distribuert progressive hedging-algoritme for å løse store instanser av EMPIRE-modellen. Metoden dekomponerer modellen per langtidsscenario for deretter å iterativt løse desentraliserte subproblemer i parallell. Algoritmenes oppførsel blir testet på en rekke forskjellige probleminstanser under variasjon av både kort- og langsiktige inndata. Den viser seg å kunne løse instanser av EMPIRE-modellen med mer enn 1,2 milliarder variabler og 1,7 milliarder beskrankninger, og oppnår et optimalitetsgap for denne instansen på 0,1 prosent etter 18 iterasjoner og ca. 70 timer. Algoritmen utviser gode egenskaper for konvergens, og produserer optimalitetsgap på under 0,35 prosent for alle instanser testet i denne oppgaven. Det observeres også at konvergenstiden for å løse instanser med varierende antall langtidsscenarioer er omtrent konstant. Dette resultatet viser algoritmens solide skaleringssegenskaper så lenge tilstrekkelige

beregningsressurser er tilgjengelig, og innebærer at tiden til konvergens hovedsakelig er drevet av størrelsen og kompleksiteten til kortsiktige inndata.

For å studere de praktiske implikasjonene av å inkludere langtidsusikkerhet i kapasitet-utvidelsesmodeller for kraftsystemer, gjøres en grundig analyse av de teknisk-økonomiske implikasjonene av å innføre stokastiske restriksjoner for CO₂-utslipp. I en sammenligning av en langsiktig stokastisk tilnærming med en langsiktig deterministisk tilnærming, viser VSS-beregninger signifikante verdier av å modellere både lang- og kortsiktig usikkerhet sammenlignet med kun kortsiktig usikkerhet, med VSS mellom 7,9-11,6 prosent for instanser med 8 eller flere langtidsscenarier. Analyser viser videre at det å inkludere færre langtidsscenarier enn dette resulterer i en neglisjerbar VSS, noe som indikerer at et tilstrekkelig antall langtidsscenarier er nødvendig for å finne verdien av å modellere langtidsusikkerhet.

Den langsiktige stokastiske tilnærmingen har også vist seg å velge sikringsstrategier (hedging strategies) gjennom økte investeringer i lav-CO₂-kraftproduksjon og infrastruktur for økt fleksibilitet til kraftsystemet, for eksempel overføringslinjer, lagringskapasitet og mer fleksibel termisk produksjon. Disse strategiene viser seg å gi noe høyere investeringskostnader i forkant, men resulterer i betydelige reduksjoner i fremtidige forventede driftskostnader i kraftsystemet, noe som indikerer at politikere kan redusere de forventet kostnadene av kapasitetsutvidelse i kraftsystemet betydelig ved å eliminere usikkerhet rundt fremtidig energipolitikk.

Table of Contents

1	Introduction	1
1.1	Structure of the thesis	3
2	Description of the Stochastic Power System Capacity Expansion Problem	5
2.1	Objective of the LSSCEPPS	7
2.1.1	Finding optimal investments in power system infrastructure	7
2.1.2	Finding optimal operational system dispatch for the power system	7
2.2	Problem scope	8
2.2.1	Geographical considerations	8
2.2.2	Dynamics and temporal considerations	9
2.2.3	Technological scope	10
2.3	Political regulations	12
2.4	Uncertainties and risks in power system capacity expansion	13
2.5	Summary of the LSSCEPPS	14
3	Review of Relevant Literature on Energy System Capacity Expansion	15
3.1	Introduction to the EMPIRE model	15
3.2	Energy system modeling approaches	16
3.2.1	Determining the scope and granularity of energy system models	16
3.2.2	Centralized vs. decentralized decision making	18
3.3	Optimization models for power systems	19
3.3.1	Operational considerations and short-term dynamics	19
3.3.2	Planning horizon and scope of infrastructure investments	20
3.3.3	Modeling the transmission network	21
3.3.4	Energy policy and political regulations	23
3.4	Summarizing the literature review	24
4	Treatment of Uncertainty in Power System Capacity Expansion Models	27
4.1	Theoretical background of stochastic optimization	28
4.1.1	Formulation of a multistage stochastic program	28
4.1.2	Representing multistage scenario trees	30

4.1.3	The value of using a stochastic model	31
4.2	Including uncertainty in power system capacity expansion models	33
4.2.1	Short-term uncertainty in power system capacity expansion	33
4.2.2	Long-term uncertainty in power system capacity expansion	36
4.3	Solving stochastic capacity expansion models for power systems	39
4.3.1	Problem size reduction with multihorizon modeling	39
4.3.2	Decomposition Methods for Multistage Stochastic Programs	41
4.4	Summarizing the first part and motivating the rest of the thesis	43
5	Mathematical Formulation of EMPIRE with Long-term Uncertainty	45
5.1	Model assumptions	45
5.1.1	Sectoral scope and choice of decision variables	45
5.1.2	Model formulation choices	46
5.1.3	Temporal assumptions	46
5.1.4	Geographical scope and unit commitment considerations	47
5.2	Model Notation	48
5.3	Mathematical model formulation	50
5.3.1	Objective function	50
5.3.2	Node flow balance	52
5.3.3	CO ₂ -emission constraints	53
5.3.4	Cumulative capacity restrictions	53
5.3.5	Storage technology constraints	54
5.3.6	Storage power and energy capacity coupling	54
5.3.7	Generator dispatch availability	54
5.3.8	Thermal production ramp-up constraint	54
5.3.9	Hydroelectric power generation constraint	55
5.3.10	Transmission flow constraints	55
5.3.11	Capacity investment constraints	55
5.3.12	Nonanticipativity constraints	56
5.3.13	Non-negativity constraints	57
6	A Distributed Progressive Hedging Algorithm for Solving EMPIRE	59
6.1	The progressive hedging algorithm	60
6.1.1	Preliminaries	60
6.1.2	Overview of the Progressive Hedging Algorithm	62
6.1.3	Applying the Progressive Hedging Algorithm to Solve EMPIRE	66
6.1.4	Obtaining Optimality Bounds	69
6.2	A distributed implementation of the algorithm	70
6.2.1	A Distributed Memory Infrastructure	70
6.2.2	Expected Performance Gain of the Distributed Implementation	72
7	Model Data	75
7.1	Model inputs	75
7.2	Procedure for generating short-term scenarios	77
7.2.1	Notation and pseudocode for the scenario generation procedure	79
7.3	Strategy for generating long-term scenario trees	81

8	Computational Study	85
8.1	Implementation	85
8.1.1	Hardware and software	85
8.1.2	Overview of implemented infrastructure	86
8.2	Test instances	86
8.3	Configurations of the progressive hedging algorithm	88
8.3.1	Progressive Hedging Parameter Calibration Methodology	88
8.3.2	Calibration of ρ	91
8.3.3	Calibration of ϵ	97
8.3.4	Calibrating Scenario Bundling	99
8.3.5	Summarizing the Progressive Hedging Algorithm Calibration	101
8.4	Comparing progressive hedging with direct solving	101
8.4.1	Elapsed Time Required for Solving the Problem	102
8.4.2	Computational Resources Required for Solving the Problem	104
8.4.3	Final results	106
8.5	Summary of the algorithm's performance	107
9	Techno-Economic Implications of Political Uncertainty	109
9.1	The effect of political uncertainty on expected costs	111
9.1.1	The Value of a Long-Term Stochastic Solution	111
9.1.2	Detailed analysis of total expected costs	111
9.2	The effect of political uncertainty on infrastructure investments	118
9.2.1	Comparing investments in the SP-approach to the RH-approach	119
9.3	Summarizing the techno-economic analyses	127
10	Conclusion	129
	Bibliography	133
	Appendix	143

List of Tables

3.1	Overview of capacity expansion models for the European power system . . .	25
5.1	Sets, indices, parameters and variables used in the mathematical model . . .	48
6.1	Sets, indices and variables for the progressive hedging algorithm	65
7.1	Sets and parameters for the short-term scenario generation procedure . . .	79
7.2	Scenario tree with policy uncertainty (27 scenarios)	83
8.1	Hardware and software used for testing	86
8.2	Test instances used in the computational study	87
8.3	Overview of the parameters to be configured in the PHA	88
8.4	Calibrating ρ under variation of long-term data	92
8.5	Calibrating ρ under variation of short-term data	95
8.6	Calibrating convergence parameter ϵ	98
8.7	Configuring bundling factor b	100
8.8	Memory availability requirements for the implemented methods	105
8.9	CPU time for the different solution methods	106
8.10	Final results comparing the solution methods	107
9.1	The Value of a Stochastic Solution for some test instances	112

List of Figures

1.1	Targeted European greenhouse gas emissions towards 2050	2
2.1	Conceptual overview of the problem to be solved	6
2.2	The short-term operational dispatch problem	8
2.3	Dynamics of investments and operational decisions in the LSSCEPPS . . .	10
2.4	Examples of controllable and uncontrollable generation technologies . . .	11
3.1	Illustration of the energy system	17
4.1	Illustrative scenario tree	30
4.2	Split variable versus compact formulation of a scenario tree	31
4.3	Stochastic multistage scenario trees with two time-scales	40
4.4	Stochastic multihorizon scenario trees with short- and long-term uncertainty	41
5.1	Geographical coverage of the EMPIRE model	47
6.1	Feasible area of a stochastic program with complicating constraints	61
6.2	Conceptual overview of the progressive hedging algorithm	63
6.3	Overview of the distributed implementation of the PHA	71
6.4	Synchronous versus asynchronous parallel program	73
7.1	Assumed fuel price and electricity demand development	76
7.2	Assumed development in technology investment costs	76
7.3	Illustration of short-term scenario sampling	78
7.4	Illustration of scenario tree with 27 scenarios	82
7.5	Scenario tree for long term development of CO2 emissions	84
8.1	Infrastructure of current implementation	87
8.2	Initial bound study for calibrating ρ	91
8.3	Initial gap study for calibrating ρ	92
8.4	Optimality gaps when varying ρ on different long-term data	93

8.5	Optimality bounds when varying ρ on different long-term data	94
8.6	Deviation from nonanticipativity under variation of long-term data	95
8.7	Optimality gaps when varying ρ on different short-term data	96
8.8	Deviation when varying ρ on different short-term data	97
8.9	Average deviation of variables deviating from nonanticipativity	99
8.10	Elapsed time per iteration with different bundling factors	100
8.11	Obtained optimality gaps at specific times when varying bundling factor	101
8.12	Elapsed time required by the PHA to solve the instances	102
8.13	Comparison of elapsed computation time for the PHA and direct solving	103
8.14	Histogram of subproblems terminating at a given time period	104
9.1	Total expected system costs per infrastructure type and technology	113
9.2	Total expected system costs per country	113
9.3	Total expected system costs per five-year stage	114
9.4	CO ₂ -emission intensities for different generation technologies	115
9.5	Total expected investment costs per time stage	116
9.6	Relative comparison of investment costs in the SP- and RH-approach	116
9.7	Total expected operational costs per five-year period	118
9.8	Relative comparison of costs of generation in the SP- and RH-approach	119
9.9	Comparison of investments in generation and transmission capacity in 2020	120
9.10	Relative comparison of accumulated infrastructure capacities in 2020	121
9.11	Comparison of investments in generation capacity in 2030	122
9.12	Comparison of investments in transmission and storage capacity in 2030	122
9.13	Relative comparison of accumulated infrastructure capacities in 2030	123
9.14	Comparison of investments in selected infrastructure types in 2040	124
9.15	Relative comparison of accumulated infrastructure capacities in 2040	126

Abbreviations and Terminology

Abbreviations

LSSCEPPS	-	Long- and Short-Term Stochastic Capacity Expansion Problem for Power Systems
EMPIRE	-	European Model for Power system Investment with Renewable Energy
IRE	-	Intermittent renewable energy
MENA	-	Middle East and North Africa
EV	-	Expected value
CAPEX	-	Capital expenditures, i.e. cost of investments
OPEX	-	Operational expenditures, i.e. cost of operations
IAM	-	Integrated assessment models
SRMC	-	Short-run marginal costs
O&M	-	Operations and maintenance
CCS	-	Carbon capture and storage
CCTS	-	Carbon capture, transport and storage
HVDC	-	High-voltage direct current
HVAC	-	High-voltage alternating current
KVL	-	Kirchhoff's voltage law
NTC	-	Net transfer capacity
RH	-	Rolling horizon (deterministic)
SP	-	Stochastic programming
PHA	-	Progressive hedging algorithm
IO	-	Input/output of data
MPI	-	Message-Passing Interface
HPC	-	High-Performance Cluster
VSS	-	Value of a stochastic solution

Terminology

System configuration	-	One specific choice for the generation capacity and production mix from different generation technologies in the European power system
Base load technologies	-	Non-intermittent power generation technologies such as coal, gas, hydro and nuclear power plants
Investment time stage	-	Time stages on the long-term time-scale
Operational time step	-	Time periods on the short-term time-scale
Short-term uncertainty	-	Stochastic input data on the short term time scale
Long-term uncertainty	-	Stochastic input data on the long term time scale
Strategic decisions	-	Decision variables on the long-term time-scale
Operational decisions	-	Decision variables on the short-term time-scale
Branching	-	A stage in a scenario tree where uncertain information is revealed
Hedging action	-	A behavior where investments are made early on to reduce the risk of poor operational performance in later periods

Chapter 1

Introduction

In recent years, much political focus has been directed towards climate-related questions, and the Paris Agreement on Climate Change in 2015 (UNFCCC, 2015) confirmed that this topic is a top priority for many governments around the world. Figure 1.1 shows that the European power sector is responsible for more than 20 percent of current greenhouse gas emissions in Europe. In addition, it is communicated in EC (2011) that significant emission reduction potentials exist in the European power sector due to expected technological improvements and reductions in the cost of renewable energy technologies. Therefore, in 2011 the European Council reconfirmed the European Union's objective to reduce CO₂-emissions by 80 to 95 percent below 1990 levels in 2050 (EC, 2011). It is further communicated that due to the large emission reduction potentials of the power system, targets for almost complete decarbonization of the sector are implied. However, even though ambitious targets for emission reductions have been communicated, it is still unclear how and when political regulations aiming to achieve these targets will be implemented, giving rise to substantial uncertainty in European energy policy going forward.

To study the implications of climate policy and technological or economic developments relevant for power systems, quantitative models are often used. Multiple different modeling approaches exist, and an increasingly appreciated tool for this purpose is optimization based modeling. The need for quantitative models in this context is evident due to the combination of a high level of technological and engineering detail together with economic behavior that needs to be modeled, giving rise to models beyond the scope of qualitative judgment. The need to co-optimize both long-term investments and short-term operational decisions over several decades and large geographical areas, in the presence of profound uncertainties, yield an enormous decision space and tend to generate computationally intractable models that current state-of-the-art optimization software is unable to solve.

Several optimization models for energy policy analysis already exist, but due to the high degree of complexity in such models, deterministic approaches are often used. By applying such a modeling approach, the evident uncertain nature of many essential input parameters is neglected, such as the timing of policy regulations, future investment costs

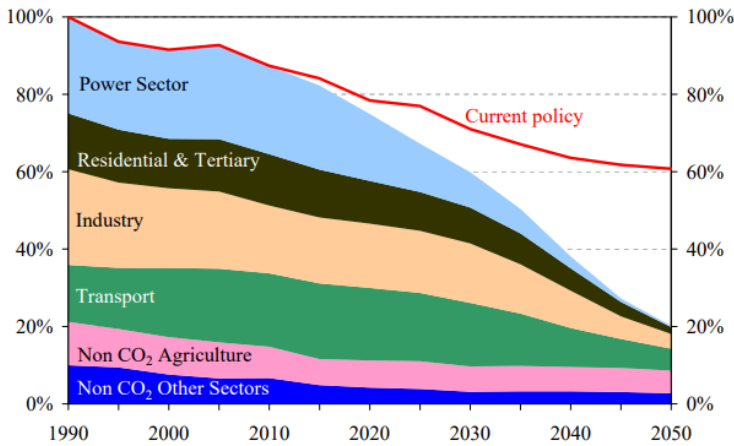


Figure 1.1: Targeted European greenhouse gas emissions towards an 80 percent reduction in 2050 (100 percent corresponds to 1990-levels), implying an almost complete decarbonization of the European power sector.

of power generation capacity, or the technological development in carbon capture and storage. By acknowledging the future as uncertain and practically impossible to forecast with a reasonable amount of accuracy, any argument for using deterministic optimization models in this context quickly loses its foundation.

The need to reflect uncertainty in optimization models for power systems sets the context for the research conducted in this thesis. The underlying hypothesis of the thesis is that the ability to include a treatment of future uncertainties can give insights beyond the scope of a deterministic analysis. The linear optimization model EMPIRE, developed at The Norwegian University of Science and Technology (Skar et al., 2016), defines the starting point of the model used in the studies in this thesis. It is a capacity expansion model for the European power system. The model was initially formulated with the ability to account for uncertainty in short-term input parameters, while an extension of the model including uncertainty in long-term input parameters was developed in Mikkelsen and Reiten (2017). However, this extension of the model is unable to scale and handle a realistic amount of long-term scenarios, establishing a need for improved solution methods and algorithmic implementations. With this foundation and the hypothesis mentioned above, some quite fundamental issues should be addressed:

1. If the future is acknowledged as uncertain, in what manner should uncertainty be incorporated into a rigorous, mathematical model?
2. How should the issue of added computational complexity from including uncertainty in an optimization model be addressed?
3. What are the techno-economic implications of considering both long- and short-term uncertainty in capacity expansion models for power systems?

The purpose of this thesis is to develop an optimization model and solution method that enables these three questions to be addressed. In addressing the first question above, the approach of large-scale stochastic optimization has been applied in an extended version of the EMPIRE model. In addition, a literature review and discussion of possible ways to represent uncertainty in both long- and short-term parameters is conducted. To address the second question, a considerable effort has been put into implementing a decomposition method, more specifically a distributed progressive hedging algorithm, that handles the increase in computational complexity from accounting for long-term stochastics in capacity expansion models. Finally, to the best of the authors' knowledge, an analysis of simultaneously including long- and short-term uncertainty in a capacity expansion optimization model for power systems has not been carried out in previous research efforts. Hence, to address the third question above, a demonstration of the techno-economic implications of considering both long- and short-term uncertainty in capacity expansion models for power systems is conducted, a demonstration enabled by the enhanced solution algorithm developed as part of the work with this thesis. As a result, the main contributions of this thesis are the following:

- A review of treatment of uncertainty in power system capacity expansion models, with a particular emphasis on handling long-term uncertainty in such models.
- A model for power system capacity expansion accounting for both long- and short-term uncertainty.
- A proprietary library of code that implements a distributed progressive hedging algorithm for solving stochastic capacity expansion models for power systems, together with a comprehensive computational study of the algorithm's performance.
- An analysis of the techno-economic implications of including political long-term uncertainty in power system capacity expansion models.

These contributions represent a natural advancement within research on energy and power system capacity expansion, due to an increasing appreciation that a proper consideration of uncertainty is imperative in such systems. In addition, these contributions advance the knowledge of decomposition methods and algorithms for solving large-scale stochastic optimization models. These methods have received increasing attention in recent years due to the development of computational power enabling such methods to be applied.

1.1 Structure of the thesis

The rest of the thesis is organized as follows. First, a comprehensive description of the power system capacity expansion problem studied in this thesis, together with relevant background for the problem, will be presented in chapter 2. Next, in chapter 3 a brief introduction to the EMPIRE model and a review of existing literature relating to modeling capacity expansion in energy and power systems is presented. Note that this chapter does not focus on the inclusion of uncertainty in such models, as chapter 4 presents a thorough

review of treating uncertainty in capacity expansion models, including a literature review of representing long- and short-term uncertainty. Following these introductory chapters, a detailed and technical description of the mathematical formulation of the extended version of the EMPIRE model including both long- and short-term uncertainty is presented in chapter 5. Chapter 6 presents the progressive hedging algorithm developed for solving this model, along with a description of its distributed, parallel implementation. Chapter 7 presents important input data to the model, including a description of the methods used for generating long- and short-term scenarios for uncertain input parameters. This is followed by a documentation and analysis of the performance of the implemented progressive hedging algorithm in chapter 8. In chapter 9 a demonstration of the significance of the solution algorithm is conducted, by analyzing the techno-economic implications of including long-term political uncertainty in the EMPIRE model. Finally, chapter 10 concludes the most important results of this thesis and suggests further research topics to be examined.

Description of the Stochastic Power System Capacity Expansion Problem

The importance of ensuring optimal development of power systems is evident for a multitude of reasons. With increased attention towards reducing global CO₂ emissions, indicated by e.g. the political targets of the EU pointed at in the previous chapter, the importance of reducing emissions from the power sector goes without saying. This also applies to other pollutants, as reducing air pollution has become an increasingly challenging task in many large cities, see for example Zhao et al. (2018) for a study of this in China. Other environmental considerations also add to the importance of expanding power systems in a balanced way. For instance, large power lines or windmills may be viewed as visual noise to local residents, and the regulation of rivers and watercourses for hydropower generation purposes may alter the local biological and ecological balance.

The task of securing a reliable supply of electricity is also an obvious target in the context of capacity expansion in power systems. As discussed in Castro et al. (2016) this target can be split into three different components; reliability and availability of electricity supply, power quality such as adequate frequencies and voltage magnitudes, and commercial quality such as the ability to handle customer requests on time without noticeable delay. Sustaining wealth creation and jobs in the power sector also adds to the importance of the problem.

In recent years there has been an exceptional technological development within renewable energy, both for energy generation and storage purposes. This development has led to steep declines in the cost of renewable energy, and these declines are only assumed to continue, see EU Reference Scenario (2016). As clean, unsubsidized renewable energy generation is about to become competitive with traditional energy generation technologies, increased adoption rates and learning effects are only assumed to speed up this development. Technological advances on the demand side of the power system, such as electric

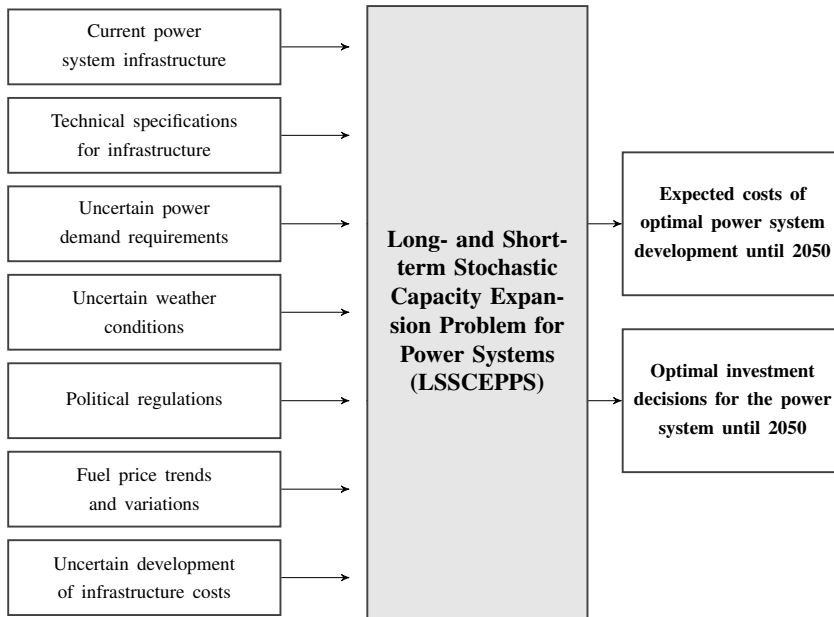


Figure 2.1: Conceptual overview of the LSSCEPPS with inputs on the left side and outputs on the right side.

vehicles, distributed generation, and smart grids, are also anticipated to have a profound impact on the power system of the future. All these technological developments, along with the other aspects discussed above, impact the task of developing and expanding the power system of the future, hence motivating the task of studying the capacity expansion problem for power systems.

With the above motivation in mind, this chapter will provide a background description and detailed discussion of central issues and attributes related to the problem to be studied in this thesis, which is the **Long- and Short-term Stochastic Capacity Expansion Problem for Power Systems (LSSCEPPS)**. Due to the geographical specificity of political regulations and a focus on Europe in the rest of the thesis, the scope of the problem will be limited to the European power system. Several subtle, yet important considerations and issues arise in the context of this problem, and the purpose of this chapter is to shed light on these to aid the reader's understanding of the problem.

Capacity expansion refers to the problem of obtaining optimal developments for a supply chain that satisfies a demand for a good, in this case, electricity. Central to the power system capacity expansion problem is the co-optimization of long-term investments and short-term system dispatch in the presence of long- and short-term uncertainty in different input parameters. The co-optimization is done in a context of electricity demand requirements, unpredictable generation from intermittent renewable energy sources, political regulations and technological restrictions. Figure 2.1 illustrates the conceptual principles of the LSSCEPPS, including inputs to the problem on the left and outputs of the problem to the right.

In section 2.1 the objective and desired outputs of the problem is presented. Section 2.2 lays out the scope of the problem in terms of geographical, temporal and technological considerations, while the relevance of political regulations in the power sector is presented in section 2.3. In section 2.4 the issue of handling uncertainties in the power system is discussed, while section 2.5 summarizes the discussion of the problem. Note that this chapter is meant to give a background overview and description of the generic problem referred to as LSSCEPPS, while modeling assumptions and choices specific for the model formulation developed as part of the work with this thesis will be elaborated and discussed in chapter 3, 4 and 5.

2.1 Objective of the LSSCEPPS

The objective of the LSSCEPPS is to identify cost-efficient and robust developments for the power system several decades ahead, given uncertain developments of important inputs to the problem in both the short- and long-term. Robustness is here defined as solutions that are resilient to several possible outcomes of the future. The costs considered in the problem include (1) the costs of investing in power system infrastructure and (2) the costs of utilizing the invested capacity to operate the system.

2.1.1 Finding optimal investments in power system infrastructure

Infrastructure investment decisions can be made in several geographical locations and multiple investment stages over a long planning horizon. The infrastructure considered for investments includes both generation, transmission or storage capacity. The costs incurred over the lifetime of an investment in one of these three types of infrastructure include both fixed capital expenditures (CAPEX) and fixed operational and maintenance expenditures (O&M) per unit of invested capacity. The technical details of these types of infrastructure will be further elaborated in section 2.2.3 below.

2.1.2 Finding optimal operational system dispatch for the power system

The short-term operational decisions for system dispatch consist of deciding how to utilize the invested and available capacity of generation, transmission and storage in a least-cost manner to satisfy operational requirements in each operational period. These decisions include how much electricity to produce from each generator, how much energy to transfer from a net supply to a net demand location, and how much each storage should be charged or discharged in each operational period. Figure 2.2 illustrates how these operational decisions are coordinated to satisfy electricity demand in a particular location and operational period h . Note that the system is also given the option of *not* meeting demand at a cost, from here denoted as lost load.

When electricity is generated from a given generation technology, variable operational expenditures (OPEX) and variable O&M costs are incurred per unit of electricity. Variable OPEX includes the cost of fuel for technologies that require this to generate electricity, e.g. coal plants or natural gas plants. In addition, both CAPEX and OPEX related to carbon

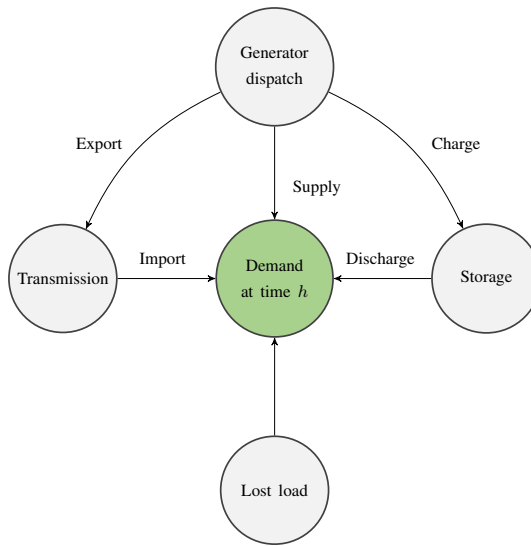


Figure 2.2: The short-term operational dispatch problem of satisfying demand in a particular location and given operational period h . The gray nodes denote decisions that need to be made to ensure satisfaction of demand during an operational period.

capture and storage (CCS) is included for generation technologies with such possibilities. The cost of not satisfying parts of the demand for electricity, i.e. cost of lost load, is also included as part of the operational costs of the system.

The operational requirements alluded to above typically include the following: Political targets for emission reductions from electricity generation, availability of generation plants at any point in time (e.g. if the wind is not blowing at a particular location, invested wind generation capacity at that location cannot be utilized in full), electricity demand requirements with a certain degree of supply security at each location and all operational periods, and certain technical constraints that are further elaborated in section 2.2.3 below.

2.2 Problem scope

Several considerations need to be made when restricting the scope of the LSSCEPPS. In this section, a discussion of issues and considerations relating to the choice of geographical, temporal and technological scope is presented.

2.2.1 Geographical considerations

An increasing acceptance that reductions in CO₂-emissions have to come from a coordinated international effort is one argument for including multiple European countries in the study. In addition, availability of energy from renewable technologies varies a lot with geography - for example, access to solar energy is more favorable in Southern Europe while conditions for offshore wind is better in the Northern part of Europe with harsher

maritime environments. For these reasons, the study should utilize a wide geographical scope. This will enable a correct identification of the trade-off between relying on local generation capacity at high-demand locations versus investing more in generation capacity where electricity can be produced in the cleanest and cheapest manner. The latter choice would lead to a larger reliance on overseas and cross-border transmission infrastructure and possibly make it easier to reduce emissions at a low cost. The choice of such a geographical scope also facilitates an integrated assessment able to capture the synergies between long-term decisions, by identifying possibly profitable investments in generation capacity that would not otherwise be profitable if transmission infrastructure into or out from that location was considered.

2.2.2 Dynamics and temporal considerations

As stated above, the purpose of the LSSCEPPS is to co-optimize both long-term investment decisions and short-term operational decisions in the power system. Note that the terms long-term decisions and investment decisions will be used interchangeably to refer to decisions to invest in generation, transmission and storage capacity, while the terms short-term decisions and operational decisions will be used interchangeably to refer to short-term decisions for how to operate the system. Due to the long-term nature of investments in power system infrastructure, planning horizons of several decades are typically applied. At the same time, to properly analyze the operational characteristics of the power system, a granular time-scale of days, hours or possibly even minutes is needed. With such a granular time-scale spanning a planning horizon of several decades, the problem size quickly becomes too difficult to handle. Therefore, two different time-scales are introduced, where investment decisions are made along a long-term time-scale and operational decisions are made along a short-term time-scale. As an example, the dynamics between investment decisions and operational decisions along both time-scales is illustrated in Figure 2.3, where infrastructure investment decisions are made along the long-term time-scale and operational decisions for utilizing the available capacity are made along the short-term time-scale.

The two different time-scales for making decisions give rise to some interesting dynamics due to the interactions between long-term and short-term decisions. Important attributes of the power system, such as weather conditions or demand for electricity, are naturally fluctuating on a short-term basis, and as a result, the usefulness of long-term investment decisions is affected by these short-term operational characteristics. These dynamics also work the other way around, as the short-term operational decisions for the system are restricted by long-term investment decisions that already have been made, e.g. utilizing a particular wind generator is limited by the amount of invested and available generator capacity.

Other characteristics of the power system are inherently long-term, such as the development of investment costs of different generation technologies. This calls for a dynamic, multi-stage approach where investments in infrastructure are allowed several times along the planning horizon. This opens up for the possibility to postpone investments if such a wait-and-see strategy has lower expected costs. Furthermore, the combination of long planning horizons and a wide geographical scope also enables a dynamic approach to long-term investments. For example, as more investments in transmission infrastructure

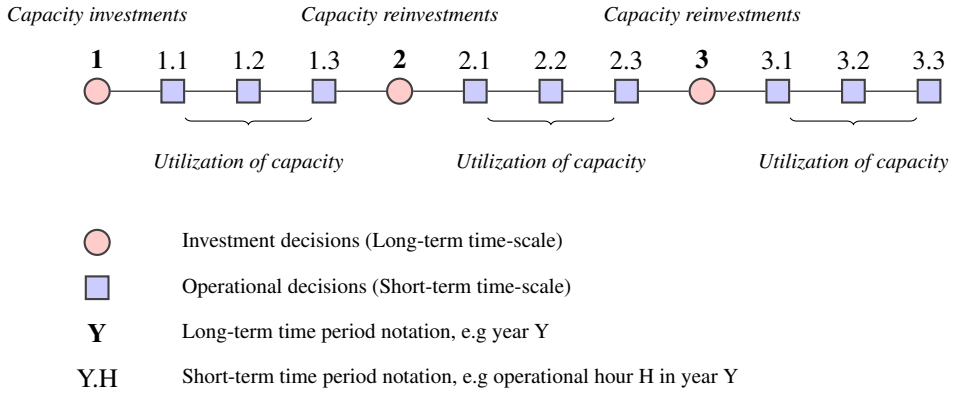


Figure 2.3: Dynamics of investments and operational decisions in the LSSCEPPS for a small example problem instance with three investment stages each followed by three short-term operational periods. Note that the figure intends to show the dynamics of decisions and does not intend to visualize any notion of uncertainty.

are made, unprofitable generation investments may turn profitable due to the added possibilities for transmitting surplus electricity to nearby locations. Such synergies are possible to identify due to the dynamic approach to investment decisions and a wide scope both geographically and temporally.

It is worth noting that the main intention of assessing operational periods and decisions as part of the LSSCEPPS is not to search for optimal operational decisions in the system, but rather to account for the impacts of operational variability on the usefulness of long-term investments. Therefore, short-term operational periods are included to validate the profitability, performance and usefulness of the infrastructure investments, since operational costs make up a significant amount of total costs during the planning horizon.

2.2.3 Technological scope

In power system planning, inputs from multiple different sectors have to be integrated. This type of planning is different from single industry planning where interactions between sectors, such as the effect of variations in natural gas prices on the demand for nuclear power, are neglected. This gives rise to an extensive technological scope for problems where power systems are analyzed, where characteristics for different technologies within generation, transmission and energy storage have to be considered in the analysis.

Attributes of generation technologies

When investing in generation capacity, several generation technologies with different characteristics are available. Decisions are made for both the amount of invested capacity and the share of different generation technologies to be invested in. The amount of invested







<p>Controllable generators</p> <p><i>Anticipated reduced share of power system in the future</i></p>	 Gas	 Coal	 Nuclear
<p>Uncontrollable generators</p> <p><i>Anticipated increased share of power system in the future</i></p>	 Wind	 Solar	 Hydro (River)

Figure 2.4: Examples of controllable and uncontrollable generation technologies

capacity in each period is restricted by reasonable upper limits for new capacity additions at each location and period of time. Typical generation technologies being considered include solar power plants, wind power plants (onshore and offshore), natural gas power plants, coal-fired power plants, nuclear power plants, hydroelectric power stations, oil-fired power plants, tidal water power plants, wave power plants, geothermal power plants and biomass-fired power plants. Note that the technological scope is not restricted to these as more technologies may be considered. Versions of relevant technologies with installed CCS-capabilities is also included in the scope of the problem.

The mentioned generation technologies have different characteristics and will affect the problem in different ways. Retirement factors are associated with some of the technologies, meaning that some of the invested capacity is made unavailable from one period to the next due to deterioration and wear and tear. In addition, anticipated lifetimes for investments in power plants are associated with the different types of generation technology, which have to be taken into account when assessing the usefulness of a capacity investment. All generation technologies that rely on fossil fuel as input also have specified properties such as heat rates, efficiency numbers for the amount of electricity produced from a given amount of fuel input and CO₂-emissions per unit of produced energy.

It is worth mentioning that there is an important distinction between intermittent, uncontrollable generation technologies such as solar and wind power on the one hand and stable, controllable baseload generation technologies such as coal-fired power plants or hydropower stations. As nobody can control the amount of sunshine or wind at a location, the availability of such intermittent generation capacity is restricted by this uncontrollable resource availability. In contrast, generation from the stable type of technologies is fully controllable, only restricted by the installed capacity and ramp-up restrictions (i.e. that a certain amount of time to start up or increase production from the current production level is required). This distinction between controllable and uncontrollable generation technologies have significant implications for the power system, particularly since ambitious CO₂-emission reduction targets call for an increased share of renewable energy which is often intermittent and uncontrollable.

Figure 2.4 gives examples of generator technologies categorized as controllable and uncontrollable power sources. Due to political ambitions of reducing greenhouse gas emissions, a transition of the power system towards a higher share of uncontrollable renewable

energy generation is anticipated. A phase-out of controllable, conventional thermal generators, such as coal and gas power plants, and an increase in the share of uncontrollable, intermittent renewable sources such as wind and solar, is therefore expected (Skar et al., 2016; Nagl et al., 2013; Richter, 2011). Consequently, an important aspect of the LSS-CEPPS in Europe is to find the most cost optimal pathway for this transition.

Attributes of transmission infrastructure

To facilitate transmission of electricity, investments in transmission networks between geographical locations is possible. Decisions are made for both the amount of invested transmission capacity and whether the investment should be made in direct current or alternating current lines (HVDC and HVAC, respectively). Both transmission line types have specified transmission loss coefficients stating the power losses associated with each type of line. Investments can be made either through expanding the capacity of existing infrastructure or through building entirely new interconnectors.

Attributes of electricity storage

Investments in storage is defined as investments in both capacity for energy storage and capacity for charging and discharging of the storages. Decisions are made for both the amount of invested capacity and the share of different storage technologies to be invested in. For some storage technologies such as certain types of batteries, there is a coupled relationship between investments in energy capacity and investments in charging and discharging capacity, for example, that discharging a battery entirely cannot be done within a very short amount of time. When charged, the storage capacity can be used as an operational source of electricity just like a generator, is depicted in Figure 2.2. Available storage technologies are quite heterogeneous and can have very different characteristics. For instance, the storage of liquid hydrogen needs a constant flow of energy to keep it cold, while other storage technologies can stay untouched for long periods without being discharged, while yet other storage technologies can self-discharge entirely if it is not discharged quickly after being charged. In addition to the mentioned characteristics, losses in charging and discharging of different storage technologies should be accounted for.

Note that although not fully commercialized in today's power system, the possibility to store electric energy from the transmission grid is anticipated to play a significant role in future power systems where intermittent renewable energy sources are anticipated to make up a significant amount of the generation capacity, as discussed in Whittingham (2012). With a forecasted increase in the amount of intermittent renewable energy capacity, storages might provide the necessary buffers needed to stabilize the power system, as physical laws state that power otherwise has to be consumed at the instant when it is produced.

2.3 Political regulations

A central part of the LSSCEPPS is the various energy policies being set by either national governments or international institutions, where the EU system is the most relevant institution for the European power system. These policies are implemented with the target

of reaching a more favorable equilibrium state than the current, such as getting to a state where it is profitable to invest in renewable energy capacity. Possible policies may include targets for shares of renewable energy production or restrictions on the amount of invested capacity in a given generation technology, transmission type or storage technology. An example of the latter is Germany's nuclear moratorium implying a complete phase-out of nuclear power in Germany by 2022 (World Nuclear Association, 2017). Restrictions may also be put in place to ensure domestic energy security without having to rely on transmission from neighboring countries, such as requirements for minimum domestic generation capacity. Further, depending on the political environment, emission policies can be enforced either through emission restrictions or by taxing emissions. The latter case would imply an inclusion of these taxes in the variable OPEX of generation technologies that emit CO₂.

2.4 Uncertainties and risks in power system capacity expansion

In the context of capacity expansion in power systems where planning horizons typically span several decades, a deliberate treatment of risks and uncertainty is imperative. Note that this section contains a generic description of risks and uncertainties relating to capacity expansion in power systems, while issues relating to the incorporation of uncertainty in power system modeling are discussed in chapter 4.

There are several approaches to dealing with the issue of uncertainty in this context: One possible approach is to not assume anything about the future, a second approach is to assume a probability distribution about the possible outcomes of the future, and a third is to assume exact knowledge about the future. Given an objective to find robust solutions to the LSSCEPPS that are resilient to different kinds of uncertainties, the second approach is argued to stand out as a reasonable approach.

Two fundamentally different types of uncertainty should be considered as part of the LSSCEPPS. The first one relates to highly frequent and unpredictable variability in the short-term, a type of uncertainty that can be included in the problem by utilizing statistical methods on historical data. Examples of such uncertainties include variability in short-term electricity demand or varying availability of renewable energy generation capacity due to unpredictable weather conditions. These uncertainties should be included as part of the problem to reflect the varying operational nature of power systems.

The second type of uncertainty relates to longer-term, low-frequency uncertainties about future trends and developments in the system. Due to the low frequency of such events, statistical methods fall short in trying to capture their impact on the system, but their potential impact may be too significant to ignore. These uncertainties may include the development of future investment costs of generation capacity due to maturation processes and learning effects, changes to policy regulations or long-term changes to electricity demand trends. Note that the two types of uncertainty presented correspond to the two different time-scales being considered in the LSSCEPPS, as discussed above in section 2.2.2.

The uncertainties discussed above may have large impacts on the choice of genera-

tion portfolio in the future power system, due to the inherent risks they represent. For instance, the risk of stranded assets due to overinvestments or the risk of undercapacity due to too low investments in generation capacity becomes more prevalent with increasing amounts of new, immature generation technologies. In addition, fluctuating electricity prices introduces the risk of not collecting enough revenue to cover the costs of capital during the lifetime of an investment in a generation plant, particularly when renewable energy technologies with close to zero variable costs, such as solar, wind or hydropower, are introduced to a larger extent. Other risks include inadequate diversification of the power supply portfolio, resulting in a power system that is vulnerable to extreme, unexpected events.

2.5 Summary of the LSSCEPPS

To summarize, the problem explored in this thesis is the co-optimization of long-term investment decisions and short-term operational decisions in the European power system several decades ahead. The objective is to find a sustainable, least-cost and robust development of the power system while securing coverage of future power demand and complying with given political regulations. The co-optimization is done in a context of uncertainty in both long- and short-term input parameters. In the rest of the thesis, this problem will be studied using the long- and short-term stochastic version of the EMPIRE model, which is a simultaneous capacity expansion and system dispatch optimization model for the European power system. The EMPIRE model will be briefly introduced in chapter 3 while modeling issues related to uncertainty will be presented in chapter 4. Finally, a detailed presentation of the mathematical formulation of the extended version of the EMPIRE model including long-term uncertainty will be presented in chapter 5.

Review of Relevant Literature on Energy System Capacity Expansion

This chapter will provide an overview of the existing literature related to capacity expansion models for energy and power systems. Note that throughout this chapter, the term energy system will refer to all sectors relevant for energy supply and demand, while the term power system will refer to the electricity sector only. The main objectives of the chapter are to (1) examine different approaches to capacity expansion modeling, (2) create an overview of the most relevant power system models that have been developed and how these deal with different modeling issues, and (3) discuss key results from studies conducted utilizing such models. Mikkelsen and Reiten (2017) presents a literature review touching on some of the similar topics, and some parts of this literature review are based on elements of the work done there.

First, to set the context for the discussions in this chapter, a brief introduction to the EMPIRE model is given in section 3.1. After this, different approaches to energy system modeling with related issues are presented in section 3.2. This is followed by a discussion of power system optimization models in section 3.3, including important features and considerations that need to be made when formulating such models. Finally, section 3.4 summarizes the literature review. Selected models described in the chapter is also summarized in Table 3.1 for convenient comparison between the model studied in this thesis and other relevant research efforts. While this chapter reviews relevant literature for energy and power system capacity expansion in general, literature relevant for the inclusion of uncertainty in such models will be presented in chapter 4.

3.1 Introduction to the EMPIRE model

In order to facilitate a comparison between the EMPIRE model studied in this thesis and other relevant capacity expansion models in the literature, a brief introduction is included here, while an extensive presentation of the model will be given in chapter 5.

A tradition of large-scale stochastic optimization has been applied when formulating the European Model for Power System Investment with Renewable Energy (EMPIRE). The model was first presented in Skar et al. (2016) and is a multistage, long-term capacity expansion and system dispatch optimization model for the European power system. In the version of the model studied in this thesis, the possibility to represent both short-term and long-term dynamics in addition to short-term and long-term uncertainties is included. The model simultaneously co-optimizes investment decisions in multiple stages with operational decisions for system dispatch. It was developed to study optimal capacity expansion in the European power system in a context of fluctuating energy demand and variable, intermittent renewable energy (IRE) production. To cope with this uncertain variability, the model was initially formulated with the ability to include uncertainty in short-term input parameters in Skar et al. (2016), while an extension of the model including uncertainty in long-term input parameters was developed in Mikkelsen and Reiten (2017).

3.2 Energy system modeling approaches

Due to the large, complex and interconnected nature of energy systems, several different approaches exist for creating models for energy systems in general and for the LSS-CEPPS in particular. Holz and von Hirschhausen (2013) makes a distinction between top-down general equilibrium models and bottom-up optimization models. An approachable introduction to equilibrium modeling can be found in Gabriel et al. (2013), and Kiuila and Rutherford (2014) discusses similarities and differences between equilibrium models and optimization models. In equilibrium models, the behavior of market participants is modeled through their decisions and interactions. Each market participant is assumed to maximize their utility subject to a market clearing condition, i.e. that supply must match demand. Supply and demand are matched by inputs such as demand functions and supply curves, and together these determine the equilibrium state of the system, including market prices and quantities. It is worth mentioning that under assumptions of price inelastic demand and perfect competition, an equilibrium model is equivalent to minimizing costs and satisfying demand in an optimization model for the energy system (Gabriel et al., 2013). This stands in contrast to the assumption of imperfect competition where some market participants have market power (see Schwenen (2014) and Sanstad and Howarth (1994) for a discussion of imperfect competition in energy modeling). The choice between these two classes of models is typically affected by several factors. Two of the most important factors in such a consideration is (1) the desired scope and granularity of the system to be studied and (2) assumptions about who are making decisions in the system.

3.2.1 Determining the scope and granularity of energy system models

When studying energy systems and energy policy questions, several modeling choices regarding scope and granularity need to be addressed. One such choice relates to the sectors to be included in the model. The energy system consists of several interacting sectors that are mutually dependent on each other, such as the power sector, the coal sector, the natural gas sector, the oil sector, the transportation sector and the heating sector. In the energy system, the sectors are interconnected in the sense that they can take the role as both

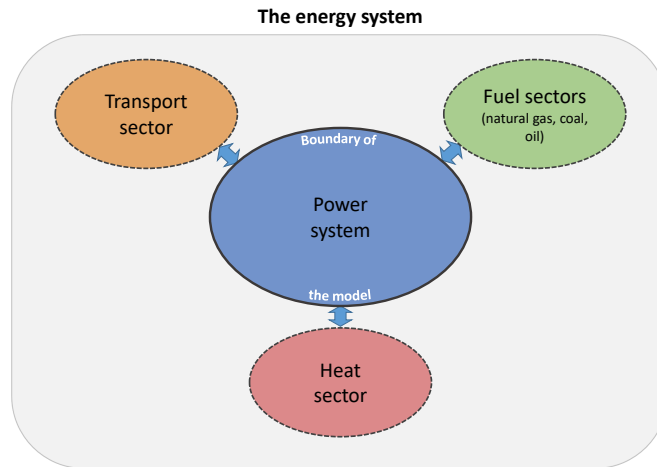


Figure 3.1: Illustration of the power system’s boundaries to other sectors of the energy system.

a consumer of other sectors’ outputs and a producer of other sectors’ inputs, as illustrated in Figure 3.1.

Hübler and Löschel (2013) uses the PACE model (Policy Analysis based on Computable Equilibrium) to study different decarbonization pathways for the European energy system towards 2050. In their model, the world is partitioned into 13 regions, where 24 different production sectors are included. Compared to the single sectoral analysis of the electricity sector spanning 31 European countries in the EMPIRE model, this is a much wider scope both sectorally and geographically.

Capros et al. (2014) introduces the PRIMES model, which is a general equilibrium model that simulates several energy sub-systems simultaneously, covering all sectors and relevant markets for the energy system. The model is applied to 28 EU member states, i.e. a similar geographical scope as in the EMPIRE model. However, similarly to the PACE model discussed above, the sectoral scope is much wider than in the EMPIRE model, since other sectors relevant for the energy system are treated as exogenous inputs in the EMPIRE model. Note that the choice of not including other sectors of the energy system in a model implies ignoring interactions and feedback loops between sectors. As an example, an increase in electricity production from natural gas-powered generators may induce a need to invest in more natural gas pipelines, possibly inducing a reduction in natural gas prices due to higher supply, which in turn may increase the demand for natural gas. Such effects cannot be modeled in a single sector model. Stated otherwise, co-optimization of both power systems and fuel sectors may find more efficient solutions for the entire energy system, but at the cost of increased computational complexity and increased requirements for input data gathering and preparation.

The TIMES model, introduced in Loulou and Labriet (2008) and Loulou (2008), is a

linear optimization model covering all sectors relevant for supply and demand of energy. The linear optimization approach is a different one than the general equilibrium approach used in the PACE-model and the PRIMES-model discussed above, but similar to the modeling approach used in the EMPIRE model studied in this thesis. The authors argue that optimization models are useful when a high level of technological detail is desired, due to the bottom-up approach of these models. However, due to this granular level of detail and the wide sectoral scope of the TIMES model, its application is limited to a single-country level only, such as in Seljom and Tomasgard (2015) where the geographical scope is limited to Denmark and in Pina et al. (2011) where the TIMES-model is applied to a Portuguese island. This illustrates the trade-off between geographical scope and sectoral scope and level of detail. When developing models to study energy or power systems, these trade-offs have to be balanced in such a way that the model is able to capture the relevant dynamics and interactions needed to study the questions of interest, but still not too detailed making the model computationally intractable.

From the discussions above it can be argued that if the purpose of a model is to study the high-level interactions between multiple sectors in the energy system, equilibrium models are of great use. However, endogenously modeling several sectors comes at the cost of higher computational complexity, thereby reducing the possibilities to model temporal and geographical characteristics in great detail. As discussed, a remedy for this issue is to assume all sectors but the one of interest as exogenous inputs to the model, as is done in single-sector optimization models such as the EMPIRE model. This implies an ignorance of feedback effects between sectors, or stated otherwise, that the power system has negligible impacts on other sectors in the energy system. However, this choice has the benefit of providing more granular results for the power system. This is evident from e.g. the difference in geographical scope between the EMPIRE model and the PACE-model presented in Hübler and Löschel (2013), as the PACE-model breaks the world into 13 regions (only one of them being Europe), while the EMPIRE model includes 31 different countries within Europe.

3.2.2 Centralized vs. decentralized decision making

The choice of modeling decisions as centralized or decentralized is an important one when modeling energy systems in general, and power systems in particular. It is well understood that these systems comprise numerous decision makers with their own agendas and considerations, making it reasonable to claim that decisions should be assumed decentralized. An assumption of centralized decision making in mathematical models results in decisions that are unlikely to happen in a system with multiple decision makers. However, this may still prove useful, since the assumption of a single decision maker with all relevant information and complete decision-making authority will let the model find an optimistic target for the system, and this target can direct and aid policy making. This stands in contrast to the results from a model assuming decentralized decisions, as such a model enables a validation of how the system and its decision makers will respond to the implementation of specified political regulations.

The distinction between centralized and decentralized decision making corresponds well with the distinction between optimization models and equilibrium models, respectively. In optimization models for energy systems, an objective to maximize social welfare

or minimize expected costs is typically used. This calls for an assumption of centralized planning leading to socially optimal solutions, thereby neglecting profitability and rationality constraints for individual market participants. This stands in contrast to equilibrium models where each participant maximizes their own objective. In a sense, both classes of models complement each other when studying energy-related policy questions, since the former type can be used to direct policy while the latter can be used to study the effect of specific policies.

With the above discussions in mind, the EMPIRE model studied in this thesis has been chosen to include the power system only, assuming interactions with other sectors in the energy system as exogenous inputs (possibly stochastic). Due to an objective of searching for optimal policies for the European power system going forward, and not to validate the outcomes of specified policies already suggested, it has been formulated as an optimization model. According to Hobbs (1995), optimization models are a natural choice for studying capacity expansion in power systems due to the bottom-up approach able to capture a high degree of complexity and technological granularity. This level of detail is required due to the need to capture the dynamics between long-term infrastructure investments and short-term scheduling of operational system dispatch. As a result, in the remaining part of the chapter, the scope of the literature review will be limited to optimization models for capacity expansion in power systems.

3.3 Optimization models for power systems

In this section, several different optimization models that are used to study capacity expansion in power systems will be introduced. While most of these models touch on many of the relevant attributes and characteristics discussed in this section, only selected characteristics will be discussed for each model. However, a table detailing the different characteristics of a number of the models presented is included at the end of the section.

3.3.1 Operational considerations and short-term dynamics

In the EMPIRE model, long-term investment decisions and short-term operational decisions are simultaneously co-optimized, which gives rise to the model's ability to identify and capture both dynamical effects and synergies along both time-scales.

A model comparable to the EMPIRE model is the Long-term Investment Model for the Electricity Sector in Europe (LIMES-EU), documented in Nahmmacher et al. (2014). LIMES-EU is a linear optimization model that minimizes investment and dispatch costs from generation, storage and transmission in Europe from 2010 to 2050. Haller et al. (2012) uses the model to explore long-term capacity expansion with high shares of intermittent renewable energy generation in the power system in the European and MENA region, however, in a deterministic setting. They find that limitations to long-term, cross-border transmission expansion increases both short-term temporal variations and geographical variations in electricity prices. That is, the long-term decision of limiting transmission investments turns out to have an impact on the operations of the system in the form of electricity price variability, showing the interplay between short-term operations and long-term decisions in the system.

Pina et al. (2011) extends the TIMES energy model to include seasonal, daily and hourly dynamics of supply and demand, which enables a more accurate study of the effects of an increased share of unpredictable renewable energy sources in the electricity system. An important finding is that such a fine-grained time-scale is necessary when studying the effects of different policy measures in systems with high shares of renewable energy. Although instructive, the study is only performed on an island outside the coast of Portugal. Note that in the EMPIRE model an hourly short-term time-scale has also been applied, but in addition, a much wider geographical scope has been used, including 31 countries within Europe. The reason why the TIMES model is unable to handle such a large geographical scope is due to the greater sectoral scope, as discussed earlier.

The issue of modeling seasonal storages in a proper manner in capacity expansion models has been discussed in Powell et al. (2012). This issue has also been addressed in a similar power system model to EMPIRE, the Dispatch and Investment Model for European Electricity Markets (DIMENSION), presented in Richter (2011). The DIMENSION model differentiates from the EMPIRE model by including options to study effects like demand side management and decentralized electricity production. In addition, it includes the possibility to represent short-term operations on an hourly time-scale with 8760 hours per year, meaning that full operational years can be studied. This enables simplified modeling of seasonal storages since the need to link storage levels between time-periods is easily accomplished when the operational time-scale spans the entire year. This is opposed to the case where only a limited number of typical days in an operational year is modeled. Using this approach, planning of seasonal energy storages such as hydro reservoirs becomes more difficult as the limited number of operational days is unable to capture the seasonality of these storages. In addition, the temporal link between the last operational hour of one operational period and the first operational hour in the next is lost. As a result, the choice of only modeling a limited number of typical operational days in EMPIRE has the benefit of reduced computational time, but at the cost of complicating the task of modeling seasonal storages in a realistic manner.

3.3.2 Planning horizon and scope of infrastructure investments

The choice of planning horizon for long-term capacity expansion models for power systems may seem evident due to the long lifetimes of infrastructure investments. Schmid and Knopf (2014) uses the LIMES-EU+ model to study the interactions between investments in European transmission infrastructure and capacity investments in renewable energy generation towards 2050. They find that the optimality of investments in transmission infrastructure in Europe is vastly impacted by the development of solar and wind investment costs the coming decades, confirming the importance of using a long enough planning horizon to incorporate such long-term developments in important input parameters.

The EMPS model is presented in Wolfgang et al. (2009) where they study the effect of deregulation of the Norwegian electricity market on reservoir levels in hydropower plants. They take investment decisions for generation capacity from the PRIMES model as exogenous inputs and utilize the extended operational modeling capabilities of the EMPS model to study optimal transmission grid expansion with the requirement of satisfying exogenous demand. The EMPS model differs from the EMPIRE model in the sense that it includes enhanced operational modeling features, but at the expense of less sophisticated

modeling of investments, as investments are taken as exogenous input. Their results show that increases in transmission capacity, thereby extending the operational flexibility of the power system, cause a reduction in average reservoir levels. This result indicates the need to model transmission expansion endogenously due to its apparent effect on how the power system is managed and operated.

Investments in storage capabilities for the power system is anticipated to increase with a rising share of intermittent renewable energy in the power system. This is studied in Gerbaulet and Lorenz (2017), where the dynELMOD model is presented. They study different decarbonization pathways for the European power system, including 33 countries in Europe, five-year investment steps and a planning horizon until 2050. They find that if a near complete phase-out of CO₂ emissions from the power system is required, most of the electricity will be provided from a combination of renewable technologies and storage capacity. They also find that as the share of renewables in the generation portfolio increases, the optimal amount of installed storage capacity increases. These results are clear indications that an endogenous treatment of storages in the model is necessary since such results are impossible to obtain with a model that excludes decisions for storage capabilities.

Krishnan et al. (2015) discusses the choice of whether to include transmission infrastructure investments as endogenous decisions in the model or not. They argue that generation and transmission investments often are substitutes, as electricity demand can be met either by local generation or by transmitting electricity from distant supply locations. In addition, generation investment decisions are often affected by the amount of nearby transmission infrastructure and hence the possibility to transmit power to other demand locations. This is also true the other way around. Therefore, it is argued that capacity expansion models should include a combined assessment of investments in both generation and transmission. Furthermore, Haller et al. (2012) finds that if transmission and storage investments are allowed, ambitious emission reduction targets set out by EU can be met by an extensive expansion of renewable energy capacities. Powell et al. (2012) also argues that the issues of intermittent and volatile sources of energy, such as wind and solar, can be mitigated through the use of different types of storage such as batteries and pumped hydro. All these results illustrate that it is important to consider endogenous investments in both generation, transmission and storage capacity in order to enable the model to capture the synergies that might emerge from an integrated assessment.

3.3.3 Modeling the transmission network

There are several different approaches to modeling the transmission network of a power system, all with different levels of realism and complexity. Siddiqi and Baughman (1995) discusses different approximations to modeling power flow networks and studies their effect on the model results. In the process of reviewing relevant literature for capacity expansion in power systems, four common approaches to modeling power flow networks have been identified.

The first type is called the copper-plate assumption, where power is allowed to flow freely from any supply location to any demand location in the model. A more realistic assumption is a net transfer capacity (NTC) approach, also called a pipe flow equivalent. In such an approach power is simply assumed to be transported from one geographical location to another with specified losses per unit of transferred energy, only restricted by

capacity restrictions and nodal balances, and not necessarily obeying Kirchhoff's voltage law (KVL).

An even more realistic modeling approach would be what is often called a DC power flow model, where, in addition to the restrictions above, the KVL is assumed to hold under certain assumptions about low resistance in the network, flat node voltage profiles and small angular differences across lines in the network. These assumptions result in a model that can detect bottlenecks in the grid and that considers active power flows, but not reactive power.

Finally, the most realistic power flow model is an AC power flow model where the KVL is assumed to hold without any further assumptions. In such a model reactive power is also modeled, however at the expense of making the model non-linear. As noted in Ryan et al. (2011), even linearized DC power flow models become non-linear if the impedance is included in the model, due to the need to divide voltage angles by line reactances, both of which are decision variables in such a formulation.

A recurring observation made when reviewing other power system capacity expansion models is the trade-off between modeling detail and computational complexity, and the case of modeling transmission networks is no different. With smaller, more detailed geographical scopes, AC or DC models might prove more appropriate, while NTC approaches (or even the copper-plate assumption) may be sufficient for lower levels of detail, such as when nations or several nations are modeled together as one region in the transmission network.

Due to the non-linearity of AC and DC power flow models, the linear pipe flow equivalent has been applied in the EMPIRE model to keep it linear. However, there do exist mitigating measures for the issue of non-linearity in DC models. The dynELMOD model presented in Gerbault and Lorenz (2017) iterates between a linear optimization model for investments and dispatch and a separate, non-linear optimization model for solving the intra-country grid expansion problem. Hence, the issue is mitigated at the expense of increased computational complexity and an increased number of iterations in the solution algorithm, but with the benefit of validating the solution on a more realistic transmission network expansion model. Note that the increased computational complexity in the dynELMOD model explains the less sophisticated modeling choices of myopic investment decisions (meaning that investments are made in sequential time steps only accounting for here-and-now knowledge) and very few operational hours (18 hours compared to up to 720 in the EMPIRE model) included in the system dispatch optimization.

In a comparative study of several different capacity expansion models for the European power system, Holz and von Hirschhausen (2013) finds that the iterative approach to intra-country grid expansion using a DC power flow model results in both lower investments in cross-border and intra-country transmission infrastructure compared to two other models where the NTC approach is used. On the other hand, Fürsch et al. (2013) also uses an iterative approach where investment and dispatch decisions are optimized using the DIMENSION model, followed by a separate optimization of grid extensions using a load flow based grid model. Contrary to the results found in Holz and von Hirschhausen (2013), they find meaningful potential value in large expansions of the power flow network, particularly when high shares of renewable energy generation is introduced in the system. Consequently, whether the use of a separate, non-linear DC power flow model

results in improved decision support for transmission expansion in power systems is an ambiguous question, supporting the use of an NTC approach in the EMPIRE model in this thesis.

3.3.4 Energy policy and political regulations

Power system models are important tools for advising governments and policy makers on energy and environmental policy issues. These models are widely used in studies of decarbonization pathways and optimal capacity expansion in power systems, particularly in the context of EU's target of almost fully decarbonizing the European power system by 2050 (EC, 2011).

There is no doubt that political regulations have major impacts on the power system. In economics, the notion of externalities is a basic concept that formalizes the benefits and costs of an individual decision maker's choices for his or her surroundings (Pindyck and Rubinfeld, 2013, p. 675). Within energy economics, the social cost of carbon is a well agreed-upon externality and a foundation for a lot of the political regulation being put in place for the energy sector. The target of these political regulations is to nudge the equilibrium state of the society into a more favorable one, as economic theory states that individual decision makers will not internalize these social costs by themselves, such as the external costs of emissions and pollution from producing, transporting and consuming energy.

Several types of political regulations have been discussed in the research literature and implemented in practice by different governments and regulatory authorities. Schmid and Knopf (2014) simulates climate policy by constraining annual CO₂ emissions in a similar manner as what is suggested in the "Roadmap for moving to a competitive low carbon economy in 2050" (EC, 2011). This kind of policy regulations is similar to those implemented in this thesis, apart from the fact that the restrictions are modeled in a stochastic manner in the EMPIRE model. This will be further elaborated in the next chapter.

Other kinds of political regulations are also found in the research literature. In Gerbaulet and Lorenz (2017) political targets to reduce carbon emissions can be included either by modeling particular emission paths, by imposing emission budgets for a specified period or by taxing emissions of CO₂. Jägemann et al. (2013) uses the DIMENSION model to study 36 different policy scenarios for the European power system towards 2050. The different political regulations considered include CO₂ emission limits, targets for renewable energy capacities, and restrictions on investments in nuclear generation capacity or CCS-capabilities. They find that in the case of restrictions to investments in either thermal generation plants (such as coal-fired or natural gas-fired plants) with CCS-capabilities or to nuclear capacity, targets for investments in renewable energy capacity become redundant. The reason is that the model finds it optimal to invest heavily in renewables to meet required CO₂ restrictions when other mitigating measures such as these are excluded. It is worth mentioning that from the perspective of enforcing political regulations, renewable share targets are probably easier to monitor than direct targets for CO₂ emissions, since measuring CO₂ emissions is subject to great uncertainty (Global Carbon Project, 2017). Although the possibility to include renewable share targets exists in the EMPIRE model, this type of political regulation has not been studied in this thesis.

The E2M2 model (Swider and Weber, 2007) is applied in a study of five different policy scenarios or policy regimes in Spiecker and Weber (2014). The focus is to study different approaches to decarbonizing the European electricity sector towards 2050, and an important conclusion made is the importance of a coordinated policy effort across borders to introduce meaningful amounts of intermittent renewable energy capacity in the European power system. The reason for this, they point to, is that in order to maximize the value of uncontrollable renewable energy in Europe, coordination and cooperation of investments in all kinds of infrastructure is needed.

3.4 Summarizing the literature review

In this chapter relevant literature for capacity expansion in energy and power systems has been reviewed. Several issues and attributes specifically related to modeling this problem has been discussed, including choice of model type, temporal and sectoral considerations for scope and granularity, system dynamics between investments and operations, transmission network modeling and political regulations.

In Table 3.1 a summarizing overview of different attributes of the most relevant models reviewed in this chapter is presented, including a comparison with the EMPIRE model studied in this thesis. Note that no relevant literature has been found to include uncertainty in the model in both the short and long term, which is the main objective of this thesis.

Yet to be discussed is the issue of incorporating stochastics in capacity expansion modeling. Although some of the models presented in this chapter have embedded functionality for including stochastics, most of them are deterministic models in both the short and long term. Since such deterministic models can lead to overly optimistic predictions of expected future costs (Wallace and Fleten, 2003), it is the authors' view that including uncertainty is of significant importance. For this reason, the next chapter will elaborate on the inclusion of stochastics in multistage capacity expansion models, both in terms of theory, methods, relevant literature on the subject and a discussion of mitigating measures to reduce computational complexity.

Table 3.1: Overview of capacity expansion models for the European power system. Abbreviations: NTC - Net transfer capacity; Gen - Generation; Transm - Transmission; Stor - Storage. References are provided in the footnotes below the table. The uncertainty column is not discussed in this chapter, but will be discussed in chapter 4.

Model name	Type of model	Investments		Operations		Geographical scope	Investment opportunities	Uncertainty		Transmission network	Demand side mgmt.
		Horizon	Steps	Days per year	Hours per day			Short-term	Long-term		
This thesis	Optimization	2010-2050	5 years	30 days	Hourly	31 countries	Gen, Stor and Transm.	Yes	Yes	NTC	No
DIMENSION ^a	Optimization	2010-2050	10 years	365 days	24 hours	28 countries	Gen, Stor, Transm.	No	No	NTC	Yes
LIMES-EU ^b	Optimization	2010-2050	5 years	6 days	8 hours	31 countries	Gen, Stor, Transm.	No	No	NTC	No
DIMENSION ^c	Optimization	2010-2050	10 years	365 days	Hourly	6 countries	Thermal gen, Stor	No	Yes	N/A	No
E2M2 ^d	Optimization	2000-2020	Yearly	12 days	12 hours	Germany	Thermal gen	Yes	No	N/A	No
EMPIRE ^e	Optimization	2010-2050	5 years	10 days	24 hours	31 countries	Gen, Stor, Transm.	Yes	No	NTC	No
TIMES ^f	Optimization	2005-2025	Yearly	12 days	Hourly	Portugal	Gen	No	No	N/A	No
EMPS ^g	Iterative simulation and optimization	2030	Once	365 days	12 hours	Northern Europe	Gen, Transm	Yes	No	NTC	No
dynELMOD ^h	Iterative simulation and optimization	2015-2050	5 years	365 days	24 hours	33 countries	Gen, Stor, Transm, National grids	No	No	DC	Yes

^aRichter (2011)

^bHaller et al. (2012)

^cFürsch et al. (2014)

^dSwider and Weber (2007)

^eSkar et al. (2016)

^fPina et al. (2011)

^gJaehnert et al. (2013)

^hGerbaulet and Lorenz (2017)

Treatment of Uncertainty in Power System Capacity Expansion Models

As nobody can forecast the future with perfect accuracy it should be acknowledged as inherently unpredictable, making uncertainty a fundamental part of most decision processes. Capacity expansion models for power systems is no exception to this since these models aim to capture the dynamic and complex development of power systems over a long planning horizon. As a result, uncertainty commonly arises in planning problems for power systems (Hobbs, 1995).

There exist multiple approaches to dealing with uncertainty in large-scale capacity expansion models. These approaches can in most cases be classified into one of two groups - uncertainty propagation or sequential decision making (Kann and Weyant, 2000). Within uncertainty propagation, uncertain parameters are sampled from their probability distributions and propagated through a deterministic model to generate distributions for the model output. Although this approach provides a nice framework for carrying out uncertainty analysis of the outputs, it does not instruct decision makers on optimal, robust decisions before the uncertainty is revealed. That is, uncertainty propagation only gives information about how uncertainty in the input parameters is transformed by the model to uncertainty in the model outputs, but it does not provide optimal policies or decisions as output. In contrast, sequential decision making frameworks, such as stochastic optimization, endogenously find sets of decisions that incorporate the effect of uncertainty in a balanced way, accounting for all possible realizations of the uncertain parameters. Frequently used methods within stochastic optimization include robust optimization (Ben-Tal and Nemirovski, 2002), chance-constrained optimization (Prékopa, 2003) and stochastic programming (Bertsimas et al., 2011; Birge and Louveaux, 2011). As the latter of these three is the chosen modeling method in this thesis, it will be introduced more formally in this chapter, and the scope of this section will henceforth be limited to relevant theory and literature covering stochastic optimization models.

The following chapter is divided into four parts. In section 4.1, fundamental theory of multistage stochastic programming for capacity expansion models is presented, providing

context for later discussions and methods used in this thesis. This is followed by section 4.2 where a literature survey related to the role of uncertainty in power system capacity expansion models is presented. Both short- and long-term uncertainty is studied, but since studying the effects of long-term stochastics is the main focus of this thesis, a particular focus has been directed towards understanding how this form of uncertainty is incorporated in the literature. Section 4.3 presents some relevant methods for solving large-scale stochastic optimization models, before section 4.4 summarizes the first part of the thesis and motivates the material presented in the rest of the thesis.

4.1 Theoretical background of stochastic optimization

Stochastic programming, as a framework for decision making under uncertainty, can be traced back to Dantzig (1955). The main objective of stochastic programming is to find optimal decisions in problems that involve uncertain input parameters, where a sequential process is defined by alternating between decisions to be made and revelation of uncertain information (Birge and Louveaux, 2011). In multistage stochastic optimization, such as in the EMPIRE model, this process is repeated multiple times. A deterministic model can tailor its solution to the input parameters due to the assumption that this particular scenario will happen with probability 1, and the solution is therefore biased towards this particular scenario. Contrary to this, stochastic models yield both cost optimal and robust solutions, in the sense that the model chooses to invest in such a manner that it is able to handle several possible realizations of the future. The purpose of this approach is to assign a value to flexible solutions, and this effect is often referred to as hedging effects (Higle and Wallace, 2003). The drawback of such a formulation, however, is increased computational complexity, particularly when uncertainty is added in multiple time-scales.

In power system modeling, infrastructure investments are typically made in multiple investment stages over a span of several decades. When optimizing over several decades, it is evident that many of the exogenously given model inputs are based on forecasts and subject to great uncertainty. Examples of inputs often considered uncertain in power system models include long-term trend developments of power demand, long-term fuel price trends, future developments of investment costs in generation capacity and governmental policy regulations (Gardner, 1996; Reinelt and Keith, 2007; Usher and Strachan, 2012). When uncertain input parameters are combined with a dynamic approach to investments, i.e. including multiple investment stages, it is referred to as multistage stochastic programming.

4.1.1 Formulation of a multistage stochastic program

In Birge and Louveaux (2011, p. 149), a very general introduction to multistage stochastic programs can be found. Decisions are made sequentially as time passes and random information influencing the system is revealed. Let $x^1, x^2(\omega^2), \dots, x^H(\omega^H)$ denote the decision vectors for the periods over the finite time horizon H , where the x^t decision variables are understood to be functions of the random events ω^t up to time $t \in \{1, \dots, H\}$. Furthermore, let ξ^t be a realization of the random vector ω^t at time t . Then, a multistage stochastic program with fixed recourse can be formulated as follows:

$$\begin{aligned}
\min \quad & c^1 x^1 + E_{\xi^2}[\min c^2(\omega^2)x^2(\omega^2) + \dots + E_{\xi^H}[c^H(\omega^H)x^H(\omega^H)]\dots] \quad (4.1) \\
\text{s.t.} \quad & W^1 x^1 = h^1 \\
& T^1(\omega^2)x^1 + W^2 x^2(\omega^2) = h^2(\omega^2) \\
& \dots \\
& T^{H-1}(\omega^H)x^{H-1}(\omega^{H-1}) + W^H x^H(\omega^H) = h^H(\omega^H) \\
& x^1 \geq 0, \quad x^t(\omega^t) \geq 0, \quad t = 2, \dots, H
\end{aligned}$$

The W^t matrices, $t \in \{1, \dots, H\}$ are assumed to be known matrices, while the right-hand side vectors $h^t(\omega^t)^T$, $t \in \{2, \dots, H\}$ and the matrices $T^t(\omega^{t+1})$, $t \in \{1, \dots, H-1\}$ are understood to take values dependent on the realizations ξ^t of the random vectors ω^t at time t . E_{ξ^t} denotes the mathematical expectation with respect to ξ^t .

The above model formulation is instructive in the sense that it formalizes how uncertainty in model input parameters can be incorporated in stochastic programming. However, such a formulation is in general infinite-dimensional due to continuous random variables. A normal approach to deal with this complication is to create an approximation of the problem by considering a finite number of realizations ξ^t of ω^t with assigned probability distributions. Dupačová (1995) presents a formulation of multistage stochastic programs that incorporates the notion of scenarios in an explicit manner:

$$\begin{aligned}
\min \quad & \sum_{s \in \mathcal{S}} \pi_s f_s(\mathbf{x}_s) \quad (4.2) \\
\text{s.t.} \quad & \mathbf{x}_s \in \mathcal{F}_s \quad \forall s \in \mathcal{S} \\
& \mathbf{x}_s \in \mathcal{F}_{NA} \quad \forall s \in \mathcal{S}
\end{aligned}$$

Formulation (4.2) is made finite-dimensional by using a decomposition based on a finite number of scenarios indexed by $s \in \mathcal{S}$. Note that vector notation has been introduced for the decision vectors \mathbf{x}_s to underline that it is a vector of decisions for all time stages $t \in \{1, \dots, H\}$, hence enabling multiple time-scales in each decision vector. For clarity, $\mathbf{x}_s = [x_s^1, x_s^2, \dots, x_s^H]$, i.e. there are $|H|$ decision stages. The cost of making decisions \mathbf{x}_s in scenario s is denoted by $f_s(\mathbf{x}_s)$, hence expected costs are minimized in formulation (4.2). Note that stochasticity is now denoted through the use of the index s on the decision vectors, as opposed to formulation (4.1) where stochasticity was denoted by the use of ω^t . \mathcal{F}_s denotes the set of feasible solutions for a given scenario $s \in \mathcal{S}$, while \mathcal{F}_{NA} is introduced to denote the set of implementable solutions. Implementability is enforced through the requirement of nonanticipativity, which is a central concept of multistage stochastic programming. If a solution to a stochastic program is nonanticipative, or implementable, it implies that decisions are only based on past and current information available, and not on any future revelations of information. This is illustrated in Figure 4.1, where all pairs of scenarios s and s' that are indistinguishable up to decision stage t satisfy the condition $x_s^\tau = x_{s'}^\tau$ for $1 \leq \tau \leq t$. In practice this implies that if two scenarios share the same node in a scenario tree, the decisions taken at that stage should be identical to satisfy the nonanticipativity constraints (King and Wallace, 2012). Note that if the requirement

of nonanticipativity were omitted, formulation (4.2) would be decomposable by scenario, meaning that each scenario problem could be solved in a separate manner before each objective value would be combined in a probability-weighted sum to yield the objective value of the entire problem. The nonanticipativity constraints are therefore an example of complicating constraints, and a brief review of exploiting this in solution methods is presented in section 4.3.

With the support of formulation (4.2), the decision stages of a multistage stochastic program can be visualized in a scenario tree, as illustrated in Figure 4.1, where the nodes represent decision variables and edges represent discrete outcomes of stochastic parameters. A path from the root node of the scenario tree to a leaf node is called a scenario.

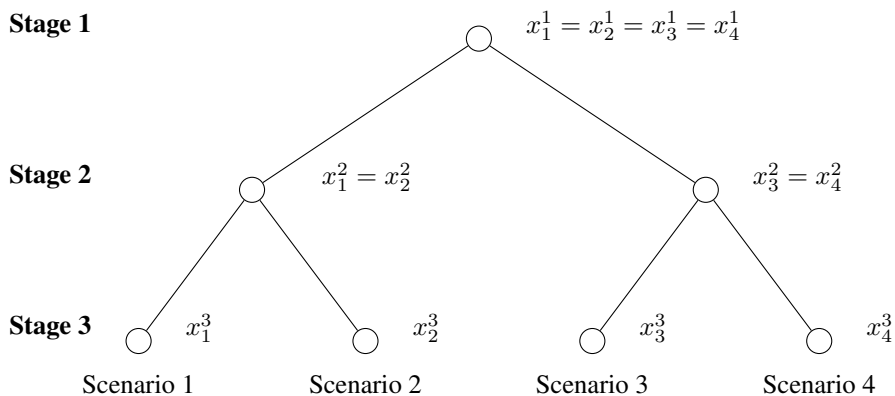


Figure 4.1: Illustrative scenario tree with three stages and four scenarios.

4.1.2 Representing multistage scenario trees

In relevant literature, multiple formulation alternatives are provided to represent decision variables in multistage stochastic programs. Two of the most used formulations are compact formulations and split variable formulations (Gassmann and Ziemba, 2013). In a compact formulation the decision variables are indexed by the nodes in the scenario tree, which implies that nonanticipativity is accounted for implicitly through the formulation. Formulation (4.1) is an example of a compact formulation. In a split variable formulation the decision variables are indexed by scenario, and as a result, nonanticipativity constraints must be explicitly defined in the formulation to enforce implementability. Formulation (4.2) is an example of a split variable formulation. Both formulations are able to represent the same multistage stochastic programs, a fact that is graphically illustrated in Figure 4.2 where (a) is the compact formulation and (b) is the split variable formulation. The circles in Figure 4.2 (b) represent the nonanticipativity constraints.

There are certain practical differences between the two formulations. As illustrated in Figure 4.2, a split variable formulation involves a matrix representation of the decision tree where nodes and scenarios are coupled by nonanticipativity constraints. This implies a large number of redundant variables and constraints, which is a clear limitation of using

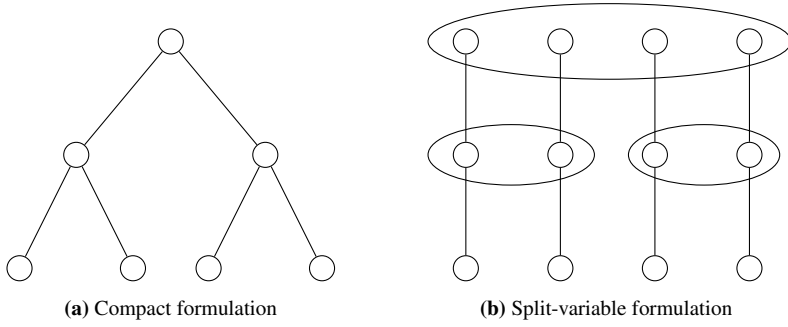


Figure 4.2: Two equivalent representations of a multistage scenario tree: (a) Compact formulation, (b) split variable formulation with explicit nonanticipativity constraints. Circles represent investment decision variables, arcs represent pathways in a scenario, and the ellipses represent the nonanticipativity constraints.

a split variable formulation as compared to a compact formulation where nonanticipativity constraints are implicitly enforced and decision variable only defined once. However, an obvious advantage of the split variable formulation is that scenario based decomposition algorithms, which are well suited for distributed programming, can easily be applied to such formulations.

4.1.3 The value of using a stochastic model

Several measures of the value of information in stochastic programming have been discussed in the literature (Bistline and Weyant, 2013). One of the most commonly used measures of this is the value of a stochastic solution (*VSS*). The *VSS* represents the expected benefit of accounting for uncertainty in the model instead of merely using a deterministic version where all uncertain input parameters have been replaced by their expected values.

VSS for two-stage stochastic programs

In Birge and Louveaux (2011) the notion of *VSS* is explained for two-stage recourse problems, where the process of evaluating a stochastic program and obtaining its corresponding *VSS* can be done in four steps. First, solve the stochastic program, or the recourse problem *RP*, where $RP = \min_x E_\xi z(x, \xi)$. Second, solve the expected value problem $EV = \min_x z(x, \bar{\xi})$ where all uncertain parameters are replaced by the expected values, i.e. $\bar{\xi} = E(\xi)$, and obtain its optimal solution denoted as $\bar{x}(\bar{\xi})$. Third, find the expected result of using the *EV* solution, *EEV*, where the first-stage decision variables are fixed to the first-stage optimal decision variables obtained from solving *EV*, i.e. $EEV = E_\xi [z(\bar{x}(\bar{\xi}), \xi)]$. Note that the second-stage decision variables can be chosen freely as functions of $\bar{x}(\bar{\xi})$ and ξ when finding *EEV*. Then, finally, for minimization problems the *VSS* can be calculated as in equation (4.3).

$$VSS = EEV - RP \quad (4.3)$$

VSS for multistage stochastic programs

For a multistage stochastic model, the definition of VSS is similar to the one for two-stage recourse problems in the sense that it is an evaluation of the value of incorporating stochastics in the model. However, calculating the VSS for multistage stochastic models is a slightly more involved procedure (Maggioni et al., 2012). In order to reflect the fact that information is gradually revealed, a rolling horizon approach should be applied, meaning that the arrival of new information should be accounted for in the VSS -calculation.

The implementation is based on solving the deterministic version of the model once for each branching point in the scenario tree. This is done to obtain decision variables for decisions to be made from the previous branching point up until the current branching point. When solving the model once for each branching point, the stochastic input parameters are replaced by their expected values according to the most recently arrived information. The process can be illustrated using Figure 4.1. First, all stochastic input parameters are set to their expected values, and the model is solved to obtain the decision variables x^1 for stage 1, the root node of the tree. After this decision, new information is assumed to arrive between decision stages 1 and 2, which should be accounted for in the rolling horizon approach. Therefore, one deterministic version of the model is solved for each branching point in stage 2, fixing stage 1 decision variables to x^1 . Hence, with reference to Figure 4.1, two models are solved: one where stochastic input data are replaced by the expected values for scenarios 1 and 2, and another where stochastic input data are replaced by the expected values for scenario 3 and 4. By solving these two models, stage 2 decision variables for the left and right hand side of the scenario tree, x_{left}^2 and x_{right}^2 respectively, are obtained. Finally, the stochastic version of the model is solved, however fixing stage 1 and stage 2 decision variables to x^1 , x_{left}^2 and x_{right}^2 , respectively. The objective value of this final model yields the *expected result of using the rolling horizon expected value solution*, the $ERHEV$, for multistage stochastic problems. Finally, the rolling horizon value of a stochastic solution is calculated as in equation (4.4).

$$RHVSS = ERHEV - RP \tag{4.4}$$

Note that since stochastic programs in general are harder to solve than deterministic programs, the VSS or $RHVSS$ can give reasonable indications whether including stochasticity in a model brings additional value or if the deterministic model simply is good enough. Hence, it can be a reasonable evaluation procedure to understand if uncertainty matters from a modeling perspective. However, an important note regarding VSS or $RHVSS$ is that these metrics are unable to capture structural differences between the solutions of the stochastic and deterministic versions of a model. That is, if the VSS or $RHVSS$ are close to zero, structural differences between optimal decisions in the deterministic and stochastic approach may still exist, and these can only be found by studying the differences between decisions made in the two different versions of a model.

4.2 Including uncertainty in power system capacity expansion models

Optimization models for capacity expansion in power systems are powerful tools for policy analysis when conclusions are consistent across several different models. However, a lot of variation in results and recommendations is also observed, thereby reducing the credibility of the conclusions drawn. Kann and Weyant (2000) argues that one reason for this variation is due to different assumptions about exogenous input parameters. A remedy for this issue is to model important input parameters in a stochastic manner. Stochastic programming has been successfully applied to power system models for several decades, where the goal is to capture the value of flexibility in such systems, as discussed in Wallace and Fleten (2003).

In chapter 2 long- and short-term uncertainties were presented as the two fundamentally different types of uncertainty that are considered as part of the LSSCEPPS. The development of important economic, technological or political conditions give rise to profound long-term uncertainties that impact central model inputs, such as projections of long-term power demand, long-term changes in fuel prices, future investment costs of generation capacity or CO₂-emission restrictions. Uncertainties in the short-term affect everyday operations of the power system and may have a notable impact on operational costs, and hence on the usefulness and profitability of infrastructure investments. Availability of intermittent renewable energy sources, inflows to hydro reservoirs, short-term fluctuations in power demand and short-term fuel price volatility are relevant examples of short-term uncertainties.

In the rest of this section, a review of relevant methods and literature relating to short-term uncertainty in capacity expansion models are presented in section 4.2.1, while a similar discussion related to long-term uncertainty is presented in section 4.2.2.

4.2.1 Short-term uncertainty in power system capacity expansion

Short-term uncertainty is reflected in optimization models by assuming selected exogenously given short-term input parameters to be stochastic. This is implemented by generating multiple scenarios for the realizations of these uncertain input parameters, typically through an application of statistical methods on historical data, often referred to as scenario generation methods. In this section a brief review of methods for generating short-term scenario trees will be presented, followed by a review of the inclusion of short-term uncertainty in relevant literature on capacity expansion models. Note that the specific method used to generate the short-term scenarios used in the studies conducted in this thesis will be presented in chapter 7.

Methods for generating short-term scenario trees

For most of the short-term input parameters that are relevant for stochastic analysis, the sample space is continuous. However, allowing continuous probability distributions for input parameters to stochastic programs leads to very large and complex problem instances. Hence, as discussed above, a discretization is normally used to approximate the sample

space. This discretization is represented through a scenario tree, where a path from the root node down to a leaf node corresponds to a scenario, i.e. one possible future realization of all the uncertain parameters.

In Kaut and Wallace (2003) methods for scenario generation and evaluation of scenario trees are presented. Different methods are suitable for different problems and applications, therefore one method is not generally better than others. One widely used scenario generation method is called conditional sampling, where realizations of uncertain inputs are sampled for each branching point in the scenario tree. The reason for its name is that when sampling of data for a given branching point is done, it is implicitly assumed that the process has already reached this point, hence the use of the word conditional. This method is appropriate for scenario trees with a lot of branching points, i.e. a lot of recourse actions. However, as stated in chapter 2, the main intention of assessing several different operational scenarios as part of the LSSCEPPS is simply to make the model account for the impacts of operational variability on the usefulness of long-term investments. Therefore, the short-term scenario tree should be generated as a simple two-stage tree where investment decisions are the first stage decisions and operational decisions are the recourse actions. In this sense, the operational decisions are made under *operational* perfect foresight (but investments are made under short-term operational uncertainty). For this reason, the method of conditional sampling is not considered further.

Another method presented involves sampling from specified marginals and correlations for the stochastic processes of interest. Although a preferred method if the statistical properties of the underlying processes were known, it is not suitable for generating short-term scenarios for the LSSCEPPS simply because marginal statistical properties are not known for the relevant uncertain short-term parameters. That being said, the moments of the historical data, such as the mean, variance, skewness and kurtosis of the historical time series, can be obtained using statistical methods. By sampling subsets of the historical data and keeping the samples that best match the moments of the entire data series, a useful method for generating short-term scenarios for the LSSCEPPS stands out. By sampling data from the exact same points in time for all uncertain short-term parameters, both autocorrelations within time series and correlations between time series for the different parameters are preserved. Due to these favorable properties, this method has been applied when generating the short-term scenarios for the studies conducted in chapter 8 and 9, and the actual procedure will be thoroughly presented in chapter 7.

Short-term uncertainty in relevant literature for power system capacity expansion

A lot of research effort has been put into studying the impact of introducing increasing amounts of unpredictable, intermittent generation capacity, such as solar and wind energy, in the power system. In Swider and Weber (2007) the E2M2 model is presented, and this is used to analyze how integration costs of wind power and operational decisions are affected by short-term uncertainty. More specifically, a recombining tree formulation (see Dupačová et al. (2000) for a presentation of this) is used to model the operation of the system as a multistage stochastic program, where uncertainty is introduced in the availability of wind power generation. Power plant investments are modeled sequentially by means of a myopic approach, meaning that investments are optimized only accounting for here-and-now-knowledge. They find that when stochastics are included in the availability

of wind power generation, larger amounts of investments in controllable power generation capacity, such as natural gas-fired or nuclear power plants, are required. This is in line with the assertion that deterministic models may provide too optimistic results, since the stochastic evaluation suggests a more flexible solution by investing more in other generation technologies.

It is worth noting the difference of the operational modeling in the E2M2 model compared to the EMPIRE model. The EMPIRE model incorporates several stochastic scenarios for the short-term inputs, but operational decisions are made under operational perfect foresight, as discussed above. In contrast, the recombining tree formulation used in the E2M2 model includes multiple recourse actions, one for each operational time-step, hence allowing a much more sophisticated operational analysis. The choice between these two approaches should depend on the main research questions of interest, as the recombining tree formulation enables a detailed operational analysis, while the formulation used in the EMPIRE model provides less operational detail and is therefore suitable for analyzing longer-term research questions.

A similar conclusion to the one in Swider and Weber (2007) is drawn in Sun et al. (2008), where a mixed-integer unit commitment model for generation investments is used in a case study on the German electricity system. They find that the negligence of stochasticity in modeling wind power generation availability results in an undervaluation of investing for flexibility and too low investments in controllable power generation.

Other methods for introducing uncertainty in capacity expansion models also exist. Sioshansi and Short (2009) use a unit commitment model for the power system in Texas to demonstrate the implications of large amounts of wind power generation on the power system. By simulating decisions in a rolling horizon model using different scenarios for wind power availability two days ahead, they find that there is a substantial additional value of wind power plants in the power system. This is due to the close to zero variable costs of wind generation, offsetting costly production when the wind blows.

An extended version of the DIMENSION model (Richter, 2011) where short-term uncertainty in both solar and wind generation availability is included is presented in Nagl et al. (2013). This version of the model is long-term static, meaning investments are only possible once. Therefore, it cannot be used to study long-term transitions of the power system, but it can be used to study operational effects of stochastics in wind and solar generation. In line with other modeling results discussed earlier, they find that including stochastics increases expected system costs, confirming the presumption that stochastic models are able to avoid the overly optimistic results often found by deterministic models tailoring solutions for a particular realization of the future. Another interesting finding is that solar generation is undervalued compared to wind generation if the negative correlation between solar irradiance and wind infeed is disregarded. This result supports the methodology used to generate short-term scenarios in this thesis, where each scenario for all uncertain short-term inputs is sampled from the same historical time periods, enabling the routine to capture correlations between short-term inputs in a proper manner.

Jaehnert et al. (2013) extends the EMPS model, which includes short-term uncertainty (Wolfgang et al., 2009), to include endogenous investment decisions. However, their approach to co-optimizing investments and operation is slightly different from the one used in the EMPIRE model. Instead of optimizing both investments and operations simultane-

ously, they iterate between a detailed, stochastic power system simulation and determining investment decisions. In contrast to investments in the EMPIRE model, investments in this study are myopic, i.e. investments are only optimized for current conditions. In their study they find that production from hydropower plants is expected to be much more volatile due to the need to balance unpredictable generation from solar and wind power. They also identify profitable investments in transmission infrastructure from the Nordics to continental Europe and the UK, primarily due to electricity surplus in the Nordics and anticipated greater demand overseas.

Seljom and Tomasgard (2015) presents a methodology for introducing short-term uncertainty in the TIMES model (Loulou and Labriet, 2008; Loulou, 2008), where they introduce a two-stage approach where investments are made under uncertainty about operating conditions and the operational decisions are the recourse actions. This is comparable to the approach presented for the EMPIRE model in Skar et al. (2016), but not to the extended version of the EMPIRE model used in this thesis. The reason for this is that in this thesis, the EMPIRE model has been extended to include uncertainty in not only short-term inputs, but also long-term inputs. The inclusion of long-term uncertainty in capacity expansion models will be discussed in the next section.

4.2.2 Long-term uncertainty in power system capacity expansion

Due to the long-term horizon of power system capacity expansion models, many of the exogenously given input parameters are highly uncertain in the long-term. For example, even though the European Union has a stated target related to emission reductions in the European power system, this does not mean that future policy may deviate from current targets due to unknown future technological, political or economic developments. Hence, policy targets are subject to great uncertainty. Put differently, omitting long-term uncertainty in an optimization model is similar to assuming perfect foresight about all long-term model inputs, possibly leading to far too optimistic estimates of the future and sub-optimal investment decisions.

In this section, a discussion of issues and methods for generating long-term scenarios for capacity expansion models is included, in addition to a review of how long-term uncertainty has been incorporated in the relevant literature.

Issues when generating long-term scenario trees

One observation from reviewing relevant literature for long-term stochastic capacity expansion modeling of power systems is that there is no unified framework for generating scenarios for these uncertain long-term parameters. As opposed to methods for generating short-term operational scenarios, generating long-term scenarios is described much more as an art than a science. That being said, some different approaches have been discussed. One approach could be to specify a joint probability distribution for all uncertain parameters and draw random realizations from this distribution. There are, however, solid arguments for why this method is not suitable in the context of long-term uncertainty. It is argued in Ryan et al. (2011) that for many of the parameters considered to be uncertain in the long term, new information is revealed on a too infrequent and unpredictable basis. Hence, it would be unwise to rely on historical data in an attempt to estimate probabilistic

properties of these long-term parameters. As discussed in Weitzman (2009), the fact that an event has not been observed in the past does not imply that ignoring them as a possible realization of the future is a good idea. As an example, it would be unwise to look at historical changes to policy regulations affecting the power system in order to gain insight into the frequency and probability of similar policy changes in the future.

As a result, one is often left with the only option of using separate forecasts for each uncertain long-term parameter, leaving out all questions about correlations between them. There are considerable amounts of evidence in the literature that both regular people and experts are poor at dealing with and anticipating correlations (Morgan and Henrion, 1990), especially when there is no or limited amounts of historical data able to back up any such correlational predictions. Therefore, similarly to Hu and Hobbs (2010) and all other research studies surveyed as part of the work with this thesis, no attempts at modeling correlations between different uncertain long-term parameters are made, implying an assumption of independence between all uncertain long-term input parameters. Whether this is a correct assumption, e.g. if the development of CO₂-emission regulations is dependent on the development of electricity demand in the years to come, is out of the scope of this thesis.

The issue of spanning a suitable outcome space of uncertain long-term, real-valued input parameters is another challenge in the context of generating long-term scenarios. Trutnevyte (2013) finds that maximally different scenarios should be assessed in order to get a proper grasp of the outcome space of such long-term input parameters. Although it is difficult, if not impossible, to identify the exact maximally different scenarios, this study at least supports the view that long-term scenario trees should span a large part of the possible outcome space.

Methods for generating long-term scenario trees

The following section gives a brief discussion of possible approaches to creating long-term scenario trees. With the above discussion in mind, these approaches should be viewed as strategies guiding this task, as no consensus methods for creating these scenario trees have been found in relevant research literature.

In Boßmann (2015) a Partial Decomposition Approach to generating long-term scenarios for power demand is described. In this approach, total demand is broken down into separate sectors, and forecasts of demand are then created for each of these sectors in a bottom-up manner. Finally, the forecasts and their associated uncertainty estimates are aggregated into a total power demand with an aggregated uncertainty measure. However useful for demand forecasts, this method is not necessarily suitable for other long-term uncertain input parameters such as uncertainty in political regulations, simply because of the lack of natural ways of breaking down political uncertainty into sub-sectors or sub-groups.

A widely used and simple approach to generate long-term scenarios is to use forecasts from experts or results from other research studies aiming at predicting the development of relevant uncertain long-term parameters. These forecasts can then form the basis for several long-term scenarios through two different methods. The first method would be to obtain external forecasts from several different sources and combine these into a scenario tree. The second method is to use one forecast as a baseline for the scenario tree and generate multiple other scenarios by perturbing this scenario through stochastic errors or

by scaling it by different factors. The latter method has been used in the studies in chapter 8 and 9, and the method will be more thoroughly presented in chapter 7.

Results from implementing long-term uncertainty in capacity expansion models in the literature

In relevant research literature, there are multiple studies on the effect of including long-term uncertainty in stochastic models for power system capacity expansion. Gardner (1996) shows that the value of technologies with shorter lead-times increase in environments with high uncertainty related to long-term demand. Reinelt and Keith (2007) uses a stochastic programming model to analyze optimal decisions for investments in generation technology subject to uncertainty in future carbon and natural gas prices. Fortes et al. (2008) applies the TIMES model on the Portuguese electricity market, and shows that seemingly cost-effective solutions to deterministic models can result in obsolete and inadequate decisions when long-term uncertainty is introduced in demand and fuel prices.

Hu and Hobbs (2010) studies the impact of uncertainties in electricity demand growth, natural gas prices and greenhouse gas regulations on investments decisions and costs in the US power sector up to 2050, using the MARKAL model (G. and Harold, 1981). Similarly to this thesis, they represent the uncertainty with scenario trees, using three different scenarios for each uncertain parameter. It also applies equal probabilities to the different scenarios, reflecting the lack of other natural choices for these probabilities. Their results show that possible regulations of greenhouse gas emissions constitute the most important long-term uncertainty, motivating the choice to study uncertainty in emission restrictions in this thesis (the analysis will be presented in chapter 9).

Kanudia and Loulou (1998) also uses the stochastic version of the MARKAL model to study the effect of long-term uncertainty in carbon mitigation measures for Québec. More specifically, similarly to the policy uncertainty studied later in this thesis, they implement uncertain CO₂ emission constraints for the power system. They pick four different scenarios, where combinations of stringent and non-stringent carbon policies are combined with high and low demand growth scenarios, and find that the inclusion of uncertainty through the use of stochastic programming yields insights that are not observed in any of the deterministic cases.

In Usher and Strachan (2012), long-term uncertainty in future fossil fuel prices and in the availability of biomass imports is introduced in a two-stage stochastic version of the MARKAL model for the UK. They study the effect of these long-term uncertainties on optimal near-term investments, and similarly to Kanudia and Loulou (1998) they find that the hedging strategies discovered by the stochastic model are structurally different from any of the deterministic scenarios studied. Their results also show that the uncertainty in fossil fuel prices is very expensive, while the uncertainty of biomass import availability is less important with regards to expected system costs. However, as a side note, it is interesting to observe that since this paper was published, the UK has started the process of exiting the EU and therefore stepping away from a set of established trade agreements, hence illustrating the relevance of such long-term uncertainties.

In Fürsch et al. (2014) the DIMENSION model is extended to assess optimal investments in thermal generators under uncertain long-term renewable energy deployment paths. It is found that uncertainty regarding political renewable share targets significantly

affects optimal investment and dispatch decisions. Compared to the EMPIRE model implemented in this thesis, this version of the DIMENSION model is long-term stochastic, but they do not include stochastics in short-term parameters.

In Messner et al. (1996) the MESSAGE model (Model for Energy Supply Strategy Alternatives and their General Environmental impact, see Messner and Strubegger (1995)) is extended with long-term uncertainty in investment costs of new generation capacity. They conclude with the promising result that letting the stochastic model endogenously find robust solutions has lower expected costs than diversifying through explicit flexibility constraints in a deterministic model. That is, they conclude that a stochastic model is better than modelers themselves at identifying optimal and robust solutions given stochastic inputs.

4.3 Solving stochastic capacity expansion models for power systems

Introducing uncertainty in multistage stochastic optimization models with multiple time-scales is a challenge from a computational perspective due to the vast increase in the number of decision variables. This happens because uncertainty is incorporated along one or more of the time-scales (Kaut et al., 2014). The results of doing this is illustrated in Figure 4.3, where ● represents long-term investment decisions and a ■ represents short-term operational decisions. The figure depicts how the scenario tree of a multistage stochastic model with two time-scales grows as various forms of stochasticity are included. In (a) neither long-term nor short-term uncertainty is included and the illustration represents a deterministic model. In (b) long-term uncertainty is included, and in (c) both long-term and short-term uncertainty has been included. As the figure illustrates, introducing uncertainty along both time-scales greatly increases the size of the scenario tree. Despite the apparent intractability of problems with this scenario trees, there exist alternative formulations and solution techniques that can cope with such models. In the remaining parts of this section, two central concepts related to this is discussed. The first concept is a technique known as a multihorizon formulation which decouples future investment decisions from past operational decisions, leading to vast reductions in the decision variable space and problem size. The second concept is a survey of decomposition techniques used for solving large-scale models when uncertainty is added and complexity increases.

4.3.1 Problem size reduction with multihorizon modeling

Alternative formulation techniques exist that can drastically contribute to reducing the problem size of capacity expansion models. One option is to apply a multihorizon formulation. This formulation, originally presented in Kaut et al. (2014), is an approach to limit the growth in problem size of multistage stochastic models with multiple time-scales. The multihorizon formulation can be illustrated with a tree structure where the evolution of decisions and revelation of uncertain information is depicted. Figure 4.4 shows an example of a multistage and multihorizon stochastic program, where (a) shows a program with long-term uncertainty, and (b) shows a program with both long-term and short-term

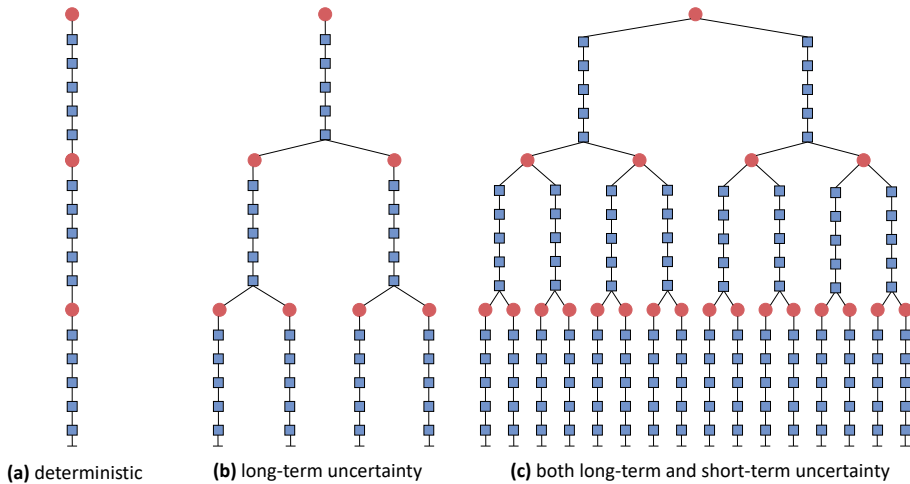


Figure 4.3: Stochastic multistage scenario trees with two time-scales illustrated for (a) a deterministic model without any uncertainty, (b) a stochastic model with long-term uncertainty, and (c) a stochastic model with both long-term and short-term uncertainty. Note that ● represents long-term investment decisions and ■ represent operational decisions.

uncertainty. Note from the figure that a result of the multihorizon formulation is that the operational periods and decisions are somewhat embedded into each long-term investment decision stage. This result comes from a set of assumptions that are implicitly made in the multihorizon formulation, as discussed below.

In Kaut et al. (2014) it is argued that the reduction in problem size in the multihorizon formulation comes from a decoupling of certain dependency structures in the scenario tree, which is a simplification that can be considered exact if two key assumptions are satisfied:

- Long-term uncertainty is independent of short-term uncertainty, and investment decisions are independent of past operational decisions. This enables a single investment stage to follow multiple operational scenarios.
- The first operational decision embedded in an investment decision stage is independent on the last operational decision embedded in nodes from the previous investment stage. Consequently, there is no connection between operational scenarios and decisions of two consecutive investment stages.

As an example, these assumptions imply that the decision of how much to be invested in new generation capacity (an investment decision in the current time period) or how much electricity to produce from a particular power plant (an operational decision in the current time period) does not depend on how much it rained a particular hour five years ago (the realization of an uncertain short-term parameter in a previous time period) or whether production from coal power plants was unusually high a particular hour several years ago

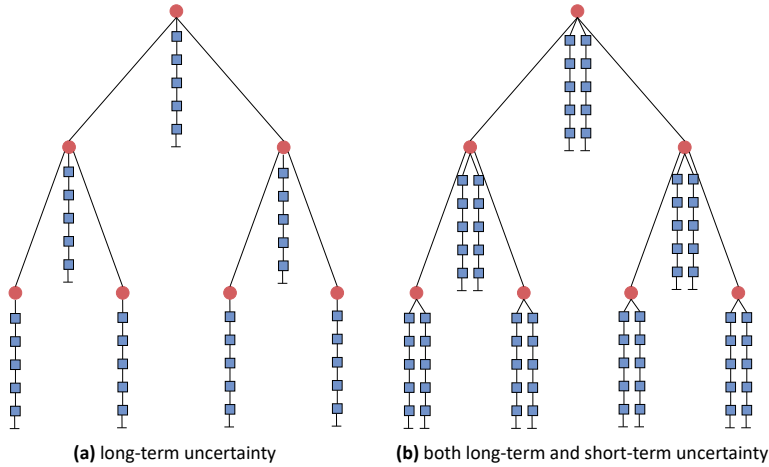


Figure 4.4: Multihorizon scenario trees with (a) long-term uncertainty and (b) both long-term and short-term uncertainty. Note that ● represents investment decisions and ■ represent operational decisions.

(an operational decision in a previous time period). In practice, this means that there is only a loose coupling between future decisions and current or past operation of the power system.

Even though the assumptions significantly contribute to reducing the problem size of a stochastic program, they come at a cost of realism. The first assumption regarding the independence of investments and past operational decisions can be considered reasonable in many capacity expansion models. This is particularly the case in models where the difference between the time-scales vary significantly, as for example with years along the long-term time-scale and hours along the short-term time-scale. The second assumption regarding lack of connection between operational decision variables can in many cases be problematic. An example is the modeling of storage in hydropower plants, where a memory aspect between consecutive long-term periods ideally should be required. Therefore, introducing a multihorizon formulation for capacity expansion models clearly comes with a benefit of reducing the size of the problem, but at the cost of realism in applications where the connection between operational decision variables between consecutive investment stages are of importance.

4.3.2 Decomposition Methods for Multistage Stochastic Programs

Even though techniques such as multihorizon formulations can contribute to reducing the problem size, power system capacity expansion models of realistic scope and granularity are still difficult to solve with current state-of-the-art optimization software. Therefore, a considerable amount of research effort has been devoted to studying various methods for solving such large-scale stochastic optimization problems. An alternative to solv-

ing stochastic programs using classical direct solving methods is to apply decomposition methods to the problem. A thorough presentation of decomposition techniques for optimization models is given in Conejo et al. (2006), while Sagastizábal (2012) elaborates on the use of decomposition methods in optimization models for energy systems.

Decomposition in this context refers to breaking up the optimization problem into smaller subproblems, where each subproblem can be solved separately in an efficient manner before the subproblems are reintegrated into a master-problem to obtain the optimal solution. Such techniques can only be applied to models which exhibit a decomposable structure. A problem is decomposable if the feasible area can be divided into independent subproblems by relaxing some complicating variables or constraints that affect the problem as a whole. Then, the decomposition procedures can utilize computational techniques to make the subproblems indirectly consider the complicating constraints or variables, progressively improving optimal decisions at the cost of iterations (Conejo et al., 2006). Depending on the choice of modeling formulation for multistage stochastic programs, several different decomposition algorithms are described in the research literature.

Nested Benders decomposition method for problems with complicating variables

A decomposition method often used to solve stochastic programming models is the Benders decomposition algorithm. The original formulation was presented in Benders (1962), and has been widely applied to solve two-stage stochastic programs in the literature, see for example Birge and Louveaux (2011). The Benders decomposition algorithm can be used when the feasible region of the original problem contains complicating variables, and is thus a particularly relevant method for multistage stochastic programs formulated and implemented using compact formulations (Conejo et al., 2006), as illustrated in Figure 4.2(a). The general idea is that the master problem sends initial feasible first-stage solutions to the subproblems, where the optimal value of the problem is progressively improved through the addition of Benders' cuts computed from the subproblems. This technique is frequently used as a solution method for power system capacity expansion models in the literature, see for example Skar et al. (2014), Abdolmohammadi and Kazemi (2013) and Sadeghian and Ardehali (2016).

Since many capacity expansion problems are formulated as *multistage* stochastic programming models, a modification of the Benders decomposition algorithm, originally developed for two-stage problems, is required for a valid implementation. Nested Benders, as described in Birge (1985), is a solution method that applies the Benders decomposition scheme recursively over a scenario tree, where the algorithm views the tree as a set of nested two-stage problems. This implies that initial decisions are passed along the scenario tree, where the total system costs are progressively improved by adding Benders' cuts from the recursively solved subproblems. Each subproblem is solved using Benders decomposition for two-stage problems. In the literature, the nested benders decomposition algorithm is frequently used to find optimal values of large-scale power system optimization problems, e.g. see Archibald et al. (1999) which uses a nested benders decomposition algorithm for reservoir optimization, or Akbari et al. (2011) which applies the technique on a transmission expansion planning problem.

Scenario-based decomposition methods for problems with complicating constraints

As opposed to the Nested Benders decomposition method, which can be used to decompose stochastic programs with complicating variables, there exist a class of solution methods that perform well when complicating constraints are relaxed. This class of methods is often referred to as scenario-based decomposition methods (Conejo et al., 2006). As the name implies, such methods decompose the problem by scenario, which can be particularly useful in problems where a split variable formulation has been chosen. Recall that in a split variable formulation of a multistage stochastic program the nonanticipativity constraints form a set of complicating constraints, binding together the decision variables across scenarios. Scenario-based decomposition methods solve each scenario (or a bundle of them) individually, and then iteratively enforce nonanticipativity by penalizing deviations in the objective function.

Lagrangian decomposition is one of the most used decomposition methods for problems with complicating constraints. In this method, complicating constraints are removed and put into the objective function as soft constraints, and deviations in the soft constraints are multiplied by *Lagrangian multipliers*. At the optimum these multipliers are set in such a manner that the optimal value of the original problem is found at the same time as the complicating constraint is satisfied without being explicitly enforced in the formulation. A more thorough description of this decomposition method can be found in Conejo et al. (2006, p. 187). An extension of this method can also be found in the same book, and is called the augmented Lagrangian decomposition method. This is similar to the regular Lagrangian decomposition method, but in addition a quadratic term is added in the objective function where the squared deviations from the complicating constraints are penalized. The benefit of the latter method is normally quicker convergence (Conejo et al., 2006, p. 222), but at the cost of not being separable by scenario. An alternative method that resembles the augmented Lagrangian method was therefore developed in Rockafellar and Wets (1991). The method presented in this thesis is a frequently applied method for scenario-based decomposition known as the Progressive Hedging algorithm (PHA). In the PHA, the complicating nonanticipativity constraints are relaxed and added as an augmented Lagrangian term in the objective function, where a set of dual multipliers are included and updated at each iteration to force the linear program to converge towards its optimal value. There exist multiple examples in recent literature where the PHA is applied to stochastic programming models of the power system, see for example Gonçalves et al. (2012); dos Santos et al. (2009). In addition, recent research on the PHA has resulted in techniques for increasing convergence rates Watson and Woodruff (2011) and methods for obtaining lower and upper bounds (Gade et al., 2016). As discussed earlier, the Progressive Hedging Algorithm is the applied solution method in this thesis, and will be explained in detail in chapter 6.

4.4 Summarizing the first part and motivating the rest of the thesis

The task of identifying optimal capacity expansion pathways for the European power system in the decades to come is a challenging one, but also a very important one for a

multitude of reasons. Irreversible and costly infrastructure investments are to be made in a context of climate change mitigation initiatives, changing dynamics of electricity demand and increasing amounts of unpredictable, intermittent renewable energy supply. In chapter 2 this problem was formalized and described as the LSSCEPPS, while chapter 3 discussed relevant issues when formulating a mathematical model for this problem, and compared the EMPIRE model to other relevant literature.

The issue of uncertainty should be viewed as an integral part of the LSSCEPPS, and only adds to the complexity alluded to above. In reviewing relevant research on stochastic capacity expansion in power systems, some recurring results were observed. An important finding is that stochastic models tend to yield structurally different solutions than any deterministic models are able to find, confirming the hypothesis that including stochastics in the model gives insights beyond the scope of a deterministic analysis. In addition, stochastic models tend to suggest solutions that have higher expected costs due to increased investments, also referred to as hedging, to ensure flexibility in the system, and they provide better hedging strategies than modelers are able to. However, a gap in existing literature related to the treatment of uncertainty in such models has also been identified. That is, to our knowledge the simultaneous inclusion of long-term and short-term uncertainty in a capacity expansion model for power systems of similar scope as in the EMPIRE model has not been observed in previous research efforts. The reason for this is probably that the size of such models quickly becomes unmanageable. This forms the foundation of how this thesis adds to current literature, and it calls for improved solution methods.

Part of the motivation for the work done in this thesis is the need for improved solution methods able to solve large-scale, multistage stochastic optimization problems including uncertainty in several time-scales, since the inclusion of uncertainty has been shown to be of importance in previous research. Therefore, as part of the work with this thesis, a considerable effort has been put into developing and implementing a distributed progressive hedging algorithm to address the issue of computational complexity alluded to in such models.

In the chapters to follow, the challenges, questions and hypotheses alluded to above will be elaborated. In chapter 5 the complete mathematical formulation of the EMPIRE model is presented, before the solution method and the distributed algorithm is presented in chapter 6. Data for the analyses conducted later is presented in chapter 7, while a computational study of the performance of the implemented solution infrastructure and a study of the techno-economic implications of the improved solution method is presented in chapter 8 and 9, respectively.

Mathematical Formulation of EMPIRE with Long-term Uncertainty

This chapter presents a mathematical formulation of the extended version of the EMPIRE model with long-term uncertainty. The EMPIRE model was initially presented in Skar et al. (2016), while an extension of the model that introduced uncertainty in long-term input parameters was developed in Mikkelsen and Reiten (2017). The formulation presented here is therefore similar to the model formulation presented in Mikkelsen and Reiten (2017). Note that since this formulation is an extension of the version of the EMPIRE model presented in Skar et al. (2016), some of the notation introduced there has been reused in this thesis.

The primary focus of this chapter will be to introduce the mathematical formulation of the EMPIRE model studied in this thesis. Although most of the important modeling assumptions and choices have already been elaborated in chapter 3 and 4, some of them are repeated for clarity and readability in section 5.1. Section 5.2 lays out the complete notation used in the model, while the complete mathematical formulation of the model is presented in section 5.3.

5.1 Model assumptions

5.1.1 Sectoral scope and choice of decision variables

A central issue related to formulating a mathematical model for the LSSCEPPS is the choice of sectoral scope, i.e. assumptions about what should be modeled endogenously in the model, and what should be taken as exogenous inputs to the model. To illustrate, as shown in chapter 3, short-term demand for electricity is often considered uncertain in stochastic capacity expansion models. If demand is assumed to neither affect or be affected

by the endogenous processes and decisions of a model, it is viewed as an exogenous input parameter. In the future, however, measures to increase the responsiveness of demand to prices and availability of electricity, such as demand response and demand side management, may be introduced. This would turn demand into an endogenous part of the problem since it would enable consumers to respond to price signals and adjust their consumption of electricity according to the instantaneous price and availability of electricity. As discussed in chapter 3, the power system in the EMPIRE model studied in this thesis is modeled endogenously, while other sectors of the energy system are modeled exogenously.

A result of this separation of the power system from the rest of the energy system is that decision variables are only introduced for decisions to be made within the power system. Decision variables are introduced for infrastructure investments in generation, transmission and storage capacity for the power system. Investments are simultaneously optimized in multiple stages and are made under both long-term and short-term uncertainty. The decision variables for investments are linear, meaning that unit commitment characteristics are neglected, as discussed in chapter 3. Decision variables are also introduced for short-term decisions for operating the power system. Short-term uncertainty is included through a two-stage approach, where investments are considered the first stage decisions made under uncertainty about long- and short-term inputs, while the operational decisions are the recourse actions made under *operational* perfect foresight.

5.1.2 Model formulation choices

A split variable formulation has been chosen to represent the long-term uncertainty of the model. As discussed in section 4.1 of the previous chapter, this formulation is well suited for scenario-based decomposition, and the details of the solution method developed will be presented in chapter 6. The choice of a split variable formulation implies that independent copies for each long-term scenario $s \in \mathcal{S}$ are made for each investment decision variable. Nonanticipativity constraints are therefore applied in the model formulation to enforce implementability, as discussed in chapter 4.

To reduce computational complexity, the EMPIRE model has been formulated using a multihorizon approach, as described in chapter 4. This is included in the model formulation by (1) *avoiding* to introduce a short-term scenario index ω on long-term investment decision variables, and (2) *avoiding* to introduce constraints that connect the operational decisions in one long-term investment stage with operational decisions made in previous investment stages.

5.1.3 Temporal assumptions

As discussed in chapter 2, two time-scales have been introduced to enable the model to capture the dynamics and interactions between long-term trends and operational short-term variability of the power system. Investment decisions are optimized along a long-term time-scale discretized into several five-year investment stages $i \in \mathcal{I}$, while operational decisions are co-optimized along a short-term time-scale discretized into operational hours $h \in \mathcal{H}$.

Instead of modeling all 8760 operational hours of an entire year, a representative subset of operational hours, denoted by \mathcal{H} , is used. This set is divided into disjoint sets of seasonal

periods, $\mathcal{H}_p, p \in \mathcal{P}$, where \mathcal{P} is the set of seasonal periods. This division is done to include representative operational data from different parts of the year. If this was omitted, it could result in that for instance only operational data from the winter was included in the model, resulting in very biased solutions.

In addition, in order to ensure feasibility of the power system even in extreme cases, both regular and extreme periods are included in the set of periods \mathcal{P} . Note that no constraints connecting different seasons are included, with the intended effect that the model is unable to prepare for extreme seasons. Operational decisions from the representative seasonal periods are then scaled into yearly figures according to a scaling factor per seasonal period, α_p .

5.1.4 Geographical scope and unit commitment considerations

In terms of geographic modeling considerations, the EMPIRE model is formulated as a nodal network of geographical nodes representing countries. Hence, a reference to a country is equivalent to a geographical node in the model. The nodes are connected by arcs representing transmission capacity between countries. Figure 5.1 depicts all 31 geographical nodes included in the EMPIRE model, including all 28 member countries of the European Union less Cyprus, plus Norway, Serbia, Bosnia-Herzegovina and Switzerland.

As discussed in chapter 3, the transmission network, i.e. the arcs between nodes, is modeled using a net transfer capacity approach, meaning that the optimal solution's feasibility within individual countries and their grid networks is not verified.



Figure 5.1: Geographical coverage of the EMPIRE model. All 28 member countries of the EU except Cyprus are included, plus Norway, Serbia, Bosnia-Herzegovina and Switzerland.

Capacity expansion is modeled in a bottom-up manner through aggregated investment decisions for each country. The choice of using a national geographic granularity is convenient for a multitude of reasons. By aggregating infrastructure investments for an entire country, the assumption of linearity in investment decision variables is made more realistic. The reason for this is that certain unit commitment characteristics, such as requirements for minimum operating times or down times, or one-offs when starting up or shutting down power plants, can be neglected when using a national granularity. Neglecting these char-

acteristics would be unreasonable in a model with a greater level of geographical detail where every single power plant in a country is modeled individually. However, on a more aggregate level, such effects play a less important role, allowing linearity of decision variables. As a result, some spatial granularity is sacrificed in order to reduce the complexity of the model.

On the other hand, a drawback of modeling power plants on an aggregate level per country is that no distinction is made between recently installed capacity and older power plant capacity. As an example, solar power in Spain is modeled as one generator in the EMPIRE model. The implication of this is that whenever a technological change or breakthrough happens to this technology, the improvement is applied to all installed capacity of the technology, and not only to capacity that has been installed after the breakthrough was made. This drawback related to technological breakthroughs being applied to all power plants has to be compared with two benefits of modeling on a national geographical scale. First, the extra modeling and data preparation efforts needed to represent unit commitment characteristics have to be considered. Second, and possibly more important, is the order of magnitude of increase in computational complexity due to the need to introduce integer variables to represent unit commitment characteristics, making the model non-linear. Due to a desire to keep the model linear, investments are modeled on an aggregated national level in the EMPIRE model.

5.2 Model Notation

This section presents the sets, indices, parameters and decision variables used in the model. The complete nomenclature can be found in Table 5.1. The notation used in the model will be further explained in section 5.3. Note that all units including monetary terms, i.e. units including €, are discounted to 2010-values.

Table 5.1: Sets, indices, parameters and decision variables used in the mathematical formulation of the EMPIRE model.

Sets and indices

\mathcal{I}	Investment stages indexed by i
\mathcal{H}	Operational hours indexed by h
\mathcal{P}	Seasonal periods indexed by p
\mathcal{H}_p	Operational hours in period p , $\forall p \in \mathcal{P}$, indexed by h
\mathcal{H}^-	$\mathcal{H} \setminus \{1\}$
\mathcal{N}	Nodes indexed by n
\mathcal{G}	Generators indexed by g
\mathcal{G}_n	Generators available in node n , indexed by g
\mathcal{T}	Distinct generator technologies indexed by t
$\mathcal{T}^{\text{AggTech}}$	Aggregated generator technologies indexed by t
\mathcal{G}_{tn}	Generators of technology t available in node n
\mathcal{A}	Arcs between nodes indexed by a
\mathcal{A}_l	A set mapping bidirectional lines l to unidirectional arcs indexed by a
$\mathcal{A}_n^{\text{in}}$	Arcs going into node n indexed by a

A_n^{out}	Arcs going out of node n indexed by a
\mathcal{L}	Transmission lines between nodes indexed by l
\mathcal{B}	Storages indexed by b
\mathcal{B}_n	Storages available in node n indexed by b
Ω	Sample space of short-term scenarios indexed by ω
\mathcal{S}	Sample space of long-term scenarios indexed by s
$\{s\}_i$	Set of long-term scenarios indistinguishable from s at stage i

Cost parameters

C_{gis}^{gen}	Investment cost for generation, €/MW
C_{lis}^{tran}	Investment cost for transmission line, €/MW
C_{bis}^{storEN}	Investment cost for storage in energy, €/MWh
C_{bis}^{storPW}	Investment cost for storage in power, €/MW
q_{gis}^{gen}	Short-run marginal cost for electricity generation, €/MWh
q_{ni}^{ll}	Value of lost load, €/MWh

Availability parameters for stochastic data

$\xi_{nh\omega}^{\text{load}}$	Electricity demand, MWh
$\xi_{gh\omega}^{\text{gen}}$	Hourly available generator capacity, share of total installed capacity
$\xi_{p\omega}^{\text{RegHydroLim}}$	Max production from regulated hydro in seasonal period p , MWh
$\xi_{ni\omega}^{\text{HydroLim}}$	Max energy production from hydro at node n , MWh

Capacity parameters

$\bar{x}_{gi}^{\text{gen}}$	Initial generation capacity, MW
$\bar{x}_{li}^{\text{tran}}$	Initial transmission capacity, MW
$\bar{x}_{bi}^{\text{storPW}}$	Initial storage power capacity, MW
$\bar{x}_{bi}^{\text{storEN}}$	Initial storage energy capacity, MWh
$\bar{X}_{gi}^{\text{gen}}$	Max allowed investment in generation capacity, MW
$\bar{X}_{li}^{\text{tran}}$	Max allowed investment in transmission capacity, MW
$\bar{X}_{bi}^{\text{storPW}}$	Max allowed investment in storage power capacity, MW
$\bar{X}_{bi}^{\text{storEN}}$	Max allowed investment in storage energy capacity, MWh
$\bar{V}_{gi}^{\text{gen}}$	Max allowed accumulated investments in generation capacity, MW
$\bar{V}_{li}^{\text{tran}}$	Max allowed accumulated investments in transmission capacity, MW
$\bar{V}_{bi}^{\text{storPW}}$	Max allowed accumulated investments in storage power capacity, MW
$\bar{V}_{bi}^{\text{storEN}}$	Max allowed accumulated investments in storage energy capacity, MWh

Technical parameters

i_{*}^{life}	Life time for investment (* used to represent g, l or b), years
η_l^{tran}	Linear line efficiency where loss is $1 - \eta_l^{\text{tran}}$
η_a^{tran}	Linear line efficiency where loss is $1 - \eta_a^{\text{tran}}$
η_b^{chrg}	Storage charge efficiency
η_b^{dischrg}	Storage discharge efficiency
$\eta_b^{\text{roundtrip}}$	Storage round-trip efficiency

γ_g^{gen}	Generator ramp-up capability
ρ_b	Storage discharge to charge power capacity ratio
β_b	Storage power to energy capacity ratio
ϵ_{gi}	CO ₂ -emissions per unit of electricity, tons of CO ₂ per MWh
$\bar{E}_{i\omega s}$	Aggregated CO ₂ -emission limit, tons of CO ₂

Other parameters

r	Discount rate
θ	Five year scale factor where $\theta = \sum_{j=0}^4 (1+r)^{-j} = \frac{(1+r)^5 - 1}{r(1+r)^4}$
δ_i	Discount factor calculated as $(1+r)^{-5(i-1)}$
π_ω	Short-term scenario probability
π_s	Long-term scenario probability
α_p	Seasonal period scale factor

Decision variables

x_{gis}^{gen}	Generation capacity investments, MW
x_{lis}^{tran}	Line capacity investments, MW
x_{bis}^{storPW}	Storage power capacity investments, MW
x_{bis}^{storEN}	Storage energy capacity investments, MWh
v_{gis}^{gen}	Installed generation capacity, MW
v_{lis}^{tran}	Installed transmission capacity, MW
v_{bis}^{storPW}	Installed storage power capacity, MW
v_{bis}^{storEN}	Installed storage energy capacity, MWh
y_{gis}^{gen}	Electricity production, MWh
y_{ahis}^{flow}	Line electricity flow, MWh
y_{bhis}^{chrg}	Storage charge, MWh per h
$y_{bhis}^{\text{dischrg}}$	Storage discharge, MWh per h
y_{nhis}^{ll}	Lost load, MWh
w_{bhis}^{stor}	Storage energy content, MWh

5.3 Mathematical model formulation

This section introduces the mathematical formulation of the EMPIRE model including long-term uncertainty in detail. First, the objective function is presented in section 5.3.1, before the constraints of the model are presented in section 5.3.2-5.3.13.

5.3.1 Objective function

The EMPIRE model minimizes total expected system costs from a social planner perspective. This is done by minimizing the sum of expected investment costs and operational costs over the planning horizon, as described in equation (5.1):

$$\min z = \sum_{i \in \mathcal{I}} \delta_i \sum_{s \in \mathcal{S}} \pi_s \{ cost_{is}^{\text{inv}} + \theta \sum_{\omega \in \Omega} \pi_\omega cost_{i\omega s}^{\text{ops}} \} \quad (5.1)$$

where

$$\delta_i = (1 + r)^{-5(i-1)} \quad (5.2)$$

is a factor that discounts costs for each five-year time-stage to current monetary value. θ , as presented in section 5.2, is a factor that scales yearly operational costs to reflect the operational costs of all five years of operation between the investment stages.

In the objective function, $cost_{is}^{inv}$ denotes the total cost of investments in generation, transmission and storage capacity for a given investment stage $i \in \mathcal{I}$ and long-term scenario $s \in \mathcal{S}$. The operational dispatch in year i , short-term scenario $\omega \in \Omega$ and long-term scenario s , is denoted as $cost_{i\omega s}^{ops}$. The operational costs of each short-term scenario ω are weighted by the short-term probabilities π_ω , and the total investment costs and operational costs for each five-year period are weighted by the long-term probabilities π_s . Descriptions of these costs are presented in detail below.

Investment costs

Equation (5.3) gives the costs of investments in capacity expansion for a given investment stage $i \in \mathcal{I}$ and long-term scenario $s \in \mathcal{S}$.

$$cost_{is}^{inv} = \sum_{g \in \mathcal{G}} c_{gis}^{gen} x_{gis}^{gen} + \sum_{l \in \mathcal{L}} c_{lis}^{tran} x_{lis}^{tran} + \sum_{b \in \mathcal{B}} (c_{bis}^{storPW} x_{bis}^{storPW} + c_{bis}^{storEN} x_{bis}^{storEN}) \quad (5.3)$$

Capacity expansion can be done in either generators $g \in \mathcal{G}$, transmission lines $l \in \mathcal{L}$ or storages $b \in \mathcal{B}$. Capacity investments in generators and transmission lines are denoted by the decision variables x_{gis}^{gen} and x_{lis}^{tran} , respectively. For storage technologies the model takes into account investments in both power and energy capacity, and therefore these investment decisions are represented by the decision variables x_{bis}^{storPW} and x_{bis}^{storEN} , respectively.

Investment cost parameters are described by c_{gis}^{gen} , c_{lis}^{tran} , c_{bis}^{storPW} and c_{bis}^{storEN} . These costs include both the costs of building the infrastructure and the fixed operational and maintenance costs accumulated over the lifetime of the asset, and are discounted to the time stage corresponding to stage $i \in \mathcal{I}$. The total investment costs are allocated over the lifetime of a single asset, but adjustments are made such that investments made towards the end of the planning horizon are reduced to reflect the costs over the usable time in the model. All costs are assumed to be linear as a function of the invested amount.

Operational costs

$$cost_{i\omega s}^{ops} = \sum_{p \in \mathcal{P}} \alpha_p \sum_{h \in \mathcal{H}_p} \sum_{n \in \mathcal{N}} \left(\sum_{g \in \mathcal{G}_n} q_{gis}^{gen} y_{ghi\omega s}^{gen} + q_{ni}^{ll} y_{nhi\omega s}^{ll} \right) \quad (5.4)$$

Equation (5.4) gives the costs of operating the system in a given investment stage i , operational scenario $\omega \in \Omega$ and long-term scenario $s \in \mathcal{S}$. The amount of generation in each generator g , hour h , investment stage i , short-term scenario ω and long-term scenario s , accounted for by the decision variable $y_{ghi\omega s}^{gen}$, is multiplied by the short-run marginal cost q_{gis}^{gen} and added to the lost load term to yield the operational costs of the system. To keep track of the node of a specific generator, the sets $\mathcal{G}_n \forall n \in \mathcal{N}$ have been introduced,

containing the set of generators at each node. The lost load term consists of the value of lost load, q_{ni}^{ll} , and the amount of demand not being satisfied, denoted by the decision variable $y_{nhi\omega s}^{\text{ll}}$. Analyses of the value of lost load are presented in London Economics (2013).

The short-run marginal cost (SRMC), q_{gis}^{gen} , is composed of several different parameters; fuel costs, variable operational and maintenance costs (VOM), carbon emission costs and carbon capture, transportation and storage costs (CCTS). To keep the model formulation linear, the SRMC is assumed to be constant.

In the summation over the set of periods \mathcal{P} , the periodic scale factor α_p is included to account for the fact that the operational costs of a particular seasonal period should be weighted differently according to its representative share of an entire year. As an example: If one seasonal period covers one week of input data, and this week is assumed to be representative for three months of the year, the α_p parameter for that particular seasonal period will be set to $52 \cdot \frac{1}{4} = 13$. Note that the task of keeping track of the seasonal period of each operational hour in the model is being handled by an indexed set of hours for each period, denoted by \mathcal{H}_p .

5.3.2 Node flow balance

Constraint (5.5) enforces balance in the hourly system dispatch, as illustrated in Figure 2.2 in chapter 2:

$$\underbrace{\sum_{g \in \mathcal{G}_n} y_{ghi\omega s}^{\text{gen}}}_{\text{Generation}} + \underbrace{\sum_{b \in \mathcal{B}_n} \eta_b^{\text{dischrg}} y_{bhi\omega s}^{\text{dischrg}} - y_{bhi\omega s}^{\text{chrg}}}_{\text{Storage handling}} + \underbrace{\sum_{a \in \mathcal{A}_n^{\text{in}}} \eta_a^{\text{tran}} y_{ahi\omega s}^{\text{flow}} - \sum_{a \in \mathcal{A}_n^{\text{out}}} y_{ahi\omega s}^{\text{flow}}}_{\text{Net import}} \quad (5.5)$$

$$= \xi_{nhi\omega s}^{\text{load}} - y_{nhi\omega s}^{\text{ll}}$$

$$n \in \mathcal{N}, h \in \mathcal{H}, i \in \mathcal{I}, s \in \mathcal{S}, \omega \in \Omega$$

The constraint forces the net generation and the net imports to equal the load (less lost load) at a given node $n \in \mathcal{N}$, hour $h \in \mathcal{H}$, investment stage $i \in \mathcal{I}$, long-term scenario $s \in \mathcal{S}$ and short-term scenario $\omega \in \Omega$. The load balance is achieved through two main mechanisms; net generation and net imports.

Net generation

Net generation consists of the produced energy, denoted by $y_{ghi\omega s}^{\text{gen}}$, and the net energy discharge from storage. Net energy discharge is decided by the amount of energy discharged from a storage, $y_{bhi\omega s}^{\text{dischrg}}$, and the amount of energy charge, $y_{bhi\omega s}^{\text{chrg}}$. The technical parameter η_b^{dischrg} gives the discharging efficiency of a storage technology. For simplicity, the set \mathcal{B}_n has been introduced to describe the available storage technologies for a given node.

As presented in the objective function, the model also allows nodes to not satisfy parts of the load at a specific hour, represented by the decision variable $y_{nhi\omega s}^{\text{ll}}$. The cost of not satisfying all demand is penalized through the value of lost load in the objective function.

Net imports

Net imports consist of the amount of energy imported from other nodes less energy exported to other nodes. To simplify notation the sets $\mathcal{A}_n^{\text{in}}$ and $\mathcal{A}_n^{\text{out}}$ are defined, which denote transmission lines into and out from node n , respectively. In order to decide the unidirectional flow on these transmission lines, the decision variable $y_{ah\omega s}^{\text{flow}}$ is used. Since power transportation involves transmission losses, the model accounts for transmission losses in the importing node only, through the parameter η_a^{tran} .

5.3.3 CO2-emission constraints

As will be presented in larger detail in following chapters, the long-term uncertainty in the analyses in this thesis is introduced through stochastic constraints for CO2-emissions. The total emissions from the system in each five-year period i , long-term scenario s and short-term scenario ω are limited by the following constraints:

$$\sum_{p \in \mathcal{P}} \alpha_p \sum_{h \in \mathcal{H}_p} \sum_{g \in \mathcal{G}} \epsilon_{gi} y_{gh\omega s}^{\text{gen}} \leq \bar{E}_{i\omega s} \quad i \in \mathcal{I}, \omega \in \Omega, s \in \mathcal{S} \quad (5.6)$$

Constraint (5.6) states that the total amount of CO2-emissions in each long-term time-stage $i \in \mathcal{I}$ is limited by an exogenously fixed threshold. This limit is denoted $\bar{E}_{i\omega s}$ and states the total aggregated amount of CO2-emissions allowed in each time period, long-term and short-term scenario. ϵ_{gi} is a parameter that, for each generator g and each time-stage i , states the emissions per unit of electricity production. It is calculated from a heat rate stating how much fuel is needed to produce one unit of electrical energy, the CO2-content per unit of fuel, and a carbon capture and storage removal fraction for each generator.

5.3.4 Cumulative capacity restrictions

The cumulative capacity restrictions

$$v_{*is}^{**} = \bar{x}_{*is}^{**} + \sum_{j=i'}^i x_{*js}^{**}, \quad i' = \max\{1, i - \lfloor i_*^{\text{life}}/5 \rfloor\}, \quad i \in \mathcal{I} \quad (5.7)$$

are bookkeeping constraints that keep track of the total invested capacity for generation, transmission, storage power or storage energy. The **-superscript is a placeholder for either gen, tran, storPW or storEN, and the *-subscript is a placeholder for either g , l or b . The \bar{x}_{*i}^{**} -parameter keeps track of the remaining capacity of investments made before the planning horizon of the model. The summation in equation (5.7) adds to this parameter the cumulative investments made in previous investment stages that are yet to be fully retired. The summation starts either in the first investment stage or later to make sure retired capacity is not included in the available capacity for the different stages.

5.3.5 Storage technology constraints

The following constraints are bookkeeping constraints that couple storage levels in consecutive hours with storage charge and discharge during that hour. Note that constraints connecting operational hours from different seasonal periods are not enforced, in accordance with the multihorizon formulation of the model.

$$w_{b(h-1)i\omega s}^{\text{stor}} + \eta_b^{\text{chrg}} y_{bhi\omega s}^{\text{chrg}} - y_{bhi\omega s}^{\text{dischrg}} = w_{bhi\omega s}^{\text{stor}} \quad b \in \mathcal{B}, p \in \mathcal{P}, h \in \mathcal{H}_p^-, i \in \mathcal{I}, \quad (5.8)$$

$$\omega \in \Omega, s \in \mathcal{S}$$

The next constraints make sure the stored energy, the charge and the discharge of a storage are forced below their respective installed capacities.

$$w_{bhi\omega s}^{\text{stor}} \leq v_{bis}^{\text{storEN}}, \quad y_{bhi\omega s}^{\text{chrg}} \leq v_{bis}^{\text{storPW}}, \quad y_{bhi\omega s}^{\text{dischrg}} \leq \rho_b v_{bis}^{\text{storPW}}, \quad b \in \mathcal{B}, h \in \mathcal{H}, \quad (5.9)$$

$$i \in \mathcal{I}, \omega \in \Omega, s \in \mathcal{S}$$

5.3.6 Storage power and energy capacity coupling

The following constraint enforces a coupling between investments in storage energy capacity and storage power capacity. This is a technical restriction that applies to certain types of storages, such as certain types of batteries.

$$v_{bis}^{\text{storPW}} = \beta_b v_{bis}^{\text{storEN}}, \quad b \in \mathcal{B}, i \in \mathcal{I}, s \in \mathcal{S} \quad (5.10)$$

5.3.7 Generator dispatch availability

$$y_{ghi\omega s}^{\text{gen}} \leq \xi_{ghi\omega}^{\text{gen}} v_{gis}^{\text{gen}}, \quad g \in \mathcal{G} \setminus \{\mathcal{G}^{\text{Hydro}}\}, h \in \mathcal{H}, i \in \mathcal{I}, \omega \in \Omega, s \in \mathcal{S} \quad (5.11)$$

These constraints restrict the production from each generator, both through installed capacities and through availability parameters. For wind and solar generation, this is where operational stochasticity is introduced. The availability parameter $\xi_{ghi\omega}^{\text{gen}} \in [0, 1]$ temporarily reduces the available installed capacity in line with how varying weather conditions affect the ability of solar panels and wind turbines to generate power. For thermal generators, $\xi_{ghi\omega}^{\text{gen}}$ is a constant capacity factor for the given technology.

5.3.8 Thermal production ramp-up constraint

Ramping up thermal generators to full production requires some time, and this coupling between thermal generation in one hour and the next is enforced by the constraint

$$y_{ghi\omega s}^{\text{gen}} - y_{g(h-1)i\omega s}^{\text{gen}} \leq \gamma_g^{\text{gen}} v_{gis}^{\text{gen}} \quad g \in \mathcal{G}^{\text{Thermal}}, p \in \mathcal{P}, h \in \mathcal{H}_p^-, i \in \mathcal{I}, \quad (5.12)$$

$$\omega \in \Omega, s \in \mathcal{S}$$

$\gamma_g^{\text{gen}} \in (0, 1)$ is a ramp up parameter that determines the possible hourly increase in production as a share of total installed capacity for a given thermal generator. The set $\mathcal{G}^{\text{Thermal}}$ is a set containing all thermal generators. Note that also here, no constraints connecting operational hours from different seasonal periods are enforced, in accordance with the multihorizon formulation of the model.

5.3.9 Hydroelectric power generation constraint

Constraints on generation from hydro plants are modeled slightly different from the rest of the generation technologies. For regulated hydro, the total production during a seasonal period is limited by a stochastic parameter representing the total availability of water in the reservoirs during that period.

$$\sum_{h \in \mathcal{H}_p} y_{ghi\omega s}^{\text{gen}} \leq \xi_{gpi\omega}^{\text{RegHydroLim}}, \quad g \in \mathcal{G}^{\text{RegHydro}}, p \in \mathcal{P}, i \in \mathcal{I}, \omega \in \Omega, s \in \mathcal{S} \quad (5.13)$$

A stochastic limit is put on the total regulated and unregulated amount of energy production from hydropower in each node

$$\sum_{p \in \mathcal{P}} \alpha_p \sum_{h \in \mathcal{H}_p} \sum_{g \in \mathcal{G}_n^{\text{Hydro}}} y_{ghi\omega s}^{\text{gen}} \leq \xi_{ni\omega}^{\text{HydroLim}}, \quad n \in \mathcal{N}, i \in \mathcal{I}, \omega \in \Omega, s \in \mathcal{S} \quad (5.14)$$

5.3.10 Transmission flow constraints

The flow on installed transmission lines is limited to the capacity of the respective line through the following constraint

$$y_{ahi\omega s}^{\text{flow}} \leq v_{lis}^{\text{tran}}, \quad l \in \mathcal{L}, a \in \mathcal{A}_l, h \in \mathcal{H}, i \in \mathcal{I}, \omega \in \Omega, s \in \mathcal{S} \quad (5.15)$$

Here, \mathcal{A}_l is a mapping from a bidirectional line l to the tuple of unidirectional arcs a defined on that line.

5.3.11 Capacity investment constraints

The EMPIRE model enforces constraints on the amount of investments per five-year time-stage and the total accumulated generation, transmission and storage capacity in each of these stages to ensure realistic capacity expansion.

In equation (5.16), generation investments for a given investment stage i , node n and long-term scenario s are limited on an aggregated basis by the parameter $\bar{X}_{ti}^{\text{gen}}$, where t is an index stating the technological type of the generator and $\mathcal{T}^{\text{AggTech}}$ denotes a set of aggregated technologies. Similarly, in equation (5.17) the accumulated investments of the aggregated generation capacity is constrained by $\bar{V}_{tis}^{\text{gen}}$.

$$\sum_{g \in \mathcal{G}_{tn}} x_{gis}^{\text{gen}} \leq \bar{X}_{ti}^{\text{gen}}, \quad t \in \mathcal{T}^{\text{AggTech}}, n \in \mathcal{N}, i \in \mathcal{I}, s \in \mathcal{S} \quad (5.16)$$

$$\sum_{g \in \mathcal{G}_{tn}} v_{gis}^{\text{gen}} \leq \bar{V}_{ti}^{\text{gen}}, \quad t \in \mathcal{T}^{\text{AggTech}}, n \in \mathcal{N}, i \in \mathcal{I}, s \in \mathcal{S} \quad (5.17)$$

Transmission investments are limited in a similar manner by the parameter $\bar{X}_{li}^{\text{tran}}$, which limits the maximum allowed investments in a transmission line l for a specific period i , node n and scenario s . The accumulated capacity investments in transmission lines are also limited by $\bar{V}_{lis}^{\text{gen}}$.

$$x_{lis}^{\text{tran}} \leq \bar{X}_{li}^{\text{tran}}, \quad l \in \mathcal{L}, i \in \mathcal{I}, s \in \mathcal{S} \quad (5.18)$$

$$v_{lis}^{\text{tran}} \leq \bar{V}_{li}^{\text{gen}}, \quad l \in \mathcal{L}, i \in \mathcal{I}, s \in \mathcal{S} \quad (5.19)$$

Investments in storage capacity are limited by the parameters $\bar{X}_{bi}^{\text{storEN}}$ and $\bar{X}_{bi}^{\text{storPW}}$, which limits the maximum allowed investments in a storage technology b in a specific time-stage i and node n for each long-term scenario $s \in \mathcal{S}$. Similarly, the accumulated capacity investments in storage is limited by $\bar{V}_{bi}^{\text{storEN}}$ and $\bar{V}_{bi}^{\text{storPW}}$, respectively.

$$x_{bis}^{\text{storEN}} \leq \bar{X}_{bi}^{\text{storEN}}, \quad b \in \mathcal{B}, n \in \mathcal{N}, i \in \mathcal{I}, s \in \mathcal{S} \quad (5.20)$$

$$v_{bis}^{\text{storEN}} \leq \bar{V}_{bi}^{\text{storEN}}, \quad b \in \mathcal{B}, n \in \mathcal{N}, i \in \mathcal{I}, s \in \mathcal{S} \quad (5.21)$$

$$x_{bis}^{\text{storPW}} \leq \bar{X}_{bi}^{\text{storPW}}, \quad b \in \mathcal{B}, n \in \mathcal{N}, i \in \mathcal{I}, s \in \mathcal{S} \quad (5.22)$$

$$v_{bis}^{\text{storPW}} \leq \bar{V}_{bi}^{\text{storPW}}, \quad b \in \mathcal{B}, n \in \mathcal{N}, i \in \mathcal{I}, s \in \mathcal{S} \quad (5.23)$$

5.3.12 Nonanticipativity constraints

Due to the formulation choice of using a split variable formulation to include the long-term uncertainty in the EMPIRE model, nonanticipativity constraints are added explicitly to the model formulation. The nonanticipativity constraints ensure that all decision variables sharing common history are set to equal values, as discussed in Mirkhani and Saboohi (2012). Note that in the progressive hedging algorithm that will be presented in chapter 6, these constraints are relaxed.

$$x_{gis}^{\text{gen}} = x_{gis'}^{\text{gen}}, \quad g \in \mathcal{G}, \quad i \in \mathcal{I}, \quad s \in \mathcal{S}, \quad s' \in \{s\}_i \quad (5.24)$$

$$x_{lis}^{\text{tran}} = x_{lis'}^{\text{tran}}, \quad l \in \mathcal{L}, \quad i \in \mathcal{I}, \quad s \in \mathcal{S}, \quad s' \in \{s\}_i \quad (5.25)$$

$$x_{bis}^{\text{storEN}} = x_{bis'}^{\text{storEN}}, \quad b \in \mathcal{B}, \quad i \in \mathcal{I}, \quad s \in \mathcal{S}, \quad s' \in \{s\}_i \quad (5.26)$$

$$x_{bis}^{\text{storPW}} = x_{bis'}^{\text{storPW}}, \quad b \in \mathcal{B}, \quad i \in \mathcal{I}, \quad s \in \mathcal{S}, \quad s' \in \{s\}_i \quad (5.27)$$

The set $\{s\}_i$ defines the set of scenarios that are indistinguishable or equivalent to long-term scenario $s \in \mathcal{S}$ in time-stage $i \in \mathcal{I}$.

Due to the properties of the multihorizon formulation where operational decisions are independent of future long-term scenarios, it is not necessary to implement nonanticipativity constraints for the operational decision variables. Recall that since the operational decision variables can be viewed as embedded within the nodes of the long-term scenario tree in the multihorizon formulation, these decision variables are implicitly defined as functions of the investment decision variables and hence do not require designated nonanticipativity constraints.

5.3.13 Non-negativity constraints

Finally, non-negativity constraints are enforced for the decision variables:

$$x_{gis}^{\text{gen}} \geq 0, \quad g \in \mathcal{G}, \quad i \in \mathcal{I}, \quad s \in \mathcal{S} \quad (5.28)$$

$$x_{lis}^{\text{tran}} \geq 0, \quad l \in \mathcal{L}, \quad i \in \mathcal{I}, \quad s \in \mathcal{S} \quad (5.29)$$

$$x_{bis}^{\text{storEN}} \geq 0, \quad b \in \mathcal{B}, \quad i \in \mathcal{I}, \quad s \in \mathcal{S} \quad (5.30)$$

$$x_{bis}^{\text{storPW}} \geq 0, \quad b \in \mathcal{B}, \quad i \in \mathcal{I}, \quad s \in \mathcal{S} \quad (5.31)$$

$$v_{gis}^{\text{gen}} \geq 0, \quad g \in \mathcal{G}, \quad i \in \mathcal{I}, \quad s \in \mathcal{S} \quad (5.32)$$

$$v_{lis}^{\text{tran}} \geq 0, \quad l \in \mathcal{L}, \quad i \in \mathcal{I}, \quad s \in \mathcal{S} \quad (5.33)$$

$$v_{bis}^{\text{storPW}} \geq 0, \quad b \in \mathcal{B}, \quad i \in \mathcal{I}, \quad s \in \mathcal{S} \quad (5.34)$$

$$v_{bis}^{\text{storEN}} \geq 0, \quad b \in \mathcal{B}, \quad i \in \mathcal{I}, \quad s \in \mathcal{S} \quad (5.35)$$

$$y_{ghi\omega s}^{\text{gen}} \geq 0, \quad g \in \mathcal{G}, \quad h \in \mathcal{H}, \quad i \in \mathcal{I}, \quad \omega \in \Omega, \quad s \in \mathcal{S} \quad (5.36)$$

$$y_{ahi\omega s}^{\text{flow}} \geq 0, \quad a \in \mathcal{A}, \quad h \in \mathcal{H}, \quad i \in \mathcal{I}, \quad \omega \in \Omega, \quad s \in \mathcal{S} \quad (5.37)$$

$$y_{bhi\omega s}^{\text{chrg}} \geq 0, \quad b \in \mathcal{B}, \quad h \in \mathcal{H}, \quad i \in \mathcal{I}, \quad \omega \in \Omega, \quad s \in \mathcal{S} \quad (5.38)$$

$$y_{bhi\omega s}^{\text{dischrg}} \geq 0, \quad b \in \mathcal{B}, \quad h \in \mathcal{H}, \quad i \in \mathcal{I}, \quad \omega \in \Omega, \quad s \in \mathcal{S} \quad (5.39)$$

$$y_{nhi\omega s}^{\text{ll}} \geq 0, \quad n \in \mathcal{N}, \quad h \in \mathcal{H}, \quad i \in \mathcal{I}, \quad \omega \in \Omega, \quad s \in \mathcal{S} \quad (5.40)$$

$$w_{bhi\omega s}^{\text{stor}} \geq 0, \quad b \in \mathcal{B}, \quad h \in \mathcal{H}, \quad i \in \mathcal{I}, \quad \omega \in \Omega, \quad s \in \mathcal{S} \quad (5.41)$$

A Distributed Progressive Hedging Algorithm for Solving EMPIRE

This chapter presents a solution method proposed for solving the EMPIRE model based on the Progressive Hedging framework introduced in Rockafellar and Wets (1991). The progressive hedging algorithm (PHA) applied to solve multistage stochastic programs decompose the problem by scenario and propose an iterative algorithm for gradually obtaining solutions and updating dual variables, and is proven to converge towards the optimal solution for linear programs. The primary objective of this chapter is to show how the PHA is adapted to solve large-scale instances of the EMPIRE model in a distributed manner.

As discussed in chapter 4, other solution methods and decomposition algorithms exist that could have been applied to solve the EMPIRE model, such as the alternating direction method (Boyd et al., 2011) or the nested benders method (Murphy, 2013). However, the PHA is chosen as the preferred solution method in this thesis for three primary reasons. First, the EMPIRE model is originally implemented with a scenario or split-variable formulation for the long-term uncertainty. Consequently, a scenario based decomposition technique is simply a more convenient choice given the current implementation. Secondly, the PHA is highly applicable for distributed implementations, meaning that the subproblems can be solved in parallel and the required time for solving the problem can in that respect be significantly reduced. Finally, the PHA has substantial support in recent literature as a frequently applied solution method for large-scale multistage stochastic programs, particularly within problems related to energy and power system modeling, making it an interesting method for the purpose of this thesis (Gonçalves et al., 2012; dos Santos et al., 2009).

In section 6.1 an overview of the PHA is provided. The first part of the section focuses on presenting the preliminaries, assumptions and algorithmic notation of the procedure in itself, while the latter part focuses on how the PHA is applied to solve the EMPIRE model specifically. Procedures for obtaining upper and lower bounds for the optimal solutions are also provided, since classical methods implemented in commercially available solvers are incapable of solving many of the test instances in this thesis to optimality. Next, in

section 6.2, the focus is to present how the algorithm is implemented in a distributed manner, with the corresponding computational challenges and advantages that follow with this implemented code infrastructure.

6.1 The progressive hedging algorithm

The progressive hedging algorithm (PHA) is first introduced in Rockafellar and Wets (1991) and is a scenario-based decomposition algorithm used to solve large-scale stochastic optimization problems (Gade et al., 2016; Watson et al., 2007). The algorithm mitigates the computational complexity of large problem instances by decomposing the problem into scenarios and iteratively enforcing nonanticipative solutions by solving penalized versions of the subproblems. As such, the original problem is divided into smaller, solvable instances, and with a sufficient amount of iterations, the algorithm is proven to converge towards the optimal solution for linear programs (Rockafellar and Wets, 1991).

6.1.1 Preliminaries

Recall that the mathematical formulation of a multistage stochastic program, as presented in chapter 4, can be represented on the following form

$$\min \sum_{s \in \mathcal{S}} \pi_s f_s(\mathbf{x}_s) \quad (6.1)$$

$$\text{s.t. } \mathbf{x}_s \in \mathcal{F}_s \quad \forall s \in \mathcal{S} \quad (6.2)$$

$$\mathbf{x}_s \in \mathcal{F}_{NA} \quad \forall s \in \mathcal{S} \quad (6.3)$$

where $\pi_s f_s(\mathbf{x}_s)$ represents the probability-weighted objective function solved for scenario $s \in \mathcal{S}$, and \mathbf{x}_s is a vector representing all decision variables in scenario s . The decision variables \mathbf{x}_s are constrained to be in the feasible area defined by \mathcal{F}_s for scenario s , and must satisfy the nonanticipativity constraints defined in \mathcal{F}_{NA} . To illustrate, assume that the feasible area of each scenario looks as depicted in Figure 6.1, consisting of a block diagonal structure defined by constraints (6.2). The nonanticipativity constraints (6.3) complicates the block diagonal structure of the problem.

The complicating nonanticipativity constraints are natural barriers for decomposition because they couple decision variables across multiple scenarios. Therefore, by relaxing these constraints and implicitly accounting for them in the objective function, the block diagonal structure can be fully exploited and the problem can be decomposed into smaller, independent subproblems. Since the subproblems have independent feasible regions, each subproblem is both smaller in size and easier to solve than the original problem. In addition, since the subproblems are independent of each other, they can be solved in a decentralized manner in parallel to reduce the required time to solve the problem.

A way of implicitly accounting for the relaxed complicating constraints in the subproblems is to introduce dual multipliers and penalize deviations from the constraints with an augmented Lagrangian penalty term in the objective function (Conejo et al., 2006). The penalty term is based on dual multipliers \mathbf{w}_s and a constant ρ , and penalizes deviations

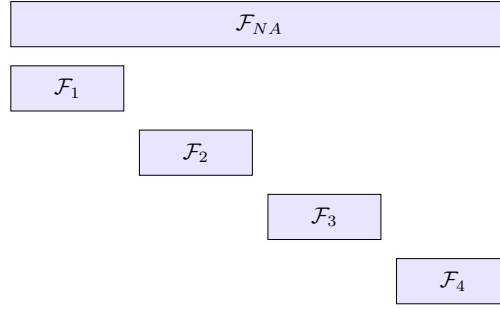


Figure 6.1: The structure of the feasible area of a stochastic program with complicating constraints. Note that if the constraints in \mathcal{F}_{NA} are relaxed, the remaining feasible area exhibits a block diagonal structure well suited for scenario based decomposition techniques.

in each subproblem's optimal decisions \mathbf{x}_s from nonanticipative solutions. The nonanticipative solution is defined as the expected value of the decision variables, denoted by $\bar{\mathbf{x}}_{\{s\}}$, where $\{s\}$ is the set of all indistinguishable scenarios for scenario s at each decision stage. Based on this, each subproblem solves the problem formulated as in (6.4) for a given scenario $s \in \mathcal{S}$:

$$\begin{aligned} \min f_s(\mathbf{x}_s) + \mathbf{w}_s^T(\mathbf{x}_s - \bar{\mathbf{x}}_{\{s\}}) + \frac{1}{2}\rho\|\mathbf{x}_s - \bar{\mathbf{x}}_{\{s\}}\|^2 \\ \text{s.t } \mathbf{x}_s \in \mathcal{F}_s \end{aligned} \quad (6.4)$$

Two issues arise with the formulation in (6.4). First, since the calculation of $\bar{\mathbf{x}}_{\{s\}}$ for each subproblem requires an optimization using decision variables from other scenarios, the problem is not separable. This property makes it hard to exploit decentralized methods for solving the problem. Secondly, in order to find the optimal solution, both optimal dual variables and the step length ρ must be determined. Therefore, deciding how to configure the optimal values of the dual variables and parameters is necessary.

To handle these two central issues, the PHA provides a framework for maintaining separability and a regime for dual multiplier updates. It coordinates an iterative search for the optimal decision variables that satisfies the nonanticipativity constraints. In order to cope with the problem of separability, the algorithm uses an approximation of the expected values of the decision variables from the previous iteration. This approximation is denoted as $\bar{\mathbf{x}}_{\{s\}}^{v-1}$, where v represents the current iteration, and can be interpreted mathematically as a projection of individual scenario solutions onto the subspace of nonanticipative solutions of the problem (Gade et al., 2016). Therefore, instead of co-optimizing decision variables across scenarios and subproblems, each subproblem only needs to optimize its designated and independent decision variables for the given scenario, resulting in separable subproblems. As such, the PHA can be interpreted as a separable approximation of the augmented Lagrangian method. To deal with the problem of finding optimal dual variables for a specific problem, the PHA defines an iterative update procedure for obtaining the optimal dual variables for a given ρ . The dual multipliers are updated at each iteration with a step length ρ so that $\mathbf{w}_s^v = \mathbf{w}_s^{v-1} + \rho(\mathbf{x}_s^{v-1} - \bar{\mathbf{x}}_s^{v-1})$. Based on these assumptions and

procedures, each subproblem can iteratively solve an independent and separable convex quadratic programming problem, as shown in formulation (6.5). Note that since $\mathbf{w}_s^T \bar{\mathbf{x}}_{\{s\}}^{v-1}$ now is defined as a constant term, it can be omitted from the objective function.

$$\begin{aligned} \min f_s(\mathbf{x}_s^v) + (\mathbf{w}_s^v)^T \mathbf{x}_s^v + \frac{1}{2} \rho \|\mathbf{x}_s^v - \bar{\mathbf{x}}_{\{s\}}^{v-1}\|^2 \\ \text{s.t } \mathbf{x}_s^v \in \mathcal{F}_s \end{aligned} \quad (6.5)$$

For each iteration of the PHA, solving formulation (6.5) yields an admissible solution for a specific subproblem, meaning that the obtained solution does not violate any constraints within a given scenario. The ultimate goal of the algorithm is to also produce an implementable solution, which refers to the quality that identical decisions are made in all scenarios as long as they share a common history, i.e. nonanticipativity across scenarios and subproblems is satisfied. This condition is achieved through a coordinated set of activities between the master- and subproblems defined in detail by the PHA, which is further explained in the remaining parts of this section.

6.1.2 Overview of the Progressive Hedging Algorithm

The PHA defines a procedure that iterates between admissible ($\mathbf{x}_s^v \in \mathcal{F}_s$) and implementable ($\mathbf{x}_s^v \in \mathcal{F}_{NA}$) solutions, and at convergence both of these properties are enforced to within a prespecified tolerance (Rockafellar and Wets, 1991). The algorithm can be summarized in six steps: (1) initialization of the problem, (2) solving the first iteration, (3) aggregation of decision variables, (4) check of convergence, (5) update of iterators and multipliers, and (6) resolving and repeating from step (3) until convergence is achieved. To give a conceptual overview of the algorithm, an illustration is given in Figure 6.2 with a detailed explanation of all included steps below.

Initialization and first iteration

The first step of the PHA is to initialize the iterator v and dual multipliers \mathbf{w}_s^0 to zero. The iterator v keeps track of the iterations and the dual multipliers are used in later steps of the algorithm. Next, each subproblem solves the formulation defined in (6.6) once for a given scenario $s \in \mathcal{S}$ with relaxed nonanticipativity constraints:

$$\begin{aligned} \min f_s(\mathbf{x}_s^0) \\ \text{s.t } \mathbf{x}_s^0 \in \mathcal{F}_s \end{aligned} \quad (6.6)$$

The intention of solving this problem is to obtain admissible scenario solutions which can be used in the next step of the algorithm. After the initialization, the algorithm enters a loop of iterations which do not terminate until a certain convergence requirement is met.

Aggregation of decision variables

The first step of the loop is conducted by the master problem and is an aggregation procedure applied to the decision variables received from the subproblems. The aggregation

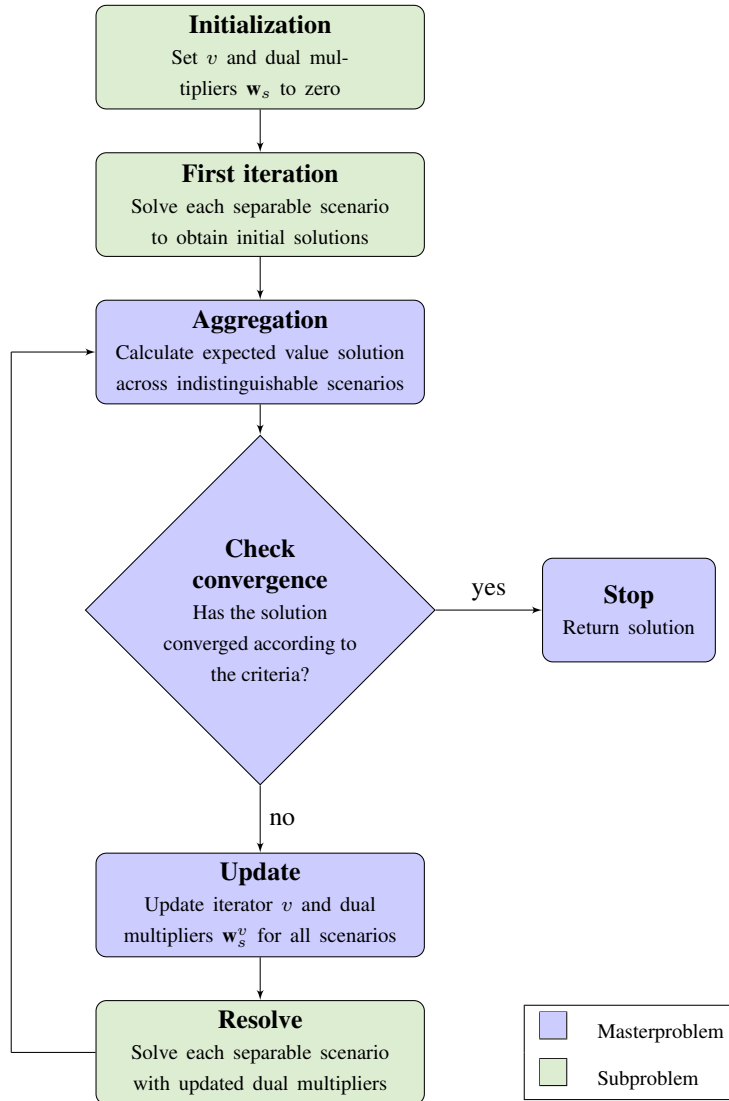


Figure 6.2: Conceptual overview of the progressive hedging algorithm

procedure generates a projection of the individual scenario solutions onto the subspace of nonanticipative solutions, where the projection is denoted as $\bar{\mathbf{x}}_{\{s\}}^v$. The projection is calculated as the probability-weighted sum of decision variables sharing the same node in the scenario tree, marginalized over these scenarios. For a given scenario $s \in \mathcal{S}$ at decision stage $i \in \mathcal{I}$ the projection can be calculated as in equation (6.7):

$$\bar{\mathbf{x}}_{s,i}^v = \frac{1}{\pi_{\{s\}_i}} \sum_{k \in \{s\}_i} (\pi_k \mathbf{x}_{k,i}^v) \quad \forall i \in \mathcal{I}, \quad \forall s \in \mathcal{S} \quad (6.7)$$

In equation (6.7) the set of all scenarios that are indistinguishable from scenario s at decision stage i is denoted as the set $\{s\}_i$. The probability for a specific scenario is denoted by π_s and the total probability of all indistinguishable scenarios to s at stage i is denoted by $\pi_{\{s\}_i} = \sum_{k \in \{s\}_i} \pi_k$.

Note that even though the aggregated solution $\bar{\mathbf{x}}_s^v$ clearly represents an implementable solution to the original problem, it does not necessarily represent admissible solutions for the individual scenario problems. The intention of this procedure is therefore to obtain an aggregated solution which can be used in later steps of the algorithm to either (1) verify if an obtained solution is both implementable and admissible within a prespecified tolerance, or (2) force the dual multipliers in a direction that pushes the subproblems closer to the optimal solution.

Check convergence

The second step of the loop is also conducted by the master problem and consists of checking whether the algorithm has converged within a prespecified tolerance ϵ . Convergence is achieved if the probability-weighted sum of absolute differences between the decision variables $\mathbf{x}_{s,i}^v$ and the corresponding aggregated variable $\bar{\mathbf{x}}_{s,i}^v$ are within an ϵ -criterion. This criterion is checked using equation (6.8):

$$\sum_{s \in \mathcal{S}} \pi_s \|\mathbf{x}_{s,i}^v - \bar{\mathbf{x}}_{s,i}^v\| < \epsilon \quad \forall i \in \mathcal{I} \quad (6.8)$$

Note that the comparison can be done either using Euclidean norms or elementwise comparison. If this criterion is satisfied, it indicates that the algorithm has reached an optimal solution that is both implementable within an ϵ tolerance of error and admissible for the individual scenarios. As a result, the algorithm can terminate and return the optimal solution. On the other hand, if the criterion is not met, the algorithm continues for yet another iteration.

The convergence criterion can also be defined such that the algorithm terminates when it reaches a prespecified optimality gap. However, as will be discussed in section 6.1.4 below, the process of obtaining upper and lower bounds from the algorithm requires the additional computational time and resources more or less equivalent to a standard iteration of the PHA. It is therefore cumbersome to apply this as a convergence criterion, and therefore an ϵ -tolerance of error as presented above is viewed as an equally good proxy for the convergence of the algorithm.

Update iterator and dual multipliers

In the third step of the loop, the iterator v is incremented and each subproblem updates its corresponding dual multipliers. The dual multipliers are used as inputs to the subproblems to gradually enforce nonanticipative solutions, and are updated according to the procedure described in equation (6.9):

$$\mathbf{w}_{s,i}^v \leftarrow \mathbf{w}_{s,i}^{v-1} + \rho(\mathbf{x}_{s,i}^{v-1} - \bar{\mathbf{x}}_{s,i}^{v-1}) \quad \forall s \in \mathcal{S}, i \in \mathcal{I} \quad (6.9)$$

In this context, ρ can be considered as a step length for the update procedure, indicating how much to penalize current deviations relative to the multiplier's previous value. A central issue related to the PHA is finding the optimal value of ρ . This is known to be a highly problem-specific issue (Gade et al., 2016; Watson and Woodruff, 2011; Watson et al., 2007), and will be further discussed in the context of the EMPIRE model specifically in chapter 8.

Resolve problem

The fourth and final step of the loop is to resolve each subproblem with the updated dual multipliers and the new aggregated solution from the master problem. Each subproblem solves the problem formulated in (6.5) for a specific scenario s , where deviations from nonanticipative solutions are implicitly accounted for through the included linear and quadratic penalty terms based on dual multipliers and the previous iteration's aggregate solution. When all subproblems are finished, the loop continues at the first step of the loop, i.e. aggregation of decision variables.

Summary of notation and algorithm

To summarize the algorithm, a detailed overview of the procedures in the PHA for a multi-stage stochastic program is given in algorithm 1. In addition, for the reader's convenience, a summary of all relevant notation used in the algorithm is given in Table 6.1.

Table 6.1: Sets, indices and variables for the progressive hedging algorithm

Sets and indices

\mathcal{I}	Set of decision stages indexed by i .
\mathcal{S}	Set of scenarios indexed by s
$\{s\}_i$	Set of all scenarios that are indistinguishable from scenario s at stage i
π	Set of probabilities π_s indexed by scenario s
$\pi_{\{s\}_i}$	Sum of probability of indistinguishable scenarios, $\pi_{\{s\}_i} = \sum_{k \in \{s\}_i} \pi_k$

Parameters

v	Progressive hedging iterator
ρ	Progressive hedging step length

Decision variables

- $\mathbf{x}_{s,i}^v$ Decision variables for scenario s at stage i in iteration v
 $\bar{\mathbf{x}}_{s,i}^v$ Aggregated decision variables for scenario s at stage i in iteration v
 $\mathbf{w}_{s,i}^v$ Dual multipliers for scenario s at stage i in iteration v

Algorithm 1: A progressive hedging algorithm for Multistage Stochastic Programs

Result: A solution satisfying implementability within an ϵ -criterion

- 1 **Initialization:**
 - 2 $v \leftarrow 0$ and $\mathbf{w}_{s,i}^v \leftarrow 0 \quad \forall s \in \mathcal{S}, i \in \mathcal{I}$
 - 3 **First iteration:**
 - 4 For $s \in \mathcal{S}$ compute $\mathbf{x}_s^0 = (\mathbf{x}_{s,1}^0, \dots, \mathbf{x}_{s,|\mathcal{I}|}^0) = \arg \min_{\mathbf{x}_s^0 \in \mathcal{F}^s} f_s(\mathbf{x}_s^0)$
 - 5 **Aggregation:**
 - 6 $\bar{\mathbf{x}}_{s,i}^v = \frac{1}{\pi_{\{s\}_i}} \sum_{k \in \{s\}_i} (\pi_k \mathbf{x}_{k,i}^v) \quad \forall i \in \mathcal{I}, \quad \forall s \in \mathcal{S}$
 - 7 **Check convergence:**
 - 8 If $\sum_{s \in \mathcal{S}} \pi_s \|\mathbf{x}_{s,i}^v - \bar{\mathbf{x}}_{s,i}^v\| < \epsilon \quad \forall i \in \mathcal{I}$ then stop
 - 9 **Iteration update:**
 - 10 $v \leftarrow v + 1$
 - 11 **Multiplier update:**
 - 12 $\mathbf{w}_{s,i}^v \leftarrow \mathbf{w}_{s,i}^{v-1} + \rho(\mathbf{x}_{s,i}^{v-1} - \bar{\mathbf{x}}_{s,i}^{v-1}) \quad \forall s \in \mathcal{S}, i \in \mathcal{I}$
 - 13 **Resolve:**
 - 14 For $s \in \mathcal{S}$ compute $\mathbf{x}_s^v = \arg \min_{\mathbf{x}_s^v \in \mathcal{F}^s} f_s(\mathbf{x}_s^v) + (\mathbf{w}_s^v)^T \mathbf{x}_s^v + \frac{1}{2} \rho \|\mathbf{x}_s^v - \bar{\mathbf{x}}_s^{v-1}\|^2$
 - 15 **Repeat:**
 - 16 Go to line 5
-

6.1.3 Applying the Progressive Hedging Algorithm to Solve EMPIRE

The split-variable formulation for representing long-term uncertainty, as presented in the version of the EMPIRE model in this thesis, exhibits a decomposable structure that can be advantageously exploited by the PHA. The feasible area of the model, as defined by constraints (5.5) - (5.41) in chapter 5, has a similar structure to the feasible area illustrated in Figure 6.1. While the nonanticipativity constraints defined for the long-term investment decisions represent the complicating constraints (5.24) - (5.27), the remaining constraints form a block-diagonal structure where none of the investment decision variables are coupled between the various long-term scenarios. Hence, by relaxing these nonanticipativity constraints, the feasible area can be decomposed by long-term scenarios and solved by applying the PHA.

In the multihorizon formulation of the EMPIRE model, operational decision variables can be viewed as embedded within the investment nodes in the long-term scenario tree. This implies that these variables neither require designated nonanticipativity constraints nor need to be explicitly accounted for in the PHA. This is because the operational decision variables are implicitly defined as functions of the investment variables. Consequently, if two scenarios share a common history up to a certain long-term decision stage and the obtained investment decisions from the PHA are implementable, then the relevant

operational decision variables must be implementable too. A practical implication of this property is that each subproblem only needs to include dual multipliers for the long-term investment variables.

Defining the subproblems for the PHA solving the EMPIRE model

When decomposing the EMPIRE model by long-term scenario, each subproblem solves a slightly modified version of the model for a particular scenario. The algorithm can also be implemented such that a bundle of multiple scenarios is solved in each subproblem, where the feasible region in each subproblem consists of the union of the included scenario's feasible regions, and nonanticipativity between the scenarios in the bundle is locally enforced. However, for simplicity, the remaining discussions assume that each subproblem solves one individual scenario. To illustrate the modified version of the EMPIRE model where a particular long-term scenario $s \in \mathcal{S}$ is solved in each subproblem of the PHA, the *objective function* of a particular subproblem is provided in equation (6.10):

$$\begin{aligned}
 z_s = \min \sum_{i \in \mathcal{I}} \delta_i \{ & \tag{6.10} \\
 & \underbrace{\sum_{g \in \mathcal{G}} c_{gis}^{\text{gen}} x_{gis}^{\text{gen},v} + \sum_{l \in \mathcal{L}} c_{lis}^{\text{tran}} x_{lis}^{\text{tran},v} + \sum_{b \in \mathcal{B}} (c_{bis}^{\text{storPW}} x_{bis}^{\text{storPW},v} + c_{bis}^{\text{storEN}} x_{bis}^{\text{storEN},v})}_{\text{Investment costs}} + \\
 & \underbrace{\sum_{g \in \mathcal{G}} w_{gis}^{\text{gen},v} x_{gis}^{\text{gen},v} + \sum_{l \in \mathcal{L}} w_{lis}^{\text{tran},v} x_{lis}^{\text{tran},v} + \sum_{b \in \mathcal{B}} (w_{bis}^{\text{storPW},v} x_{bis}^{\text{storPW},v} + w_{bis}^{\text{storEN},v} x_{bis}^{\text{storEN},v})}_{\mathbf{w}^T \mathbf{x}} + \\
 & \underbrace{\frac{1}{2} \rho * \left[\sum_{g \in \mathcal{G}} (x_{gis}^{\text{gen},v} - \bar{x}_{gis}^{\text{gen},v-1})^2 + \sum_{l \in \mathcal{L}} (x_{lis}^{\text{tran},v} - \bar{x}_{lis}^{\text{tran},v-1})^2 + \sum_{b \in \mathcal{B}} ((x_{bis}^{\text{storPW},v} - \bar{x}_{bis}^{\text{storPW},v-1})^2 + (x_{bis}^{\text{storEN},v} - \bar{x}_{bis}^{\text{storEN},v-1})^2) \right]}_{\frac{1}{2} \rho * \|\mathbf{x}^v - \bar{\mathbf{x}}^{v-1}\|^2} + \\
 & \underbrace{\theta \sum_{\omega \in \Omega} \pi_{\omega} \text{Cost}_{i\omega s}^{\text{ops}}}_{\text{Operational costs}} \}
 \end{aligned}$$

Equation (6.10) is tailored specifically for the EMPIRE model and is equivalent to the objective function in formulation (6.5). In the formulation $x_{*is}^{*,v}$ refers to the long-term investment decisions at iteration v , where an asterisk refers to either a generator $g \in \mathcal{G}$, a transmission line $l \in \mathcal{L}$ or a storage $b \in \mathcal{B}$ for scenario s at investment stage $i \in \mathcal{I}$. In

addition, δ_i is a discount factor, and $\theta \sum_{\omega \in \Omega} \pi_{\omega} cost_{i\omega s}^{ops}$ is the scaled expected operational costs for a set of short-term scenarios Ω at investment stage i . The PHA specific notation consists of the dual multipliers $w_{*is}^{*,v}$ (denoted without vector notation), the constant step length ρ , and the aggregated investment decision variable from the previous iteration $\bar{x}_{*is}^{*,v-1}$.

Defining the master problem for the PHA solving the EMPIRE model

The master problem is required to perform the aggregation procedure of the long-term investment variables, check for convergence at each iteration, update dual multipliers and to coordinate the activities in the subproblems. As discussed above, the aggregation procedure in the master problem is only necessary for the long-term investment variables. Hence, for a specific generator g , investment stage i and scenario s the aggregation procedure to obtain $\bar{x}_{gis}^{gen,v-1}$ can be performed as in equation (6.11). In each iteration, this calculation is made for all investment stages, all long-term scenarios and all generators, transmission lines, and storages. Note that equation (6.11) is similar for transmission lines l and storages b .

$$\bar{x}_{gis}^{gen,v-1} = \frac{1}{\pi_{\{s\}i}} \sum_{k \in \{s\}i} (\pi_k x_{gis}^{gen,v}) \quad (6.11)$$

Similarly, validating the convergence criterion is only necessary for the long-term investment variables. In equation (6.12) the procedure is exemplified for a particular generator g and investment stage i :

$$\sum_{s \in \mathcal{S}} \pi_s |x_{gis}^{gen,v} - \bar{x}_{gis}^{gen,v}| < \epsilon \quad (6.12)$$

If there exist one or more investment variables at a particular investment stage where the criterion in equation (6.12) is not satisfied for prespecified ϵ -tolerance, the PHA has by definition not converged, and the algorithm will continue for another iteration. However, when convergence is achieved, the algorithm terminates and returns the obtained solution as model output.

The obtained solution

A convenient property of the EMPIRE model is that the aggregated solution generated by the master problem at each iteration is both implementable and admissible. The reason for this is twofold: First, the long-term investment variables are only constrained by upper limits on investments in each investment stage, as presented in constraints (5.16) - (5.23) in chapter 5, and by the non-negativity constraints (5.28) - (5.41). It is therefore evident that a probability-weighted sum of these investments also will satisfy these constraints. Second, regardless of the available capacity determined by the investment decisions, the operational requirements can always be fulfilled through the option of increasing lost load in the solution. Therefore, the aggregated solution from the master problem is always a primal feasible solution that can be reported as a suggested solution obtained by the PHA.

6.1.4 Obtaining Optimality Bounds

Optimality bounds are useful when assessing the quality of a solution generated by the PHA. Knowledge of both upper and lower bounds of an obtained solution is particularly useful for instances of the EMPIRE model that are too large to handle for commercially available solvers where the optimal solution is unknown. Therefore, a method for finding both lower and upper bounds from the PHA solving the EMPIRE model is provided.

Obtaining lower bounds

In Gade et al. (2016) a method for obtaining lower bounds (LB) for the PHA applied to mixed integer problems is presented. The same procedure is applied in this thesis to obtain lower bounds for the solutions obtained by the PHA for the EMPIRE model. For a given set of dual multipliers, the lower bound can be calculated by solving the optimization problem given in (6.13):

$$z^{LB} = \min \sum_{s \in \mathcal{S}} \pi_s (f_s(\mathbf{x}_s^v) + \mathbf{w}_s^T (\mathbf{x}_s^v - \bar{\mathbf{x}}_s^v)) \quad (6.13)$$

$$\text{s.t } \mathbf{x}_s^v \in \mathcal{F}_s \quad \forall s \in \mathcal{S}$$

This lower bound can be calculated in any iteration of the PHA. However, the calculation requires the additional computational resources more or less equivalent to a standard iteration of the PHA, the only difference being that the objective function in the lower bound calculation does not include a quadratic term. The produced bound is specific for a given set of dual multipliers \mathbf{w}_s^v and aggregated solution $\bar{\mathbf{x}}_s^v$.

Obtaining upper bounds

An upper bound is the best known solution to the primal problem. As argued above, the aggregated long-term investment variables generated by the master problem in each iteration is, in fact, a valid primal solution. Therefore, by re-optimizing the original problem with all investment variables fixed to their aggregated value produced by the master problem in the PHA, an upper bound can be found at any iteration of the algorithm. This requires similar computational resources to the calculation of a lower bound and can be calculated at any iteration of the algorithm.

Defining the optimality gap

In this thesis, two definitions of optimality gaps are used to assess the quality of the obtained solutions. In cases where the optimal objective value of a certain test instance is known, the relative gap from the upper bound (ub) and the optimal solution (z^*) is provided. This gap is calculated as in equation (6.14):

$$\text{Gap}(ub \text{ to } z^*) = \frac{ub - z^*}{ub} \quad (6.14)$$

In cases where the optimal cost is unknown, the relative gap between the upper bound (ub) and the lower bound (lb) is given. This gap is calculated as in equation (6.15):

$$\text{Gap } (ub \text{ to } lb) = \frac{ub - lb}{ub} \quad (6.15)$$

Both gaps are expressed as a percentage. The upper bound is used in both cases to express the relative difference, because this is the optimal solution generated by the algorithm which would have been communicated as the final solution produced by the PHA.

6.2 A distributed implementation of the algorithm

In the PHA there is a clear distinction between the procedures performed by the master and subproblems. This is illustrated in the conceptual overview of the algorithm in Figure 6.2. Since each subproblem solves a problem for an individual scenario that is independent of all other scenarios, the subproblems can be solved in parallel at each iteration. This is beneficial because it allows for significant reductions in the elapsed time required for solving an iteration of the algorithm, particularly if the alternative is to solve the subproblems sequentially. In the remaining parts of this chapter, the objective is to introduce how a distributed version of the PHA is implemented, along with giving a brief overview of important concepts and terms relevant for the thesis.

6.2.1 A Distributed Memory Infrastructure

In general, parallel programs can be designed as shared memory or distributed memory programs (Pacheco, 2011). Because of the significant computational resources in terms of memory availability and CPU processing capacity required to solve a single subproblem when the PHA is used to solve the EMPIRE model, the discussion regarding parallel programming in this thesis is limited to distributed memory programming. A distributed memory system consists of a collection of core-memory pairs (i.e. processors) connected by a network. Each core-memory pair can perform independent computations, but the memory associated with an individual core is directly accessible only to that core. Therefore, all communication and exchange of information between the cores need to be implemented through a message-passing system.

The standard implementation of message-passing is called Message-Passing Interface (MPI), which is a library of functions enabling collective communication between processes in a distributed memory system. For a complete introduction to MPI programming see Pacheco (2011). A central benefit of a distributed memory system utilizing message-passing through MPI is the possibility of parallelization of the program across a distributed set of nodes on a High-Performance Computing (HPC) cluster. This implies that the available resources are no longer constrained by the limited resources on a local machine, but rather by the combined resources across all nodes in the cluster connected by MPI. Today there exist multiple implementations of MPI with support for most programming languages. One of the most frequently used implementations for MPI in distributed memory programming is the open-source version OpenMPI for the C programming language. This is also the implementation applied in this thesis.

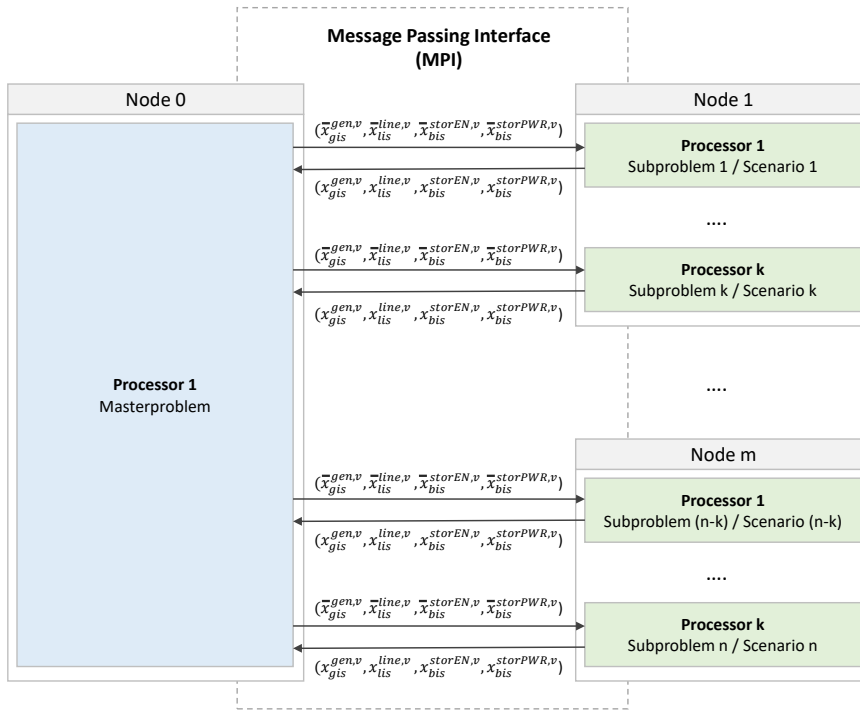


Figure 6.3: Overview and illustration of the distributed implementation of the PHA on a set of $m + 1$ nodes each with k independent processors of a problem instance of the EMPIRE model with n scenarios solved by n subproblems and one master problem. The illustration assumes that each subproblem is designated to a particular processor.

In the distributed implementation of the PHA, both the master problem and each of the subproblems are allocated to dedicated processors both within and across nodes in the HPC-cluster. Consequently, since the problems are physically separated from each other, they utilize MPI for exchanging information about long-term investment variables and dual multipliers during the course of the PHA. The subproblems utilize MPI to send obtained, admissible investment variables to the master problem after an iteration, and the master problem utilizes MPI to send updated dual multipliers and aggregated, implementable investment variables to the subproblems. The process of coordination and communication between the master problem and the subproblems is illustrated in Figure 6.3. The figure also shows how the implemented master- and subproblems are organized in terms of the distributed memory infrastructure, here depicted with n subproblems each solving an individual scenario and $m + 1$ nodes each with k independent available processors. Note that the algorithm implements a bidirectional communication process as all master- and subproblems communicate both ways. Also, none of the subproblems require communication with each other in this implementation.

6.2.2 Expected Performance Gain of the Distributed Implementation

The expected performance gain of a distributed implementation of the algorithm relative to a sequential implementation relates to (1) memory efficiency and (2) expected reduction in computational time to solve the problem. In a distributed implementation, the subproblems are solved and stored in RAM in a decentralized manner at separate memory locations. Since the memory requirements for a single subproblem is much smaller than the sum of memory requirements for all the subproblems, a distributed implementation allows for higher memory efficiency while solving the same problem, though at the cost of distributed resources and time spent on input/output operations.

The most significant performance gain of a distributed implementation compared to a sequential implementation is the achieved reductions in computational time spent on solving the problem. Assume the computational time of the fully serialized implementation of the program is denoted as T_{serial} and the computational time of the distributed implementation is denoted as $T_{parallel}$. Then the obtained speedup S of the distributed program is defined as in equation (6.16):

$$S = \frac{T_{serial}}{T_{parallel}} \quad (6.16)$$

If p processors are available, then the best possible speedup of the distributed implementation is when $T_{parallel} = \frac{T_{serial}}{p}$, or equivalently $S = p$. If this is the case, the distributed program has obtained *linear speedup*, which happens for the distributed implementation of the PHA if p is equal to the number of subproblems.

Another element that has a significant impact on the computational time required to solve a distributed program is whether it is synchronous or asynchronous. While an asynchronous program can operate in its own pace, synchronous programs must wait until all processes have reached a particular stage in the execution cycle before any process can continue from that stage. The characteristics of such programs are illustrated in Figure 6.4. The PHA for solving the EMPIRE model is implemented as a synchronous program. This is due to the aggregation procedure and convergence verification in the master problem, which requires that the long-term investment variables have been received from all subproblems at each iteration.

In theory, the computational time required to solve two single subproblems of the PHA of identical size should take approximately the same time at any two processors with the same technical specifications. In practice, however, this is often not the case. In chapter 8 this property is shown to be a major challenge for computational time when executing code on a shared HPC-cluster. Transforming the current method into an asynchronously distributed program is, therefore, an interesting topic for further research.

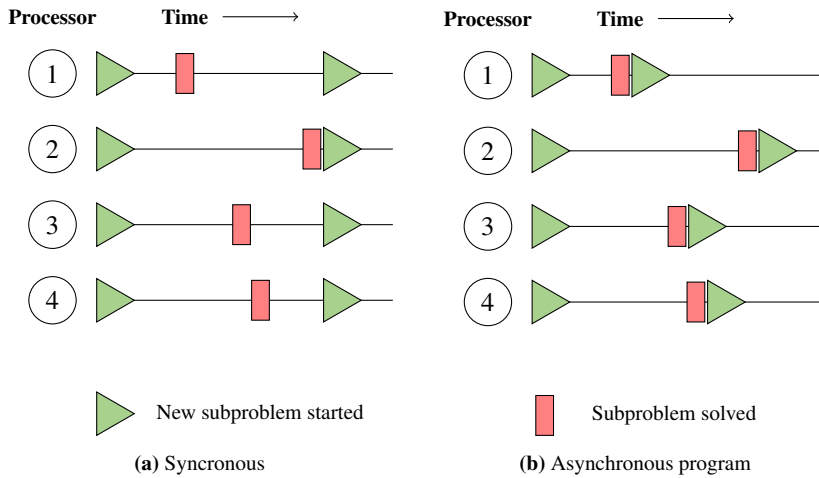


Figure 6.4: Synchronous versus asynchronous parallel program.

Model Data

A central part of analyzing the LSSCEPPS with the EMPIRE model is the data given as exogenous inputs. The objective of this chapter is to establish an understanding of the input data used in the remaining part of this thesis, with a particular emphasis on describing the implemented scenario generation procedures for short- and long-term uncertainty. In section 7.1 some of the most important data used for the analyses conducted in chapter 8 and 9 is presented. In section 7.2 the procedure for generating short-term scenarios is described, while section 7.3 presents the applied procedure for creating long-term scenarios.

7.1 Model inputs

The input data used in the studies conducted in this thesis is collected from multiple sources. To establish the conditions for the long-term dynamic developments in the model, the EU reference case published in 2016 by the European Commission (EU Reference Scenario, 2016) is used as a primary source. This reference case describes trends and scenarios within energy, transportation and greenhouse gas emissions until 2050 for the 28 member states of the EU. In Figure 7.1 the long-term developments in fuel prices and total demand from 2010 to 2050 provided by this source is presented. Note that long-term investment time-stages of five years are used in this thesis, meaning that long-term input data is provided for every fifth year from 2010-2050.

Other input data, such as assumed developments in investment costs for generation technologies, are gathered from other sources, such as ZEP (2013). In Figure 7.2 the investment costs for solar capacity, wind capacity and battery energy capacity is presented. The assumed investment costs, fixed operational and maintenance costs, variable operational and maintenance costs, thermal generator efficiency, carbon capture, transport and storage costs, derived short-run marginal costs and initial capacities for all relevant technologies is provided in the appendix, ensuring reproducible results.

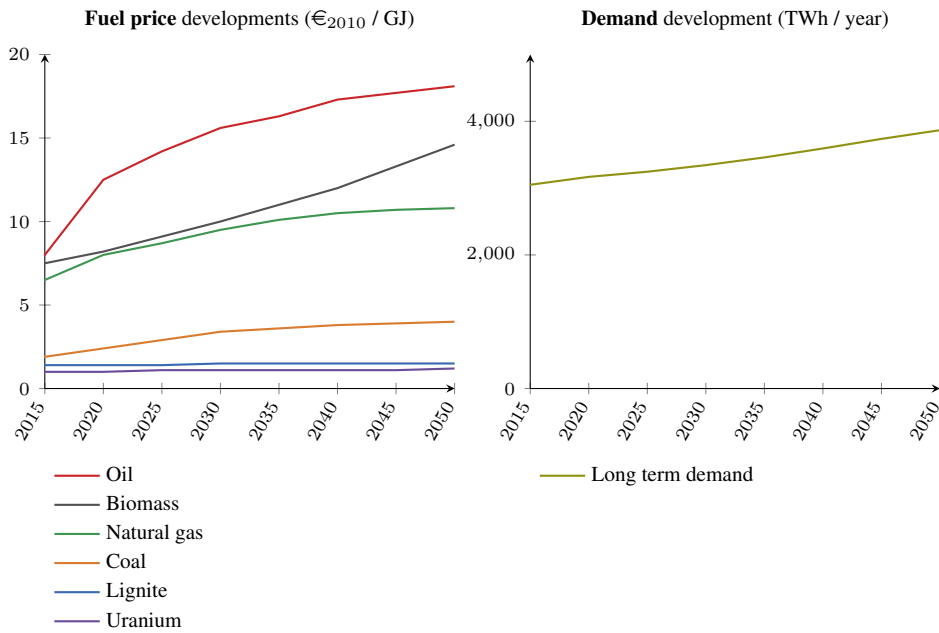


Figure 7.1: Assumed fuel price and electricity demand development in Europe from 2010-2050.

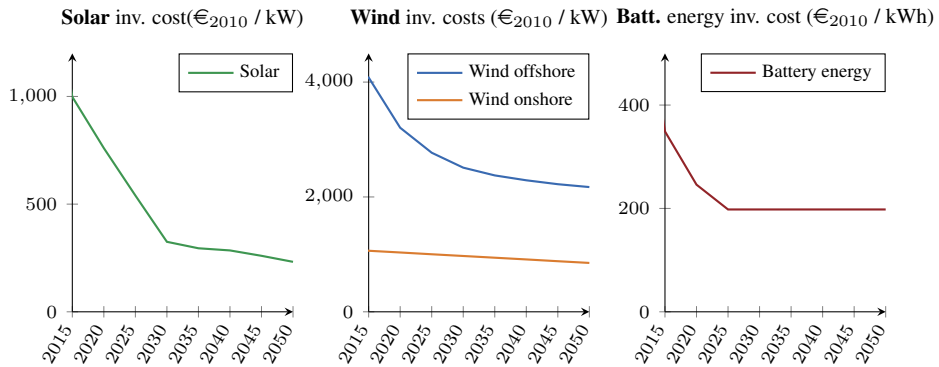


Figure 7.2: Assumed development in technology investment costs from 2010-2050 for solar, wind and battery energy capacity.

7.2 Procedure for generating short-term scenarios

In this section, the procedure used for generating short-term scenarios for the uncertain operational input parameters to the model is presented. This method is based on the scenario generation procedure presented in Skar et al. (2016), but has been extended in two ways: First, the use of different short-term scenario trees in each long-term time-stage has been implemented, and second, moment matching has been introduced in the procedure to improve the quality of the obtained scenario trees. As discussed in chapter 4, the main intention of assessing several different operational scenarios is to capture the short-term dynamics and uncertainty of the power system, preventing the model from tailoring the solution to a particular scenario. The goal of the generation procedure is to obtain a representative sample of the uncertain short-term inputs, hence enabling the model to account for operational fluctuations when making long-term investment decisions. For this reason, the short-term scenario tree is generated as a simple two-stage tree where investments are the first stage decisions and the operational decisions are the recourse actions made under *operational* perfect foresight. In addition, to ensure representative data sets, seasonal periods are used to divide the operational year into disjoint subsets. Each subset represents a particular time of the year, and by sampling data from each seasonal period of the year, the probability of obtaining biased samples is greatly reduced. As discussed in chapter 5, the scenarios are made up of both regular and extreme seasonal periods, where the former make up most of the representative hours in the data sets and the latter is introduced to ensure feasibility of the model even in extreme scenarios.

As discussed in chapter 4, short-term uncertainty can be included in several different input parameters to power system models. In this thesis short-term uncertainty has been included in four different inputs:

1. Electricity load
2. Solar PV generation
3. Wind generation
4. Rain inflow to hydro reservoirs and run-of-the-river generation plants

The short-term scenarios are generated by selecting several random subsets of historical time series of the desired length for each parameter, followed by utilizing statistical methods to choose the sample that best matches the first four moments of the entire time series (i.e. the mean, variance, skewness and kurtosis). This procedure is repeated for each new scenario included and for every long-term time stage, meaning that different short-term scenario trees are used in each five-year period. By sampling data from the exact same time periods for all uncertain parameters, as illustrated in Figure 7.3, both autocorrelations within time series and correlations between time series for different parameters are preserved. The colored parts of the data series in the figure also illustrate a possible example scenario for the uncertain short-term input parameters used in the EMPIRE model.

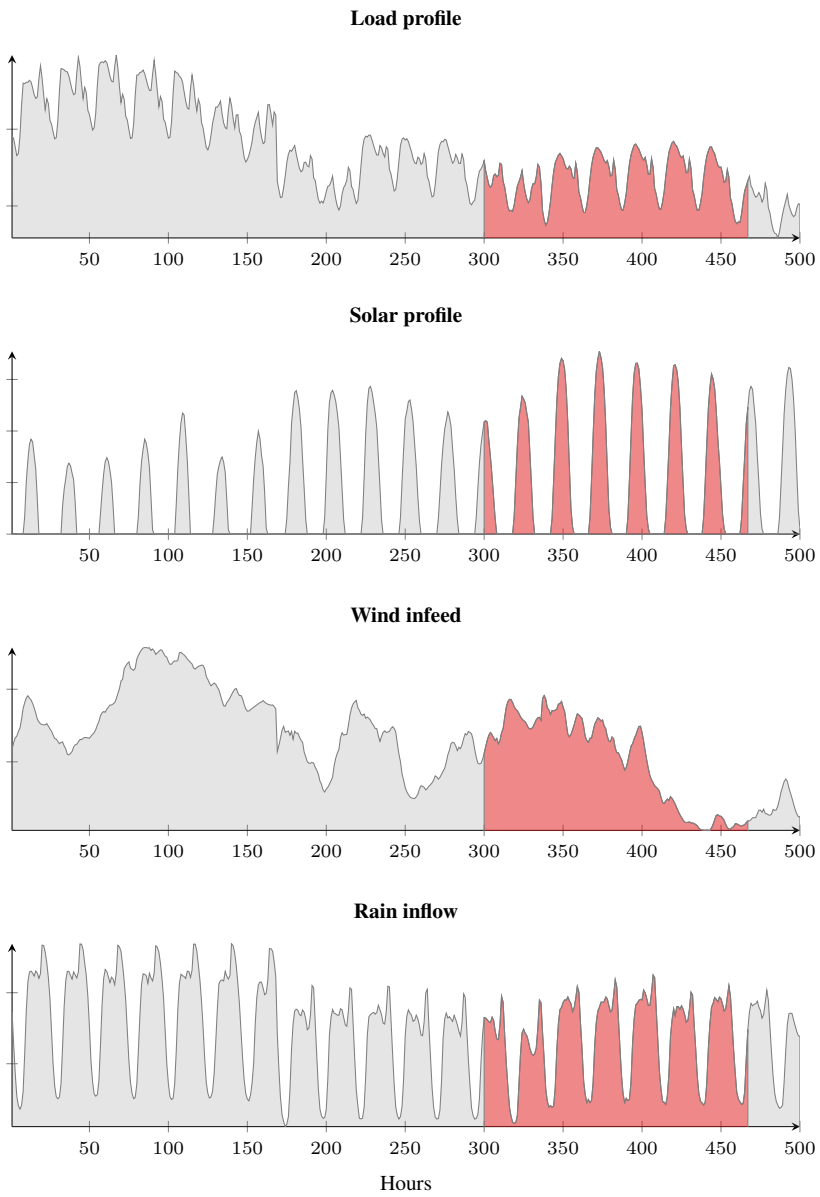


Figure 7.3: Illustration of short-term scenario sampling with hours on the x-axis. Note that sampling from the same consecutive time periods for all uncertain parameters preserves both autocorrelations within and correlations between the sampled scenarios.

7.2.1 Notation and pseudocode for the scenario generation procedure

A detailed overview of the procedure for generating short-term scenarios for the regular seasonal periods is presented in algorithm 2. Before the procedure for the scenario generation is presented, some notation is introduced in Table 7.1.

Table 7.1: Sets and parameters for the short-term scenario generation procedure

Sets and indices

\mathcal{Y}	Set of years for which historical time series are available, indexed by y .
$\mathcal{H}^{\text{full}}$	Set of all hours in a year, with range $[1, 8760]$.
$\mathcal{P}^{\text{full}}$	Set of full seasonal periods within a historical year indexed by p .
$\mathcal{H}_p^{\text{full}}$	Set of hours in full seasonal period p , $\forall p \in \mathcal{P}^{\text{full}}$.
Ω	Set of short-term scenarios indexed by ω .
\mathcal{I}	Set of investment decision stages indexed by i .

Parameters

$\theta_{*hy}^{\text{param}}$	Raw data from historical data series. $h \in \mathcal{H}^{\text{full}}$, $y \in \mathcal{Y}$.
$\xi_{*hi\omega}^{\text{param}}$	Stochastic input parameter for the EMPIRE model. $h \in \mathcal{H}^{\text{full}}$, $i \in \mathcal{I}$, $\omega \in \Omega$.
l	Number of hours in each regular seasonal period p .
K	Number of sample scenario trees generated before moment matching.

Algorithm 2: Short-term scenario generation routine for regular seasonal periods

Result: Set of K scenario trees with $|\Omega|$ scenarios per scenario tree for each five-year investment stage

```

1 initialization;
2 Inputs:  $l, K$  ;
3 for each five-year time-stage  $i \in \mathcal{I}$  do
4   for  $k \in \{1, \dots, K\}$  do
5     for each short-term scenario  $\omega \in \Omega$  do
6       Select a random year  $y \in \mathcal{Y}$ ;
7       for each season  $p \in \mathcal{P}^{\text{full}}$  do
8         Sample a random number  $h_p$  in the range  $[1, \frac{8760}{|\mathcal{P}^{\text{full}}|} - (l + 1)]$ ;
9         for  $j \in \{1, \dots, l\}$  do
10           $h = j + l \cdot (p - 1)$ ;
11           $h' = h_p + (j - 1)$ ;
12           $\xi_{*hi\omega}^{\text{param},k} \leftarrow \theta_{*h'y}^{\text{param},k}$  ;
13        end
14      end
15    end
16  end
17 end
```

In the work with this thesis, the scenario generation procedure has been implemented in Matlab. The scenario trees are generated using data from $|\mathcal{Y}|$ different historical years. The raw data from these time series is denoted by $\theta_{*hy}^{\text{param}}$, where param refers to a particular uncertain parameter, i.e. either solar, wind, load or rain. The * is a particular identifier for the given parameter, e.g. for solar it would be a particular solar plant, and for load it would be a country. The set $\mathcal{H}^{\text{full}}$ consists of the range $[1,8760]$, hence leap-years are neglected. This set is partitioned into $|\mathcal{P}^{\text{full}}|$ seasonal periods, denoted by $\mathcal{H}_p^{\text{full}}$, $p \in \mathcal{P}$. The size of the sets $\mathcal{H}_p^{\text{full}}$ is then simply $\frac{8760}{|\mathcal{P}^{\text{full}}|}$. This partitioning is done to ensure that representable input data from the entire course of the historical years is used as input to the model.

The result of algorithm 2 is one set of K scenario trees with $|\Omega|$ scenarios for each five-year investment stage i . After this procedure has been performed, moment matching is used on the K scenario trees for each five-year stage i to find the one that best matches the statistical properties of the historical data series. The moment matching is done by calculating the total sum of the absolute value of relative differences in the mean, variance, skewness and kurtosis between scenario tree k and the entire historical data series. The scenario tree that best matches the four moments, i.e. that obtains the lowest sum in the above calculation, is kept and used as input data for that time-stage i . This procedure is repeated for each five-year investment stage $i \in \mathcal{I}$, resulting in $|\mathcal{I}|$ scenario trees with optimized moments.

To ensure feasibility in peak periods of load, extreme seasonal periods are generated by selecting a random year $y \in \mathcal{Y}$ and finding

$$h_y^{\text{extreme load}} = \arg \max_h \sum_{n \in \mathcal{N}} \theta_{nh_y}^{\text{load}} \quad (7.1)$$

i.e. the historical hour in year y where the total load in the entire European power system reached its highest value. An extreme season can then be obtained by finding the full historical day that $h_y^{\text{extreme load}}$ is a part of, and using data from these 24 hours as an extreme season.

To generate the input data for the test instances studied in the computational study in chapter 8 and the techno-economic analyses in chapter 9, the short-term scenario generation procedure presented has been applied to generate three different short-term scenario trees – the first with two scenarios and 72 operational hours (1 regular seasonal period of 24 hours and 2 extreme seasons of 24 hours each, for a total of 3 full days) in each scenario, the second with three scenarios and 240 operational hours (4 regular seasonal periods of 48 hours and 2 extreme seasons of 24 hours each, for a total of 10 full days) in each scenario, and the third with three scenarios and 720 operational hours (4 regular seasonal periods of 168 hours and 2 extreme seasons of 24 hours each, for a total of 30 full days) in each scenario. All three will be used in the computational study in chapter 8 to verify the performance of the implemented PHA for different scenario trees, while the techno-economic analyses in chapter 9 will be performed using the third scenario tree with three scenarios and 720 consecutive hours in each scenario.

7.3 Strategy for generating long-term scenario trees

In this section, the strategy for generating long-term scenario trees for the EMPIRE model is presented. Even though the EMPIRE model and the solution method presented in this thesis is generalized to any form of long-term uncertainty, this section intends to show long-term scenario generation procedures for policy uncertainty specifically. The political uncertainty is implemented through stochastic restrictions on the total amount of allowed CO₂-emissions across Europe per five-year time-stage $i \in \mathcal{I}$ in each short-term scenario $\omega \in \Omega$ and long-term scenario $s \in \mathcal{S}$. The limits are denoted by $\bar{E}_{i\omega s}$ in the mathematical formulation.

As discussed in chapter 4 the procedures for generating scenario trees to represent long-term uncertainty are described much more as an art than a science, and should therefore be viewed as guidelines or strategies instead of exact methods. Although no unified framework for creating these scenario trees has been observed in the relevant literature, some examples of scenario trees for long-term uncertainty in emission restrictions have been found.

In Condevaux-Lanloy and Fragnière (2000) uncertainty related to CO₂-emission constraints is studied using the SETSTOCH-tool for energy and environmental planning. They implement in total three long-term scenarios; one stringent scenario where emissions are drastically limited with probability 0.5, one moderate in-between scenario with probability 0.2 and one "business as usual"-scenario where no emission constraints are enforced, with probability 0.3.

Uncertainty in emission reduction constraints is also introduced in Laia et al. (2014), where a unit commitment model is used to maximize expected profits for a price-taking production agent when scheduling energy generation. Here, three different scenarios for stochastic emission constraints are included; a baseline scenario level, one scenario with upper limits on the emission of 20% higher than the baseline scenario, and one scenario with upper limits 20% lower than the baseline scenario. A uniform, discrete probability distribution is applied.

Investments in the Belgian energy system in the context of uncertainty about the maximum annual CO₂-emissions allowed is studied in Aertsens et al. (1999). Four different scenarios with equal probabilities are applied, where the average CO₂ emissions up until 2030 are to be reduced by differing amounts. In the first scenario there are no emission constraints, and in the three last scenarios, the average annual emissions are limited to 0%, 8% and 25% below 1990 levels, respectively.

As these three examples depict, different approaches are used in the research literature when generating long-term scenario trees for emission reductions. Both uniform and non-uniform probability distributions are used, and both symmetric and non-symmetric scenario trees are observed.

In the scenario trees used in the analyses in this thesis, communicated EU targets are used as guidelines to anchor the expected value of the scenario trees. That is, the expected values of the scenario trees used are in line with an 80% reduction of CO₂ emissions in the European power system until 2050 compared to 1990 levels. From this baseline, scenarios are created by allowing policies to deviate from this trend in each branching stage of the scenario tree. Supported by the assertion in Trutnevyte (2013) that maximally different scenarios should be assessed to get a grasp of the possible outcome space, an attempt to

Scenario tree with 27 scenarios

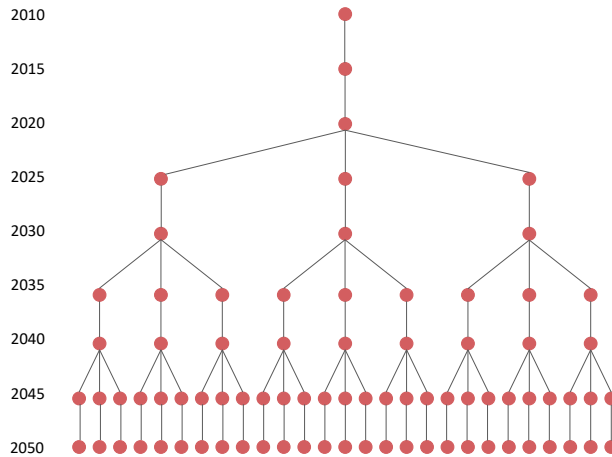


Figure 7.4: Scenario tree with 27 long-term scenarios. In each branching stage, three new branches emerge, corresponding to a branching factor of 3. Branching happens in 2020, 2030 and 2040. Note that due to the multihorizon formulation, the operational periods can be viewed as embedded within the investment nodes and are left out in this figure.

span a large part of the outcome space has been made. Note that no attempts at modeling autocorrelations between different time-stages of the long-term scenario tree have been made, implying an assumption of independence between time-stages.

The procedure for generating the long-term scenario trees used in the analyses in chapter 8 and 9 goes as follows: First, define a branching factor that indicates the number of branches in each branching stage in the scenario tree. In the test instances, a branching factor of either two or three has been used, meaning that in each branching stage two or three different developments in the emission limit for the next stages emerge. Second, choose the branching stages, i.e. the five-year stages where branching in the scenario tree will happen. For the scenario trees used in this thesis, 4 scenarios correspond to a branching factor of two and branching in stage 3 and 5 (corresponding to 2020 and 2030, respectively). For the scenario tree with 8 scenarios, a branching factor of two and branching in stage 3, 5 and 7 has been used, i.e. branching stages corresponding to 2020, 2030 and 2040. For the scenario tree with 27 scenarios, a branching factor of three and branching in stage 3, 5 and 7 has been applied. The scenario tree with 81 scenarios is similar to the one with 27 scenarios, only extended with an additional branching in stage 8 (corresponding to 2045). In Figure 7.4 the scenario tree for 27 scenarios has been illustrated. In chapter 9 the techno-economic implications of solving the EMPIRE model with this particular long-term scenario tree will be studied.

In each branching stage of the test instances, a change in the trend of emission re-

Table 7.2: Scenario tree data with policy uncertainty (27 scenarios). The political uncertainty is implemented through stochastic restrictions on the total absolute amount of allowed CO₂-emissions across Europe per unit of time. Units are given in Mt CO₂ per year.

Scenario	2010	2015	2020	2025	2030	2035	2040	2045	2050	Probability
1	1300	1138	975	1029	1083	1138	1192	1246	1300	0.001
2	1300	1138	975	1029	1083	1138	1192	1138	1083	0.002
3	1300	1138	975	1029	1083	1138	1192	1029	867	0.007
4	1300	1138	975	1029	1083	1029	975	1029	1083	0.002
5	1300	1138	975	1029	1083	1029	975	921	867	0.004
6	1300	1138	975	1029	1083	1029	975	813	650	0.014
7	1300	1138	975	1029	1083	921	758	813	867	0.007
8	1300	1138	975	1029	1083	921	758	704	650	0.014
9	1300	1138	975	1029	1083	921	758	596	433	0.049
10	1300	1138	975	921	867	921	975	1029	1083	0.002
11	1300	1138	975	921	867	921	975	921	867	0.004
12	1300	1138	975	921	867	921	975	813	650	0.014
13	1300	1138	975	921	867	813	758	813	867	0.004
14	1300	1138	975	921	867	813	758	704	650	0.008
15	1300	1138	975	921	867	813	758	596	433	0.028
16	1300	1138	975	921	867	704	542	596	650	0.014
17	1300	1138	975	921	867	704	542	488	433	0.028
18	1300	1138	975	921	867	704	542	379	217	0.098
19	1300	1138	975	813	650	704	758	813	867	0.007
20	1300	1138	975	813	650	704	758	704	650	0.014
21	1300	1138	975	813	650	704	758	596	433	0.049
22	1300	1138	975	813	650	596	542	596	650	0.014
23	1300	1138	975	813	650	596	542	488	433	0.028
24	1300	1138	975	813	650	596	542	379	217	0.098
25	1300	1138	975	813	650	488	325	379	433	0.049
26	1300	1138	975	813	650	488	325	271	217	0.098
27	1300	1138	975	813	650	488	325	163	0	0.343
Exp. val.	1300	1138	975	856	737	618	498	379	260	N/A

ductions may happen. For test instances with a branching factor of two, the development of emission restrictions can either continue flat with probability 0.3 or continue with a similar trend as targeting zero emissions from 2020 until 2050 with probability 0.7. With a branching factor of three, the trends are either slightly upwards towards 2010 emission levels with probability 0.1, slightly downwards with probability 0.2 or targeting zero emissions in 2050 with probability 0.7. By applying these probabilities the result is scenario trees with expected developments in emission restrictions of 80% reduction in 2050 compared to 1990-levels, i.e. similar to EU targets. The scenario tree with 27 scenarios has been depicted in Figure 7.5, and the data for this illustration can be found in Table 7.2. The data for the rest of the scenario trees used in this thesis can be found in the appendix.

Scenario tree representing uncertainty in **CO₂-emission restrictions** (Mt/year)

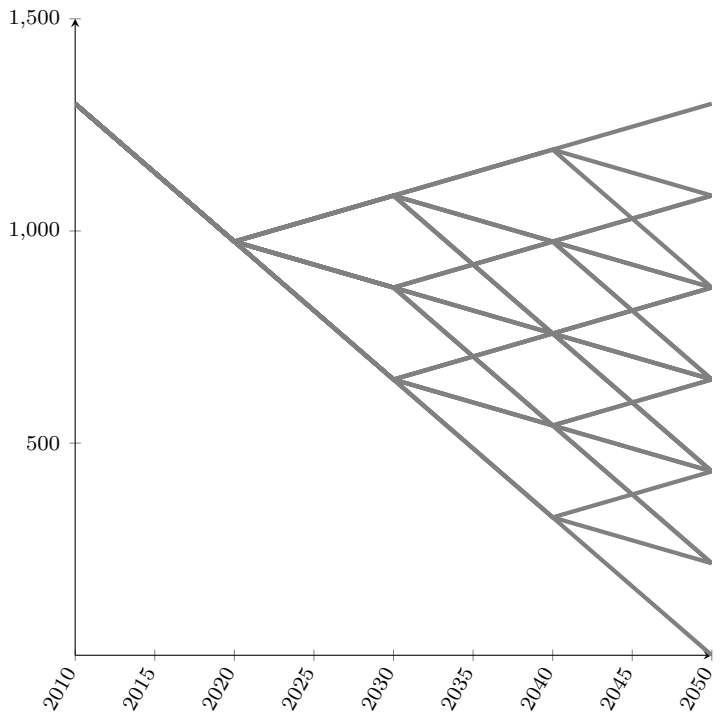


Figure 7.5: Scenario tree with 27 scenarios, depicting the long term development in policy uncertainty in emission restrictions.

Computational Study

In this chapter, the progressive hedging algorithm (PHA) presented in chapter 6 is thoroughly calibrated, documented and tested. The objective of the chapter is to obtain an optimal configuration of the algorithm and use this to test both the performance of the algorithm and the quality of the generated solutions on various test instances of the EMPIRE model. For sufficiently small test instances, the algorithm is compared with a direct solution method, which refers to solving an instance directly without decomposing the problem and relaxing the nonanticipativity constraints. For larger test instances that are intractable for direct solving, optimality bounds are used to assess the quality of the solutions.

The chapter is organized in four sections. In section 8.1, a brief overview of the current implementation and infrastructure is provided. Next, in section 8.2, a description of relevant test instances is given. These test instances are then used in section 8.3, where an extensive calibration of the algorithm’s parameters is performed and a final configuration is proposed. Lastly, the final configuration is used to obtain results from the algorithm in section 8.4, where a comparison between the obtained results from the PHA and the direct solution method is provided. As this chapter focuses on the computational performance of the PHA, an assessment of the techno-economic implications of the obtained solutions using the PHA has been designated to chapter 9.

8.1 Implementation

In this section, a presentation of the hardware and software used in the computational study is provided, along with an overview of the implemented system infrastructure.

8.1.1 Hardware and software

The technical specifications of the software and hardware used to conduct the analyses in this chapter are listed in Table 8.1.

All computations have been performed on a *shared* cluster at the Norwegian University of Science and Technology, known as the Solstorm Cluster. This is a shared cluster utilized

Table 8.1: Hardware and software used when testing the Progressive Hedging Algorithm.

Processor	3.4GHz Intel E5
Memory	512GB RAM
Available nodes	10
CPUs per node	24
Operating System	Linux 3.10.0
Xpress-IVE version	1.24.18
Xpress-optimizer version	31.01.09
Mosel version	4.0.8
C-compiler	GCC v4.8.5

by multiple other research initiatives at the university which currently lacks any form of resource allocation and queuing systems. Be aware that this implies that the results related to elapsed times required to solve the problem in this chapter may have been affected by interfering traffic during program executions.

8.1.2 Overview of implemented infrastructure

The implemented algorithmic infrastructure for solving the EMPIRE model consists of three separate modules, as illustrated in Figure 8.1. The first module consists of gathering and generating scenarios for the input data, including implementations of the scenario generation routines described in chapter 7. Data from the first module is then given as input to the second module consisting of the implementation of the progressive hedging algorithm described in chapter 6. The final module consists of procedures for efficient analysis of the extensive amounts of outputs from the PHA solving the EMPIRE model. The analyses in this chapter focus on the performance of the implemented code in the second module.

In the distributed implementation of the PHA, the subproblems are solved in parallel on the Solstorm cluster. MPI is used as the communication interface between the master and subproblems, and by default, MPI defines and creates one *process* per subproblem. In this thesis, each process is assigned to a designated processor/CPU with private memory (this is an implementation choice explicitly made in this thesis, and not necessarily a requirement for other parallel implementations). Each processor on the cluster has multiple cores that can be utilized for shared-memory parallelization by the Xpress solver within each subproblem. The shared-memory parallelization procedure is an integral part of the Xpress solver and hence not a part of the implemented algorithmic infrastructure conducted as part of this thesis.

The distributed implementation is, as mentioned in chapter 6,

8.2 Test instances

Throughout this thesis, the term test instance refers to a unique set of input data and number of scenarios for the model. All test instances are constructed based on the model data

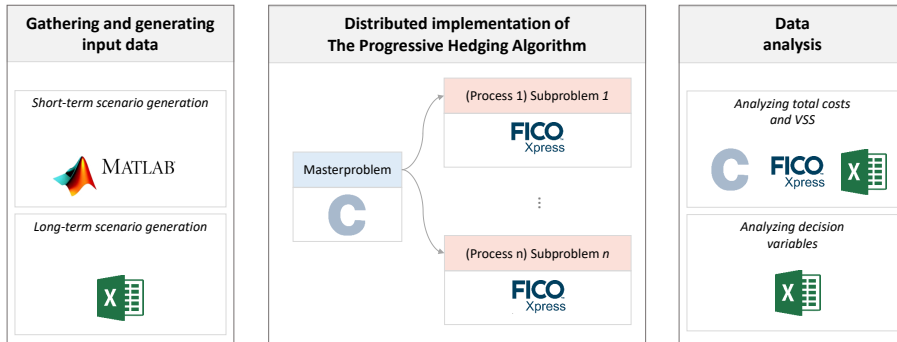


Figure 8.1: Infrastructure of current implementation

and scenario generation procedures described in chapter 7. To avoid overfitting the model parameters to a particular set of input data, multiple test instances are included for both calibration and performance testing. An overview of all relevant test instances is shown in Table 8.2.

The test instances differ in three ways: (1) the number of operational hours included in each typical operational period, (2) the number of short-term scenarios and (3) the number of long-term scenarios. Therefore, to easily identify the differences between each test instance, they are denoted by the following naming convention: <operational hours>_<short-term scenarios>_<long-term scenarios>.

Table 8.2: Overview of the test instances used in the computational study. The term branching stages refers to a set of indices on the long-term time scale where a branching occurs in the long-term scenario tree according to a branching factor. Problem sizes marked with a (*) indicates that the problem sizes are estimated, since no available commercially available software is able to set up or solve the test instance.

Test instance	Operational hours	Short-term scenarios	Long-term scenarios	Branching stages	Branching factor	Problem size	
						Rows (10^6)	Cols (10^6)
72_2_4	72	2	4	3,5	2	5.8	4.0
72_2_8	72	2	8	3,5,7	2	11.6	8.0
72_2_27	72	2	27	3,5,7	3	39.2	27.1
240_3_4	240	3	4	3,5	2	28.9	19.4
240_3_8	240	3	8	3,5,7	2	57.9	39.9
240_3_27	240	3	27	3,5,7	3	195.3*	134.6*
720_3_4	720	3	4	3,5	2	87.9	59.8
720_3_8	720	3	8	3,5,7	2	174.0*	119.5*
720_3_27	720	3	27	3,5,7	3	587.4*	403.4*
720_3_81	720	3	81	3,5,7,8	3	1762.2*	1210.2*

The stochasticity in the test instances is represented both along the short- and long-term time-scale. As can be seen from Table 8.2, the number of operational hours varies between 72, 240 and 720, i.e. 3, 10 and 30 consecutive days. Additionally, either 2 or 3 short-term scenarios are used in the different test instances to represent operational uncertainty and variability. Similarly, the number of long-term scenarios included in the test instances range between 4 and 81. The long-term scenarios form symmetric scenario trees in the sense that the same number of new branches, denoted the branching factor, emerge from each node in each branching stage of the long-term scenario tree. As an example, a branching factor of 3 and branching stages at time 3, 5 and 7 results in a scenario tree with a total of 27 scenarios, as depicted in Figure 7.4 in chapter 7. Note that although political uncertainty is the selected type of long-term uncertainty studied in this thesis, these test instances are generalized for any type of long-term uncertainty.

In Table 8.2 the problem size of each test instance is presented. Observe that the problem size of the different test instances varies significantly with the included number of operational hours and the number of scenarios. The mark (*) indicates that the test instance is insolvable through direct solution methods, and hence the problem size is estimated based on scaling of equivalent test instance with a single long-term scenario. Since such estimates omit nonanticipativity constraints, these estimates should be considered as a lower bound for the problem size.

8.3 Configurations of the progressive hedging algorithm

In this section, a comprehensive documentation of the performance of the PHA is provided, including a thorough calibration to determine an optimal configuration of different parameters in the algorithm. At first, the calibration methodology is presented, before the most important model parameters are tested and calibrated. In addition, the algorithm is tested for different bundling factors, i.e. for different numbers of scenarios included per subproblem of the PHA. At last, some concluding remarks relating to the optimal configuration of the parameters in the algorithm is presented.

8.3.1 Progressive Hedging Parameter Calibration Methodology

In the PHA there are three key parameters that need to be calibrated. These parameters are the step length ρ , the convergence criterion parameter ϵ and the bundling factor b which indicates the number of long-term scenarios to be solved per subproblem. An overview of these parameters with a brief description is given in Table 8.3. In the following paragraphs, the calibration methodology for these three parameters is presented.

Table 8.3: Overview of the parameters to be configured in the progressive hedging algorithm

Parameter	Description
ρ	Parameter used in the subproblem's objective function and dual multiplier update procedure
ϵ	Convergence parameter that indicates the strictness of the implementability requirement
b	Bundling parameter stating the number of long-term scenarios solved per subproblem

Determining step length ρ

The performance of multiplier methods, such as the PHA, is in general sensitive to the choice of ρ (Watson and Woodruff, 2011). This parameter both defines the step length in the update procedure of the dual multipliers and scales the quadratic penalty term in the objective function in each of the subproblems. Finding an optimal value of the parameter is known to be challenging, and usually there is a trade-off between fast convergence for the algorithm and tight optimality bounds (Gade et al., 2016).

In the literature there exist no unison framework for determining the optimal value of ρ . Therefore, in most cases the value is empirically determined, where the order of magnitude of the value seems to be highly dependent on the problem and input data. In Mulvey and Vladimirou (1991) the ρ -value is obtained through testing and is found to yield best results for values less than 1. In Listes and Dekker (2002), for a different problem, it is found that the best ρ -value lies in the range between 50 and 100. Watson and Woodruff (2011) argues that the optimal obtained ρ -value thus is an artifact of data-scaling and should be updated dynamically at each iteration of the PHA based on the obtained decision variables and the cost-coefficients of the specific problem. A literature survey for existing methods for updating ρ can be found in Zehtabian and Bastin (2016).

In this thesis ρ is defined as a static parameter and therefore does not change between iterations of the PHA. An approximation of the optimal value of ρ is found empirically through testing. A reasonable initial range of the parameter is found through conducting tests on the smallest data set, before a selected interval within this obtained range is applied on all test instances. Multiple test instances are used to find the optimal value of ρ to identify if there are any instance specific conditions affecting the choice of optimal ρ . Interesting indicators for finding ρ is the gap from the optimal solution, tightness of obtained bounds and the number of iterations and computational time required until convergence.

Determining convergence criterion ϵ

The convergence criterion defines when an obtained solution from the PHA is considered good enough with respect to implementability requirements. As described in chapter 6, the convergence criterion in this thesis is based on determining a fixed ϵ defining the maximum allowed deviation from the nonanticipativity constraints for a particular decision variable. This is argued to be a reasonable choice for convergence criterion since it is both fast and computationally cheap to make this convergence check at each iteration.

As with methods for determining the optimal value of ρ , there are no consensus methodologies for determining ϵ in the literature. A common approach is therefore to define it as a reasonably small value specific to the problem (Gade et al., 2016; Watson and Woodruff, 2011). For example, in Gonçalves et al. (2012) it is argued that an ϵ of 50 is a reasonable convergence criterion, since decision variables for the given problem can take values in the range between 10 and 30 000. In this thesis, a bound-study using multiple test instances is conducted to calibrate a reasonable value of ϵ , with the intention of identifying a relationship between the value of ϵ and the obtained optimality gaps.

Determining scenario bundling b

In Gade et al. (2016) it is shown that decomposing the scenario trees by bundles of scenarios of size $b > 1$ rather than individual scenarios (i.e. $b = 1$), leads to accelerated convergence of the PHA through reductions to the required number of iterations and tighter optimality bounds. The challenge, however, in particular in combination with large problem instances such as the EMPIRE model, is that the elapsed time for solving a single iteration of a subproblem increases significantly with bundling of multiple scenarios. In some cases, the problem instances may even get so large that commercially available solvers are incapable of solving the bundled subproblems. Therefore, there is a trade-off between reducing the number of iterations required to reach optimality and the total elapsed time for solving the problem. The methodology applied in this thesis for determining the optimal bundle of scenarios b is based on testing, where bounds, required iterations and total time elapsed for solving the problem to optimality are studied to find the optimal value.

Relevant terms for the calibration

To explain the convergence properties of the PHA, four relevant terms are included in the figures and tables presented in this chapter. For convenience, an explanation of the individual terms is provided below:

- **Bounds:** Bounds refer to the optimality bounds calculated by the PHA. A bound is referred to as either a lower bound (lb) or an upper bound (ub), and these are calculated as explained in chapter 6. The unit of the bounds is given in €_{2010} .
- **Gaps:** Gaps refer to the relative deviation between an upper bound (ub) and a lower bound (lb), or, for instances where the exact solution can be obtained, the relative deviation between an upper bound and the optimal value (z^*). The unit is given in %.
- **Deviation:** Deviation refers to the sum of the absolute value of total deviation of all nonanticipativity requirements for all investment decision variables. The unit is given in MW or MWh, depending on the type of investment decision variable.
- **Elapsed time:** Elapsed time refers to the wall clock time for solving the problem, excluding bound computations. Recall that since the programs are executed on a shared cluster, the timing might be affected by interfering traffic. The units are most often given as (hours:minutes).

The next paragraphs document the calibration of the various parameters in the algorithm. For all test instances, a maximum number of iterations is set to limit the total time allowed to spend on computations. The parameters are tested on multiple test instances, and since the solution method in combination with static input data would yield the same results if run multiple times, each configuration is only tested once per test instance. The objective of the remaining parts of this section is both to document important properties of the algorithm for different input data sets and to search for an optimal configuration for later usage of the algorithm.

8.3.2 Calibration of ρ

Determining the initial range of ρ

To find a reasonable range for the value of ρ for the test instances, an initial bound study is conducted on one of the instances. Upper and lower bounds are computed for test instance 72.2.4 at each iteration to assess how the value of ρ affects the quality of the solutions found by the PHA. The results of the bound study are shown in Figure 8.2.

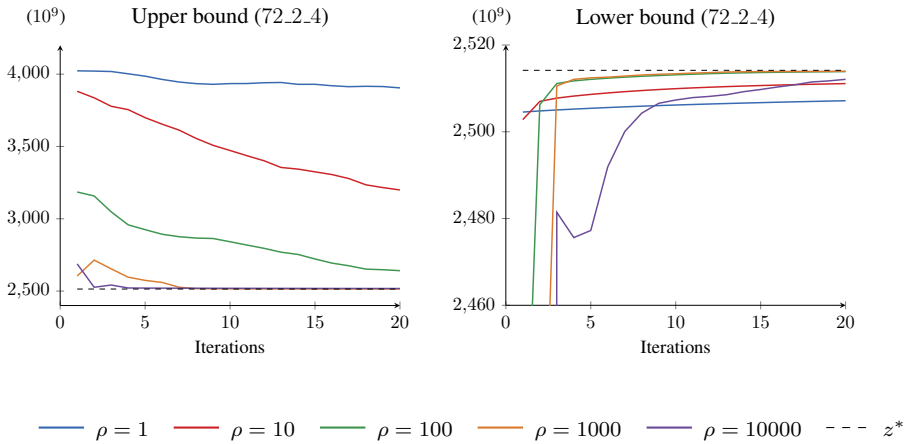


Figure 8.2: Upper and lower bounds for 72.2.4 with different values of ρ over 20 iterations.

Based on Figure 8.2, it can be seen that the choice of ρ clearly affects both (1) the quality of bounds and (2) the number of iterations required for convergence. For $\rho = 1$ and $\rho = 10$ both the upper and lower bounds only slightly improve over the course of 20 iterations, indicating that these values likely are too low for the given test instance. On the other end of the scale, $\rho = 10000$ converges after just a few iterations, but exhibits an oscillating behavior in the lower bounds, which might indicate that this value is too large for the particular test instance. The behavior and rate of convergence for $\rho = 100$ and $\rho = 1000$ seems to be more sound, as both the upper and lower bounds converge towards the optimal solution in a reasonable amount of iterations. Therefore, a preliminary conclusion based on this study is that $\rho = 1$, $\rho = 10$ and $\rho = 10000$ likely are outside the scope of optimal ρ -values and hence omitted from further testing, and that the optimal value of ρ lies between 100 and 1000.

In Figure 8.3 the optimality gaps per iteration are illustrated along a logarithmic scale. The figure shows that for $\rho = 1000$ the algorithm obtains an optimality gap of 0.1 % after approximately 10 iterations, which is the tightest gap obtained by all values of ρ for the given instance and number of iterations. Due to these preliminary results, a value of $\rho = 1000$ is chosen as the initial starting point for the remaining calibrations, where also $\rho = 500$ and $\rho = 2000$ are included in the calibration to avoid overfitting ρ to a particular test instance. The next steps of the calibration involve understanding how differences in long-term data affect the optimal choice of ρ , before analyzing these effects when varying short-term data.

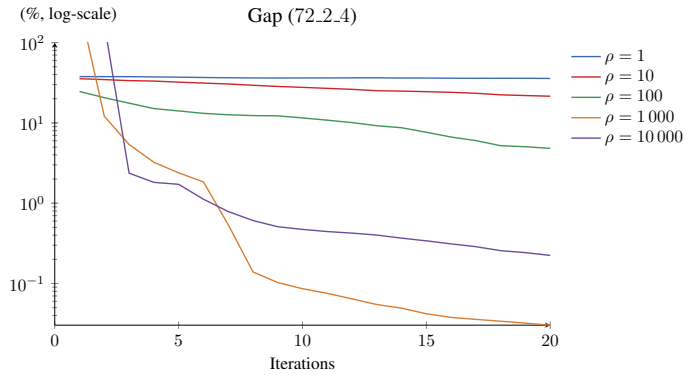


Figure 8.3: Optimality gaps for 72.2.4 with different values of ρ over 20 iterations.

Calibrating ρ under variation of long-term data

An analysis has been conducted to understand whether the optimal choice of ρ is affected by variation of the long-term data in the test instances. Table 8.4 shows the results from solving test instances with the same short-term operational input data, i.e. 72 short-term hours and 2 short-term scenarios, but with different numbers of long-term scenarios. The convergence criterion ϵ is set to 2, which later in this section is shown to be a sufficiently low value to obtain satisfactory bounds for all test instances. The best obtained optimality gap per test instance is marked with green.

Table 8.4: Calibrating ρ for instances with 72 short-term hours and 2 short-term scenarios under variation of long-term scenarios. Convergence criterion $\epsilon = 2$ and maximum iterations of 100 is applied.

Test instance	ρ	Elapsed time (H:M)	Iterations (#)	Gap (%)		Bounds (10^9)	
				(ub to z^*)	(ub to lb)	(lb)	(ub)
72.2.4	500	05:06	61	0.005 %	0.006 %	2514.142	2514.296
	1000	03:15	39	0.014 %	0.018 %	2514.053	2514.511
	2000	01:48	21	0.045 %	0.066 %	2513.623	2515.284
72.2.8	500	09:11	93	0.150 %	0.160 %	2546.787	2550.874
	1000	04:42	51	0.117 %	0.140 %	2546.458	2550.015
	2000	01:49	20	0.371 %	0.582 %	2541.630	2556.519
72.2.27	500	08:49	71	0.216 %	0.226 %	2552.955	2558.736
	1000	04:43	38	0.308 %	0.343 %	2552.431	2561.207
	2000	02:47	22	0.338 %	0.539 %	2548.176	2561.973

The results presented in Table 8.4 illustrate that the algorithm obtains tight optimality bounds regardless of the choice of ρ within the specified range. All choices of ρ generate relative gaps from ub to lb of less than 0.6 %, and relative gaps from ub to z^* of less than 0.4 %. Still, an interesting observation is that $\rho = 500$ and $\rho = 1000$ seem to be more

versatile and robust for all test instances as they consistently produce tighter bounds than $\rho = 2000$. This illustrates the benefits of using lower values of ρ , which clearly increase the quality of the obtained solutions. On the other hand, one of the disadvantages of using lower values of ρ is the decreased rate of convergence. This is elucidated in the observation that $\rho = 2000$ converges faster for all test instances both in terms of elapsed time and in number of iterations, which clearly emphasize the trade-off between speed of convergence and tightness of bounds when determining an optimal value of ρ .

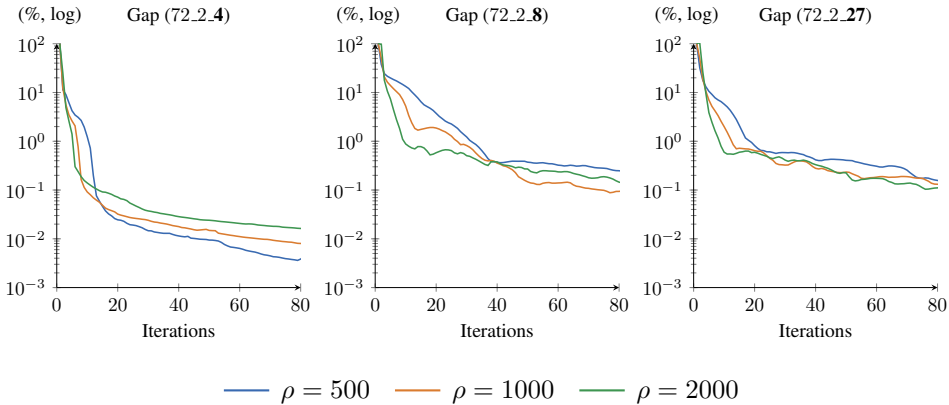


Figure 8.4: Optimality gaps under the variation of long-term data sets for test instances 72.2.4, 72.2.8 and 72.2.27, for different values of ρ . Note that the y-axis is logarithmic.

In Figure 8.4 the development of optimality gaps are shown for the test instances forced to run over the course of 80 iterations. It can be seen from the figure that as more long-term scenarios are introduced, the more iterations are required to obtain tight bounds. As more long-term scenarios are included, the number of investment variables increase as well. This results in an increase in the number of dual multipliers in the problem, which needs to be iteratively updated and enforced towards its optimal value. Thus, a possible explanation for why the optimality gaps increase with the number of long-term scenarios could be that it is harder to obtain the correct dual multipliers when the number of multipliers increases.

An important insight from Figure 8.4 is that allowing the algorithm to run for a given number of iterations, instead of determining an ϵ to define the termination criterion, might result in slightly different optimal values of ρ . For example, in Table 8.4 it is clear that $\rho = 500$ provides the best optimality gap for the test instance with 27 long-term scenarios 72.2.27, which converges after 71 iterations for $\epsilon = 2$. However, by letting the instance run for 71 iterations with $\rho = 1000$ and $\rho = 2000$ as well, it can be seen from Figure 8.4 that both $\rho = 1000$ and $\rho = 2000$ in fact produce better gaps than $\rho = 500$ at that particular iteration. From this figure it can also be observed that the optimality gaps seem to be more stable for lower numbers of long-term scenarios, indicating that the increased amount of dual multipliers introduced in test instances with more long-term scenarios induce more instability to the gap calculations.

From Figure 8.4 it can further be observed that at some point there is a diminishing marginal improvement on the optimality gaps of an additional iteration of the algorithm.

For example, in the figure there is a significant improvement of the gaps until somewhere between 20 to 40 iterations until it starts flattening out. This behavior can be explained by inspecting the optimality bounds for the first 20 iterations illustrated in Figure 8.5. Here it is shown that the fast convergence in the early iterations mostly is a result of improvements in the upper bounds, which initially are quite poor until they approach the optimal solution after approximately 5 to 20 iterations. In addition, it seems like the initial quality of the upper bound is highly problem specific, as there are large differences between the value of the upper bounds across all test instances in early iterations. The lower bound, on the other hand, seems to converge toward the optimal solution much faster than the upper bound, and in addition it seems to consistently converge approximately at the same iteration for all long-term scenarios. Based on these results, it is hard to infer any direct relationship between the number of long-term scenarios and the rate of convergence, as it seems to be highly instance-specific.

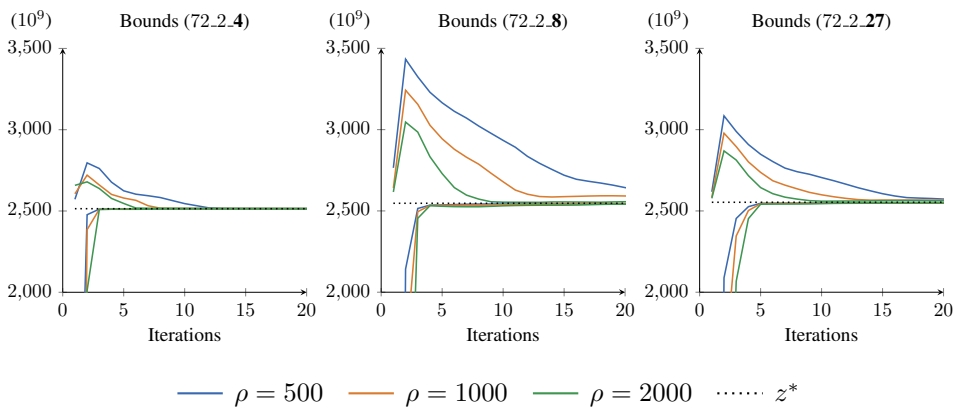


Figure 8.5: Lower and upper bounds for test instances 72.2.4, 72.2.8 and 72.2.27 for 20 iterations and different values of ρ .

The value of ρ also impacts the development of the (absolute value of the) deviation from the nonanticipativity requirements per iteration of the algorithm. A finding in the study is that higher values of ρ lead to a more oscillating development in the deviations from these requirements. This effect is illustrated in Figure 8.6, where $\rho = 2000$ clearly exhibits a more oscillating development than the other two values of ρ , which is particularly visible for $\rho = 500$. The oscillating development in the deviation for large values of ρ may indicate that such values for ρ lead to unstable solutions that converge to local optima. This is therefore an argument for using values of ρ in the lower parts of the range.

The findings above illustrate that the initial range of ρ -values is sufficient for finding tight optimality gaps when varying long-term data for the given test instances. In general, it is found that lower values of ρ produce tighter bounds, but at the cost of more iterations. This is consistent for all test instances. However, introducing more long-term scenarios results in larger numbers of dual multipliers, making it harder for the PHA to obtain tight bounds. In addition, it is found that using large values of ρ lead to more oscillation in terms of the deviation from the nonanticipativity requirements, which might lead to unstable

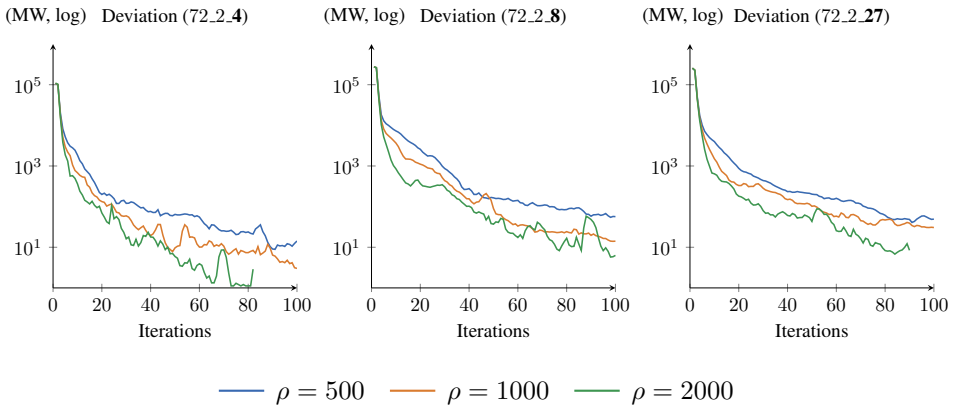


Figure 8.6: Total deviation from the nonanticipativity requirements per iteration for 72.2.4, 72.2.8 and 72.2.27, for different values of ρ . Note that the y-axis is logarithmic.

solutions obtained from the PHA.

Calibrating ρ under variation of short-term data

The analyses in the previous paragraphs showed how variations in long-term data affect the choice of optimal ρ for test instances with 72 operational hours and 2 short-term scenarios. In the following paragraphs, the focus is directed towards understanding how different short-term data affects the choice of ρ , holding the long-term data fixed. In Table 8.5 the results of calibrating ρ on three test instances with 27 long-term scenarios and different short-term data is provided. The convergence criterion is, as before, set to $\epsilon = 2$, and the maximum allowed number of iterations is limited to 100. The best obtained optimality gap per test instance is marked with green.

Table 8.5: Calibrating ρ for instances with 27 long-term scenarios under variation of short-term data. Convergence criterion is $\epsilon = 2$ and maximum iterations is 100.

Test instance	ρ	Elapsed time (H:M)	Iterations (#)	Gap (%)		Bounds (10^9)	
				(ub to z^*)	(ub to lb)	(lb)	(ub)
72.2.27	500	08:49	71	0.216 %	0.226 %	2552.955	2558.736
	1000	04:43	38	0.308 %	0.343 %	2552.431	2561.207
	2000	02:47	22	0.338 %	0.539 %	2548.176	2561.973
240.3.27	500	26:18	28	–	0.078 %	2713.883	2715.996
	1000	15:08	16	–	0.168 %	2712.747	2717.318
	2000	16:58	18	–	0.245 %	2711.484	2718.135
720.3.27	500	66:47	23	–	0.070 %	2622.254	2624.251
	1000	28:00 ¹	10	–	0.204 %	2620.722	2626.070
	2000	33:55	12	–	0.225 %	2620.500	2626.414

The results presented in Table 8.5 illustrate that the PHA obtains tight optimality bounds for the specified range of ρ also under variation of short-term data. All choices of ρ generate relative gaps from ub to lb of less than 0.6 %, and the best obtained gaps for the largest test instances 720_3_27 and 240_3_27 are found to be less than 0.1 %. Still, it is evident from the results that also when varying short-term data the trade-off between the number of iterations required to meet the convergence criterion and tight optimality bounds is present. Based on the total elapsed time required to solve the problem for the largest test instance 720_3_27, approaching almost three full days, reducing the number of iterations might be beneficial, or even necessary, for practical use of the implemented algorithm.

An interesting effect observed from the results in Table 8.5 is that the number of iterations required to converge is significantly reduced for 240_3_27 and 720_3_27 as compared to 72_2_27 (and all the other test instances with 72 operational hours and 2 short-term scenarios previously presented). The optimality gaps for the larger test instances are also tighter. An observation from Figure 8.7, which plots the optimality gaps for the three test instances over the course of 30 iterations, is that the optimality gaps in 240_3_27 monotonically decrease in an ordered manner under variation of ρ . This is different from the behavior observed in 72_2_27 where the gaps are fluctuating. This might indicate that the specified range of ρ fits 240_3_27 and 720_3_27 even better than 72_2_27, and that there exist instance specific properties affecting both the performance of the algorithm's rate of convergence and the quality of the obtained solution.

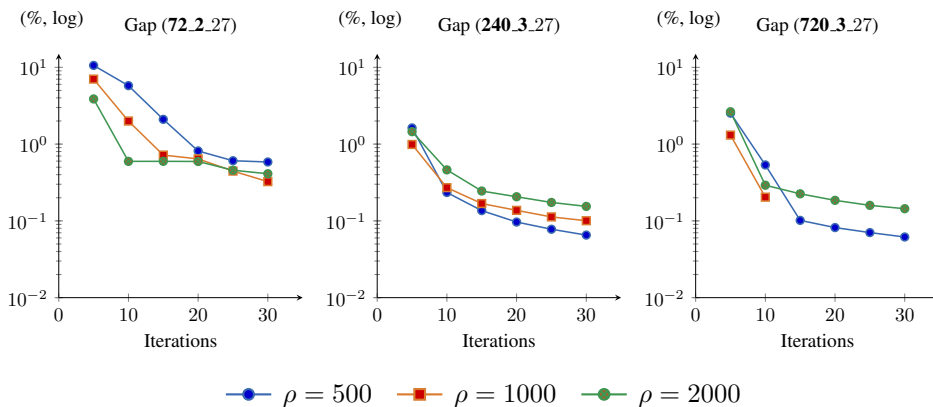


Figure 8.7: Optimality gaps under variation of short-term data sets for 72_2_27, 240_3_27 and 720_3_27, for different values of ρ . The gaps are calculated at every fifth iteration. The test instance 720_3_27 with $\rho = 1000$ was executed multiple times, but due to interfering traffic on the shared cluster none of the executions were successful at converging. Note that the y-axis is logarithmic.

A finding from Table 8.5 is that runs with $\rho = 1000$ converges faster than runs with $\rho = 2000$ for test instance 240_3_27. This result differs from all other test results presented so far where instances with high values of ρ converge faster, and is a consequence of the

¹The test instance 720_3_27 with $\rho = 1000$ was executed multiple times, but due to interfering traffic on the shared cluster none of the executions were successful at converging.

oscillating effects seen on the decision variables when ρ gets too large. In Figure 8.8 the oscillations in terms of total sum of deviations from the nonanticipativity requirements are shown for 72_2_27 and 240_3_27. For 240_3_27 an early oscillation of the deviation can be observed, resulting in an increased number of iterations required to solve the problem.

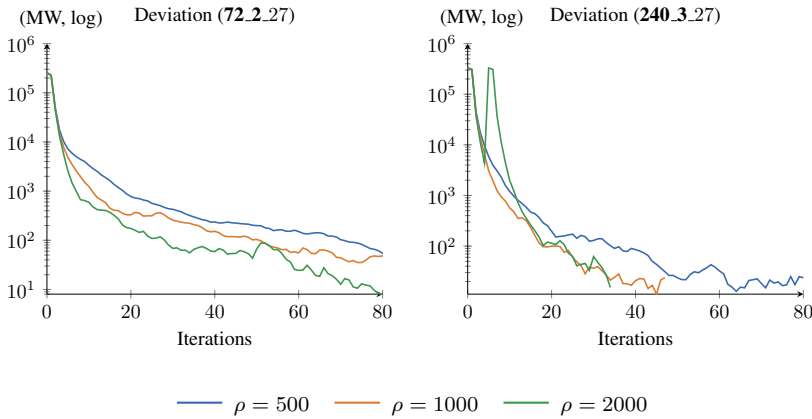


Figure 8.8: Total deviation from nonanticipativity requirements when varying ρ on 72_2_27 and 240_3_27. Testing made with $\epsilon = 1$ and maximum iterations equal to 80.

Concluding remarks regarding calibration of ρ

The results presented in this section illustrate that the initial range of ρ -values is sufficient for finding tight optimality bounds when varying both short-term and long-term data for the given test instances. It is worth noting that the test instances presented in this section are either fixed to the short-term data with 72 operational hours and 2 short-term scenarios, or with 27 long-term scenarios. Nonetheless, during testing it has been found that the convergence properties and the quality of the solutions obtained are similar for other test instances with different short- and long-term data.

It has further been shown above that the value of ρ cannot be tailored for all test instances, as it varies with the properties of the given problem. Still, it is reasonable to believe that an optimal value of ρ for the test instances presented in this thesis lies around or below $\rho = 1000$. This is mainly due to the oscillating effects that are observed when increasing ρ to 2000, leading to a sort of premature, local convergence with a resulting reduction in the bound quality. Therefore, for the remaining part of this thesis, ρ will be set to values in the lower part of the initially proposed range of ρ -values.

8.3.3 Calibration of ϵ

A study has been conducted to understand the relationship between the choice of ϵ and (1) the rate of convergence and (2) the quality of the obtained solutions. Table 8.6 presents the relationship between different values of ϵ and the optimality gaps, as well as the number of iterations and elapsed time required for solving the problem. For obtaining the results,

the value of ρ is set to 1000 and the number of iterations is limited to 100 iterations for 72_2_8 and 240_3_8 and 40 iterations for 720_3_8. The best obtained gap per test instance is marked with green.

Table 8.6: Calibrating convergence parameter ϵ for various test instances. $\rho = 1000$ and maximum number of iterations is limited to 100 for 72_2_8 and 240_3_8, and 40 for 720_3_8.

Test instance	ϵ	Elapsed time (H:M)	Iterations (#)	Gap (%)		Bounds (10^9)	
				(ub to z^*)	(ub to lb)	(lb)	(ub)
72_2_8	1	09:12	100	–	–	–	–
	2	04:42	51	0.117 %	0.140 %	2546.458	2550.015
	10	01:02	11	3.094 %	3.375 %	2539.648	2628.344
	20	00:26	4	15.859 %	16.292 %	2533.93	3027.093
240_3_8	1	23:40	53	0.047 %	0.078 %	2704.453	2706.555
	2	09:22	21	0.081 %	0.141 %	2703.641	2707.460
	10	02:26	5	0.266 %	0.433 %	2700.732	2712.483
	20	02:03	4	2.312 %	3.542 %	2671.230	2769.306
720_3_8	1	111:10	40	–	–	–	–
	2	59:46	21	–	0.158 %	2521.063	2525.042
	10	26:27	6	–	0.945 %	2502.415	2526.278
	20	12:06	4	–	2.630 %	2515.119	2583.056

In terms of the time and iterations required to solve the problem, it can be seen from Table 8.6 that high values of ϵ require relatively few iterations and less elapsed time for convergence. A low number of iterations comes at a cost of poor optimality gaps, perhaps best illustrated by the 16.3 % optimality gap for $\epsilon = 20$ and test instance 72_2_8. At the same time, it can be seen that low values of ϵ leads to significantly more computational effort in terms of iterations for finding an optimal solution satisfying the convergence criterion. In fact, if $\epsilon < 2$ both 72_2_8 and 720_3_8 are incapable of converging within their predefined maximum number of iterations. Therefore, calibrating the value of ϵ to account for both a sufficient optimality gap and the time required to solve the problem is of the essence.

The average deviation of all decision variables deviating from their nonanticipativity requirements is a metric found to be a reasonable proxy for ϵ . This metric can be used to determine a range of values of ϵ which results in acceptable optimality gaps within a reasonable number of iterations. In Figure 8.9 the number of iterations of the PHA is plotted along the x-axis, and the corresponding average deviation and optimality gaps are plotted along the left and right y-axis respectively. The figure illustrates that to obtain an optimality gap of 1.0 % for the test instance 72_2_27, 11 iterations are required, which yields an average deviation of variables of 3.9. Consequently, since the average deviation is a proxy of ϵ , by setting ϵ to 4 this would imply that the algorithm terminates after approximately 11 iterations at an optimality gap of approximately 1 %. In addition, as can be seen from the figure, the optimality gap below 1 % only marginally improves over the course of 40 iterations, which is an argument for finding a sufficient value of ϵ that produces good enough solutions without the use of too large amounts of computational resources or time.

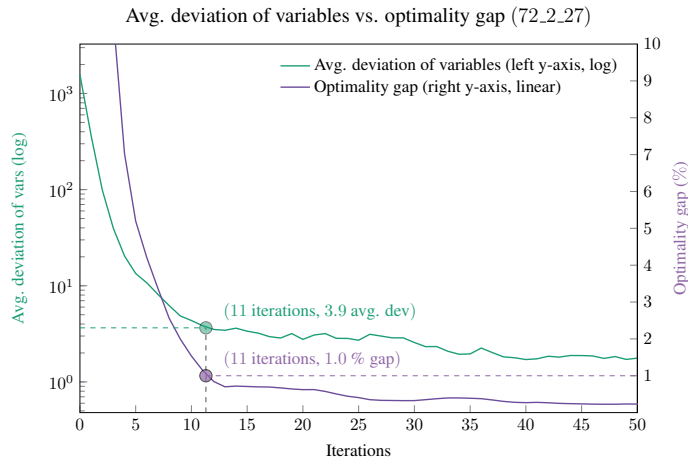


Figure 8.9: The figure depicts the average deviation of all variables deviating from the nonanticipativity constraints versus the optimality gap per iteration for 72.2.27. Iterations of the PHA is plotted along the x-axis, and the corresponding average deviation and optimality gaps are plotted along the left and right y-axis respectively.

The findings above illustrate the clear trade-off between rate of convergence and quality of obtained solutions with respect to the parameter ϵ . It seems like setting ϵ to around 2 results in a threshold for which all test instances in Table 8.6 are capable of converging within a reasonable amount of iterations. At the same time, it seems that this choice for ϵ provides sufficient optimality gaps, where all gaps are less than 0.2 %. In 72.2.27 there are around 175'000 investment variables, each taking values in the range between 0 and 135'000 MW or MWh (depending on the type of investment variable) in the optimal solution. Allowing a probability-weighted deviation of a single decision variable to deviate with at most 2 MW or MWh can therefore be considered acceptable.

8.3.4 Calibrating Scenario Bundling

In Table 8.7 the results of running the PHA on 72.2.8 and 240.3.8 with variations in scenario bundling is presented. The results are generated with $\rho = 1000$ and $\epsilon = 2$, and with a bundling factor b which indicates the number of long-term scenarios that are bundled with nonanticipativity constraints within each subproblem. The best obtained optimality gap per test instance is marked with green.

The results from Table 8.7 show that increasing the bundling factor clearly improves the quality of the optimality bounds. Solving for a bundle of four scenarios per subproblem for both of the test instances yields optimality gaps of less than half of any of the gaps produced by bundling 2 or 1 scenario per subproblem. This is possible because fewer unique dual multipliers are included in the total problem. In addition, it can be seen that fewer iterations are needed with higher bundling factors for convergence. Note that the obtained effects from bundling 2 scenarios per subproblem are significantly less than bundling 4 scenarios per subproblem.

Table 8.7: Configuring bundling factor b , which indicates how many scenarios to be solved per subproblem in the progressive hedging algorithm. Convergence criterion $\epsilon = 2$ and $\rho = 1000$.

Test instance	b	Elapsed time (H:M)	Iterations (#)	Gap (%)		Bounds (10^9)	
				(ub to z^*)	(ub to lb)	(lb)	(ub)
72_2_8	1	04:38	51	0.117 %	0.140 %	2546.458	2550.015
	2	12:44	34	0.075 %	0.154 %	2545.013	2548.937
	4	08:50	17	0.020 %	0.026%	2546.894	2547.545
240_3_8	1	09:22	21	0.081 %	0.141 %	2703.641	2707.460
	2	26:38	19	0.077 %	0.118 %	2704.183	2707.366
	4	46:13	11	0.030 %	0.052 %	2704.695	2706.093

A disadvantage with bundling is the increase in elapsed time per iteration. In Figure 8.10 the average elapsed time per iteration for various bundling factors is shown. As can be seen from the figure, the elapsed time required to solve a single iteration more than doubles when the bundling factors doubles. In addition, for some test instances that are sufficiently large, introducing bundling factors are often not applicable because the subproblems are not possible to solve. Hence, determining the bundling factor is a trade-off between tightness of the optimality bounds and the time and resources available for computations.

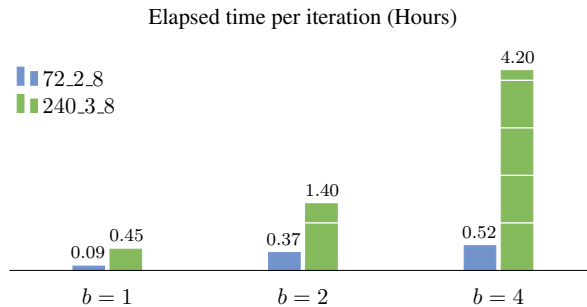
**Figure 8.10:** Elapsed time per iteration with different bundling factors for 72_2_8 and 240_3_8.

Figure 8.11 shows the optimality gap at specific times for test instance 240_3_8 for various bundling factors. A finding from these results is that using smaller bundling factors, illustrated with orange in the figure, produces tighter optimality gaps faster than using larger bundling factors. To facilitate for more agile testing, and also be less dependent of computational resources with high memory availability to solve larger bundles of scenarios, the further calibration and testing conducted in this thesis assumes a bundling factor of 1 so that one subproblem only solves a single scenario. Nonetheless, it should be noted that if the objective is to obtain extensively tight bounds, a bundling factor should be used to achieve the desired target.

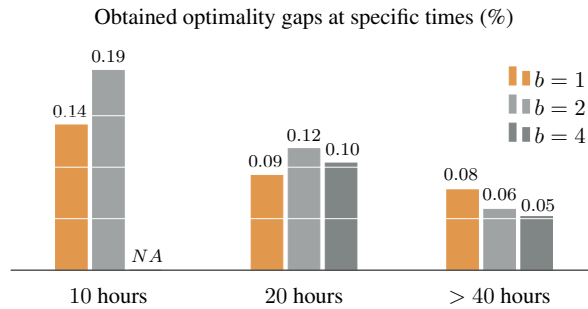


Figure 8.11: Obtained optimality gaps at specific times when varying bundling factor for test instance 240_3_8. Convergence criterion $\epsilon = 0.0001$ and $\rho = 1000$.

8.3.5 Summarizing the Progressive Hedging Algorithm Calibration

In this section, the configuration procedure for ρ , ϵ and b has been presented. The optimal choice of ρ was shown to be highly instance-specific, but is likely to have a functional value in the range between 100 and 2000 for the relevant test instances. The choice of ρ clearly is a trade-off between tight optimality bounds and the number of iterations and elapsed time required for convergence. This is illustrated by the observation that $\rho = 2000$ converged in fewer iterations with looser bounds than $\rho = 500$ for all test instances. In addition, observations from some of the tests illustrate that running the PHA with $\rho = 2000$ results in oscillating effects and premature convergence of the algorithm, which was not observed for the other values of ρ tested for. A reasonable trade-off between sufficient optimality bounds and fast convergence is thus to choose $\rho = 1000$, which is used in the latter part of this study. This value of ρ seems to be stable under the variations of both short- and long-term input data.

The optimal value for the convergence criterion ϵ is estimated to be in the range between 1 and 5. Defining ϵ in this range is shown to produce an optimality gap of less than 1 % for several test instances. In terms of the bundling constant b , it is shown that bundling indeed improves the tightness of the optimality gap. However, a major drawback of bundling is that the time required for solving the problem is significantly increased, as the time it takes for solving one iteration increases exponentially. Hence, the final configuration used in the remaining parts of this thesis is $\rho = 1000$, $\epsilon = 2$ and $b = 1$.

8.4 Comparing progressive hedging with direct solving

The remaining parts of this chapter are devoted to comparing the performance of the PHA with the direct solving method. The study is conducted to better understand the advantages and challenges of using the PHA to solve the EMPIRE model, as compared to solving the problems directly whenever this is possible. The comparison is done in three steps. First, a comparison of the elapsed time required to solve the test instances by the two methods is presented. Second, the differences in computational resources required by the methods are considered, with a particular emphasis on the necessary requirements within memory

availability and CPU capacity. Finally, a comparison between the final results of solving the test instances with both methods is shown in the latter part of the section.

8.4.1 Elapsed Time Required for Solving the Problem

The primary objective of implementing the PHA is to solve problems that the direct solving method is not capable of solving. Therefore, achieving a reduction in the elapsed time for solving a problem with the PHA if the problem is sufficiently small to be managed by the direct solver is not an objective in itself with the implementation. Nonetheless, the PHA possess solid convergence properties and scales well as the number of long-term scenarios and problem size increase.

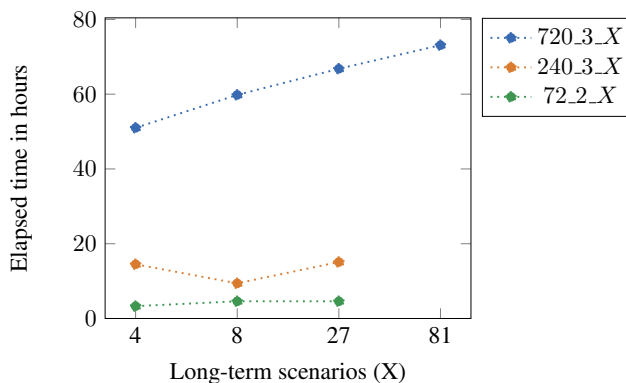


Figure 8.12: Elapsed time when solving the test instances with the PHA. Parameters $\epsilon = 2$, $\rho = 1000$ and $b = 1$

The elapsed time required by the PHA for solving test instances with different short- and long-term data is shown in Figure 8.12. Based on these results, it is apparent that the main driver of the elapsed time for solving the test instances with the PHA is related to the size of the short-term operational data, and that the number of long-term scenarios included has limited effects on the overall elapsed time to achieve convergence for the algorithm. This finding implies that the required time for solving a problem can be considered more or less constant under variation of long-term data when solved with the PHA, as long as there are sufficient computational resources available.

The direct solving method turns out to be much less robust than the PHA when considering the effect of changes in the number of long-term scenarios on the elapsed time required to solve the problem. In Figure 8.13 it is shown that the time required to solve one of the test instances directly, increases exponentially as the number of long-term scenarios increase. As previously shown, the PHA exhibits a more or less constant pattern unaffected by the changes in long-term scenarios. Therefore, in addition to fulfilling its primary objective with solving problem instances that are intractable for the direct solving method, the PHA can also solve particular instances faster than the direct solving method as the number of long-term scenarios and problem complexity increases sufficiently.

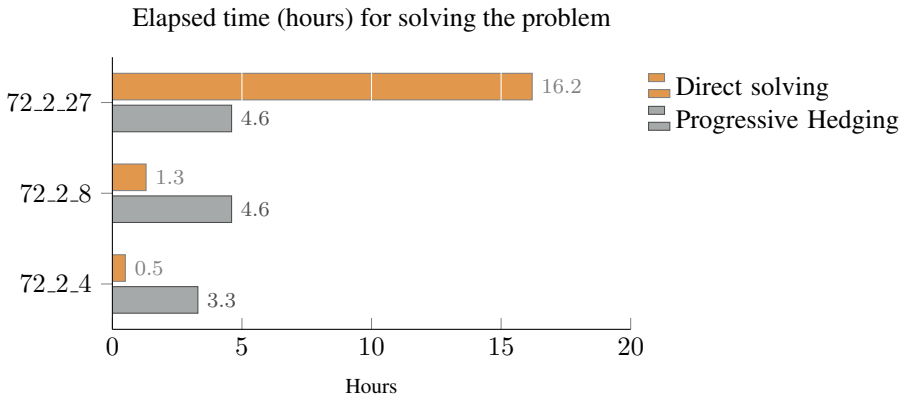


Figure 8.13: The elapsed time required for solving three test instances with different long-term data by the direct solving method and the Progressive Hedging Algorithm. Parameters $\epsilon = 2$, $\rho = 1000$ and $b = 1$.

Since the PHA is implemented as a distributed program, some of the elapsed time is devoted to input / output (IO) of data, i.e. communication, between the parallel processes. This is an example of an overhead-cost that is not present in the direct solving method, as it solves the problem instance in one particular program execution spawning a single process (potentially utilizing multiple cores). In many large-scale distributed programs the time spent on IO is significant and contributes to a radical increase in the elapsed solution time. For the PHA this is far from the case and the time spent on IO is at most negligible. For a test instance with 27 long-term scenarios, approximately 0.1 seconds is related to IO between the processes during each iteration, which for the smallest test instance 72.2.27 is about 0.03 % of the elapsed time of solving one particular iteration. It is therefore apparent that the time spent on solving the particular subproblems is much more expensive compared to the overhead cost related to IO in the parallelization.

As compared to the direct solving method, which solves the entire problem in one program execution, the PHA is an iterative algorithm solving multiple smaller programs in parallel. The combination of the PHA being both iterative, synchronously implemented and distributedly executed on a shared cluster with interfering traffic, has a significant impact on the elapsed time required to solve the problem. These factors are challenging for the PHA and does not in any noteworthy manner impact the direct solving method.

In practice, a synchronous parallel program executed on a shared cluster is challenging because the elapsed time for solving each subproblem at a particular iteration varies drastically with the interfering traffic and balance of computational resources. In theory, each subproblem should approximately terminate at the same time. In practice, however, this has not been the case for program executions on the shared cluster with the PHA. In certain cases significant differences in the elapsed solution time per iteration have been observed, the reason being that some subproblems run programs on nodes that are experiencing heavy traffic from other users. Due to the synchronous implementation this delays the entire process because all subproblems must wait for the last subproblem to finish until the algorithm can proceed to the next iteration. In Figure 8.14 a histogram illustrates the

frequency of subproblems that terminates after a certain amount of time for one iteration of a test run of instance 720_3_27. As can be seen from the figure, there is a small tail of subproblems terminating far later than all others, which increase the total elapsed time for the given iteration from 80 to 260 minutes. This significantly reduces the overall performance of the algorithm and is a practical problem greatly affecting the elapsed time for solving the problem for the PHA specifically. The direct solving method, on the other hand, is less exposed to this problem as computations are not decentralized across multiple nodes and processors.

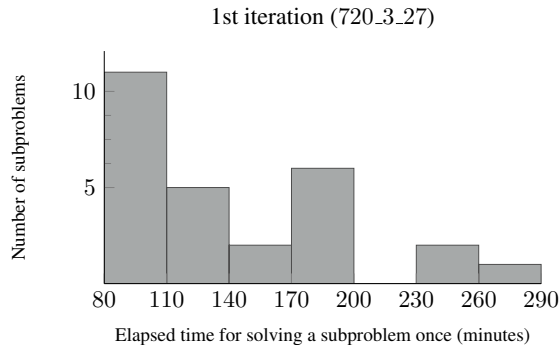


Figure 8.14: Histogram showing the frequency of subproblems in the 720_3_27 test instance terminating within specified time intervals. The example illustrates the experienced challenge with running a distributed, synchronous parallel program on a shared cluster, where interfering traffic cause increases in the elapsed time required for some of the subproblems in the PHA.

Summarized, the PHA exhibits interesting properties which makes it highly suitable for solving problems with multiple long-term scenarios. The PHA is both able to solve problems with a high number of long-term scenarios and, in fact, once the number of long-term scenarios and problem complexity increases sufficiently the PHA is observed to reach convergence faster than the direct method. Through testing, it is shown that the algorithm scales well, but only under the assumption that computational resources are available, which enables additional scenarios to be added to new processors. The following part of the computational study is included to get an understanding of the computational resources required by the PHA for solving a particular problem.

8.4.2 Computational Resources Required for Solving the Problem

The PHA is able to solve large instances of the EMPIRE model, much larger than the instances that the direct solving method is capable of. This is due to the extensive parallelization and distributed computations across multiple processes on a shared cluster. This allows the algorithm to utilize the computational resources in a different manner than the direct solving method, replacing the need of *one* large resource with good computational specifications with *multiple* resources, possibly with poorer specifications. As a result, the computational requirements of the two methods differ both in terms of (1) memory availability and (2) CPU capacity.

In terms of memory availability, there are clear differences between the requirements of the PHA and the direct solving method. A summary of the memory requirements is given in Table 8.8. In the PHA each individual subproblem requires less memory than the comparable total problem solved directly. This enables the subproblems in the PHA to be solved on computer hardware with lower available memory capacity than what is required for solving the total problem directly. Still, if the memory requirements per subproblem are aggregated to compare the total requirements of a single iteration of the PHA with the direct solving method, it is apparent that the total memory requirements of the PHA vastly exceed the ones of the direct solving method. The aggregated memory mimics the sum of the distributed memory capacity utilized by all processes when the PHA is solved in parallel. For example, solving 240_3.4 with the PHA in parallel requires as much as 41.6 GB aggregated memory in each iteration (10.4 GB per subproblem and 4 subproblems). This is almost the double of what is required by the direct method for solving the same problem, which only requires a maximum of 23.1 GB. Therefore, even though each subproblem requires less memory than the total problem, the aggregated memory capacity for the parallel version of the PHA exceeds the requirements of the direct solving method.

Table 8.8: Memory availability requirements for the progressive hedging algorithm and the direct solving method. The requirements refer to the maximum available memory capacity that is needed to solve a problem, either in one subproblem, aggregated for all subproblems in parallel, or directly. The table is included to illustrate the differences in memory utilization between the methods.

Test instance	Progressive Hedging			Direct Solving
	Required memory per subproblem (GB)	Number of subproblems (#)	Aggregated required memory in parallel (GB)	Total required memory (GB)
72_2.4	2.1	4	8.4	8.4
72_2.8	2.1	8	16.8	16.7
72_2.27	2.1	27	56.7	43.7
240_3.4	10.4	4	41.6	23.1
240_3.8	10.4	8	83.2	46.2
240_3.27	10.4	27	280.8	–
720_3.4	30.1	4	120.4	100.4
720_3.8	30.1	8	240.8	–
720_3.27	30.1	27	812.7	–

The distributed PHA requires a large number of available CPUs to solve all subproblems during a single iteration. In Table 8.9 the *CPU time* is shown for both the PHA and the direct solving method. Note that the notion of CPU time is different from the elapsed time to solve the problem previously used as a metric for time complexity in this chapter. The CPU time is the time a CPU spends on processing instructions of a computer program, as opposed to waiting for IO or being in low-power mode. In programs that utilize multiple cores in its execution, the CPU time might exceed 100 percent of the elapsed time to solve the problem. Since each subproblem in the PHA spans one process that utilizes multiple cores, the CPU time therefore gives an indication of the required resources to solve a single iteration of the algorithm. As can be seen from the table, the required resources to

solve a single iteration of the PHA significantly exceeds the required resources for solving the problem directly.

Table 8.9: The CPU time for the progressive hedging algorithm (1 iteration) and the direct solving method. The table is included to illustrate the large differences in CPU resources needed between the methods. Note that CPU time refers to the time a CPU spends on processing instructions of a computer program, and is different from the elapsed time to solve the problem, previously used as a metric for time complexity.

Test instance	Progressive Hedging (per iteration)			Direct Solving
	CPU time per subproblem (Minutes)	Max number of subproblems (#)	Total CPU time (Minutes)	Total CPU time (Minutes)
72_2_4	73	4	294	120
72_2_8	152	8	1 219	252
72_2_27	464	27	12 529	1 531
240_3_4	304	4	1 215	405
240_3_8	616	8	4 924	556
240_3_27	2 145	27	57 921	–
720_3_4	1 079	4	4 317	789
720_3_8	2 405	8	19 237	–
720_3_27	8 115	27	219 116	–

The results presented in this section indicate that the aggregated computational resources required for solving a single iteration of the distributed PHA significantly exceed the requirements for solving the problem directly. However, due to the decomposition of the large problem into smaller subproblems in the PHA, the algorithm is able to utilize the hardware infrastructure differently and hence divide the aggregated load into decentralized computations, with the result that much larger problem instances can be solved.

8.4.3 Final results

To summarize the above discussions, a comparison between the final results of solving the test instances with both the PHA and the direct solving method is conducted. The intention of this study is to better understand the quality of the solutions obtained by the PHA relative to the exact solution and the optimality bounds. In Table 8.10, the final results of solving the test instances with the different methods are presented. The parameters ρ , ϵ and b are set according to the suggested value from the calibration procedure in the primer parts of this chapter, such that $\rho = 1000$, $\epsilon = 2$, and $b = 1$. Note that the optimal value of ρ was previously found to be specific for the various instances. For comparison across test instances, all results in Table 8.10 are generated from $\rho = 1000$, even though other values of ρ was found to produce even tighter bounds for particular test instances. This is done to enable comparisons of the elapsed time required to solve the problem instance and the required number of iterations to reach the convergence criterion.

²The results were generated with $\rho = 500$

Table 8.10: The final results of comparing the progressive hedging algorithm with the direct solving method. Parameters $\rho = 1000$, $\epsilon = 2$ and $b = 1$.

Test instance	Direct solving		Progressive Hedging				
	Optimal cost	Time	Best known ub	Time	Iterations	Gap	
	(10^9)	(H:M)	(10^9)	(H:M)	(#)	(ub to z^*)	(ub to lb)
72_2.4	2514.164	00:29	2514.511	03:15	39	0.018 %	0.014 %
72_2.8	2547.036	01:18	2550.015	04:42	51	0.117 %	0.140 %
72_2.27	2553.321	16:14	2561.207	04:43	38	0.308 %	0.343 %
240_3.4	2716.757	02:59	2717.703	09:59	20	0.035 %	0.041 %
240_3.8	2705.270	09:14	2707.460	09:22	21	0.081 %	0.141 %
240_3.27	–	–	2717.318	15:08	16	–	0.168 %
720_3.4	2532.895	13:33	2534.147	51:08	13	0.049 %	0.081 %
720_3.8	–	–	2525.042	59:46	21	–	0.158 %
720_3.27 ²	–	–	2624.251	66:47	23	–	0.070 %
720_3.81	–	–	2615.249	73:07	18	–	0.117 %

From Table 8.10 it can be seen that all of the optimality gaps are found to be tighter than 0.35 % for the test instances. In addition, by comparing the obtained solutions from the PHA with the exact solution from the direct solving method for relevant test instances, all of the gaps are found to be tighter than 0.31 %. Both these results indicate that the PHA is capable of finding solutions that are sufficiently close to the optimal solution.

As a proof of concept, the algorithm is applied to solve the test instance 720_3.81, including 81 long-term scenarios, with over 1.2 billion variables and 1.7 billion constraints. When solving this instance with the PHA, an optimality gap of 0.2 % was obtained in less than 48 hours, and a gap of 0.1 % was obtained in about 73 hours. This illustrates that the algorithm scales with additional long-term scenarios, as long as computational resources are available to handle the increased number of subproblems.

8.5 Summary of the algorithm's performance

In this chapter, a computational study of the PHA has been conducted. The main focus has been to (1) calibrate and understand the properties of the parameters used in the algorithm, and (2) assess the quality of the obtained solutions.

In the calibration procedure, it was shown that the optimal choice of ρ is highly problem specific and varies for the different sets of short- and long-term input data. Nonetheless, an initial range of ρ -values was found, and further tests showed that satisfactory optimality gaps are provided within a reasonable number of iterations for all test instances. The value of the convergence criterion ϵ and the bundling factor b per subproblem was also studied and was found to have a smaller impact on the convergence properties of different test instances. The ϵ -parameter was set to 2, as this choice was shown to generate satisfactory optimality gaps for all test instances. In addition, the bundling factor b was calibrated to 1 to allow for agile testing.

In the latter part of the chapter the performance and solutions obtained with the PHA

were compared to the direct solving method. It was shown that the distributed implementation of the PHA is capable of handling the increased complexity resulting from including a large number of long-term scenarios. The algorithm showed impressive properties of scalability with increasing numbers of long-term scenarios, as long as computational resources are available. The final results obtained from solving the test instances with both the PHA and the direct solving method was presented, showing that the PHA finds tight optimality gaps for all test instances in a reasonable amount of time.

In the next chapter, to verify the implications of including long-term uncertainty in capacity expansion models, a thorough analysis of the techno-economic implications of modeling short-term operational uncertainty and long-term political uncertainty through stochastic emission restrictions has been conducted. The study is conducted on the test instance 720_3_27 presented in this chapter.

Techno-Economic Implications of Political Uncertainty

In chapter 2-4 the problem of capacity expansion in power systems was introduced, including a review of how this problem can be modeled mathematically and how uncertainty can be incorporated in the model. Further, in chapter 5, the version of the linear optimization model EMPIRE with long-term uncertainty was presented, followed by a method and algorithm for solving this model in chapter 6. Chapter 7 presented important input data and methods for generating long- and short-term scenarios for the model, while chapter 8 provided a thorough review of the performance of the implemented progressive hedging algorithm. Although a lot of the work conducted as part of this thesis has consisted of developing the mentioned solution method and algorithmic infrastructure in order to be able to solve large-scale stochastic programs, an analysis of the techno-economic implications of including long-term uncertainty in the LSSCEPPS should also be performed. This analysis is based on the hypothesis that the inclusion of long-term uncertainties in the model can give insights beyond the scope of an analysis based on a long-term deterministic approach. Therefore, in this chapter the value of the extensive implementation work will be demonstrated by analyzing the results from solving model instances with a large number of long-term scenarios for political uncertainty. In the model, the political uncertainty has been implemented through stochastic long-term development of CO₂-emission constraints.

As will be further elaborated in section 9.1 below, a sufficiently large amount of long-term scenarios has to be included in the model to capture the value of modeling long-term uncertainty. Therefore, a test instance with 27 long-term scenarios has been used in the analyses in this chapter. This is considered to be enough to illustrate the effect of including long-term uncertainty, but still not too much to grasp for policymakers. In addition, the largest short-term data set has been used to capture as realistic operational characteristics as possible. As a result, all analyses in this chapter are conducted using the 720_3_27 test instance, as presented in Table 8.2 in chapter 8. For reference, the scenario tree for 27 long-term scenarios is presented in Table 7.2 and Figure 7.5 in chapter 7.

As discussed in chapter 4, the foundation of stochastic optimization is the alternation between decisions to be made and revelation of uncertain information, followed by new recourse decisions to be made. This structure is enforced for the short-term uncertainty in the model by separating investment variables from operational variables, but for the long-term uncertainty, this structure is not enforced without further ado. The reason for this is that in the model formulation presented in chapter 5, investments are allowed after long-term uncertainty is revealed, but before a new operational period is considered. As a result, the model can tailor investments for each long-term scenario after the uncertainty is revealed but before their usefulness and profitability is assessed in an operational period. Hence, without extensions to the model formulation presented in chapter 5 it can be viewed as a long-term rolling horizon deterministic scenario analysis with short-term uncertainty, and not a model with both long- and short-term stochastics.

To capture the structure of alternation between investment decisions and revelation of long-term uncertainty, a delay from the timing of the investment decision to the time the capacity is available needs to be introduced. This is implemented in the model by not allowing investments in stages after long-term uncertainty revelation, i.e. after a branching stage in the long-term scenario tree. This modeling choice is equivalent to assuming a five-year building process for all infrastructure technologies. Note that in stages where uncertain long-term information is not revealed, there are no issues with assuming that capacity is available at the instant the decision is made (possibly apart from negligible differences in the discount factor for the timing of payments), since the building process can commence earlier in order to make the capacity available when needed. Also note that this argument only holds for long-term deterministic models, simply because optimal decisions from long-term stochastic models cannot be implemented before the uncertainty has been revealed.

As presented in the scenario tree including 27 long-term scenarios in chapter 7, the revelation of long-term uncertainty happens in investment stage 3, 5 and 7. These stages are denoted branching years in Table 8.2 in chapter 8. In terms of actual years these stages correspond to 2020, 2030 and 2040, since the planning horizon of the model spans nine five-year investment stages from 2010 (corresponding to investment stage 1) to 2050 (corresponding to investment stage 9). As a result of the time-delay discussion above, investments are not allowed in the model in investment stage 4, 6 and 8, corresponding to 2025, 2035 and 2045, respectively. It is also worth mentioning that since the EMPIRE model was originally developed to optimize power system capacity expansion from 2010-2050, 2010 and 2015 are included in the model even though they are historical years. Therefore, investments are not allowed for the first two stages corresponding to 2010 and 2015, meaning that only already installed infrastructure can be utilized when optimizing the operations of the system for these five-year periods.

In Figure 2.1 in chapter 2, the two most important outputs from a model for the LSS-CEPPS were presented – (1) the expected costs of optimal power system development during the planning horizon considered, and (2) the optimal infrastructure investment decisions during this horizon. The techno-economic analyses conducted in this chapter will be structured according to these two outputs. Section 9.1 embarks on a deep-dive into the implications of including long-term political uncertainty on the total expected, discounted costs of the system, while section 9.2 analyzes the implications of long-term political un-

certainty on the optimality of infrastructure investment decisions. Since the backbone of the treatment of uncertainty in this thesis is the hypothesis that a stochastic programming (SP) approach can give insights that a rolling horizon (RH) deterministic approach is unable to identify, the analyses in both sections will be centered around a comparison between these two fundamentally different modeling approaches. A summary and discussion of the most important techno-economic implications identified in the analyses will be provided at the end of the chapter in section 9.3.

9.1 The effect of political uncertainty on expected costs

9.1.1 The Value of a Long-Term Stochastic Solution

In section 4.1.3 of chapter 4, the difference between using the SP- and the RH-approach when formulating a mathematical model was explained. It was argued that the RH-approach yields the *expected result of using the rolling horizon expected value solution* (ERHEV), and that the value of including stochastics in the model (the VSS) can be obtained using equation (4.4) from that chapter, i.e. by finding the difference in objective value between the SP- and the RH-approach. Note that this VSS-calculation yields the value of including both long-term and short-term uncertainty compared to assuming perfect foresight about long-term parameters and only including uncertainty in short-term inputs. This subtle detail has an important implication for how the VSS should be interpreted. That is, it implies an assumption that the engineers designing the power system have accounted for short-term operational fluctuations, but that investment decision makers have neglected the low-frequent uncertainties affecting the long-term parameters in the model.

Table 9.1 presents the results from VSS-calculations for multiple different test instances. Similarly to the previous chapter, test instances are denoted by the naming convention <operational hours>.<short-term scenarios>.<long-term scenarios>. The values in the table indicate that introducing long-term political uncertainty in the model has significant value when a sufficient amount of long-term scenarios are included, ranging from 7.9% to 11.6% in the cases of 8 and 27 long-term scenarios. It is also worth noting that in the cases of 4 long-term scenarios, the VSS is negligible, indicating that more branching stages in the long-term scenario tree, and therefore a higher number of long-term scenarios, is necessary to capture the value of modeling long-term uncertainty. This observation supports the choice of using a test instance with 27 long-term scenarios in the analyses conducted in this chapter.

9.1.2 Detailed analysis of total expected costs

In this section, the total expected system costs for the SP- and the RH-approach will be analyzed in detail. The hypothesis that the SP-approach results in hedging actions compared to the RH-approach will also be analyzed. The terms hedging action, hedging behavior or hedging investment refers to the behavior of spending more on investments in infrastructure capacity early in the planning horizon in order to reduce future expected costs. Such strategies reduce the need for remedy investments later in the planning horizon. The term

Table 9.1: The Value of a Stochastic Solution for some test instances

Test instance	Best known stochastic solution (bn € ₂₀₁₀)	Rolling horizon det. solution (bn € ₂₀₁₀)	VSS	
			(bn € ₂₀₁₀)	(%)
240_3_4	2692.0	2693.6	1.6	0.1 %
240_3_8	2705.3	3060.9	355.6	11.6 %
240_3_27	2715.3	3011.3	296.0	9.8 %
720_3_4	2497.4	2501.6	4.2	0.2 %
720_3_8	2526.3	2742.4	216.1	7.9 %
720_3_27	2624.3	2854.8	230.6	8.1 %

remedy action or remedy investment will throughout this chapter refer to cases where too low amounts of capacity have been installed in early stages, resulting in a need to invest heavily, possibly at a high cost, to satisfy the operational requirements of certain scenarios. Thus, remedy actions can be viewed as the opposite of hedging actions.

To set the context for the rest of the analyses in this section, three descriptive charts of the expected costs over the planning horizon is presented. Note that all expected costs presented in this chapter are long-term and short-term probability weighted sums discounted to 2010-values and denoted in billion €. In the charts to follow, the optimal expected costs for the 720_3_27 test instance is broken down into different components – investment costs and operational costs. Investment costs are further divided into five categories – the costs of investing in low-CO₂ generation capacity, high-CO₂ generation capacity, transmission capacity, storage power capacity and storage energy capacity. Furthermore, the operational costs are divided into the cost of power generation and the cost of lost load. In the first three descriptive charts, only a split between investment costs and operational costs has been applied.

In Figure 9.1 the optimal expected system costs generated by the SP-approach are broken down by infrastructure type and technology. Note that the split between different generation technologies and for transmission is aggregated to a less granular level of detail compared to the technologies presented for the input data in the appendix. This is done to simplify the analyses. From Figure 9.1 it is observed that a few key generation technologies, in addition to investments in transmission and storage, make up most of the expected costs. In addition, the figure shows that apart from the cost of lost load, only fuel requiring generation technologies add to the operational costs of the system.

A similar breakdown of the expected system costs is done per country in Figure 9.2. Although a handful of countries contribute a lot to the total expected system costs, it is evident that many smaller countries also contribute with a meaningful amount to the expected costs.

In Figure 9.3 the expected costs are broken down per five-year investment stage. In addition, a comparison between the SP- and the RH-approach has been included. Note that due to the discounting of future costs to 2010-values, the expected costs in the figure have a downward trend. Also note that as discussed in chapter 5, operational costs are only optimized for a limited amount of typical hours in the model, in this case, 720 hours or 30 full days. The operational costs for these 30 full days are then scaled to reflect the costs of operating the power system over a full five-year period. As a result, operational costs are

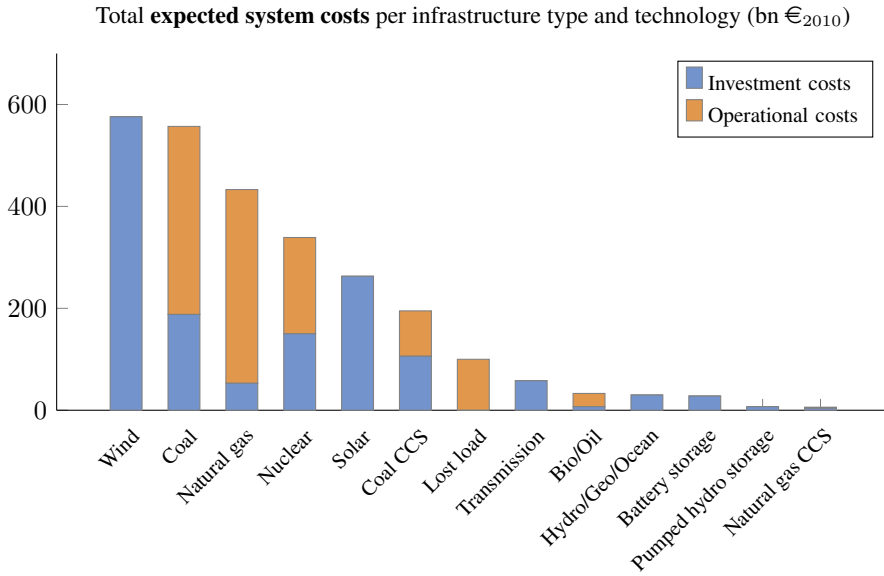


Figure 9.1: Breakdown of total expected, discounted system costs per infrastructure type and generation technology, generated by the stochastic programming (SP) approach.

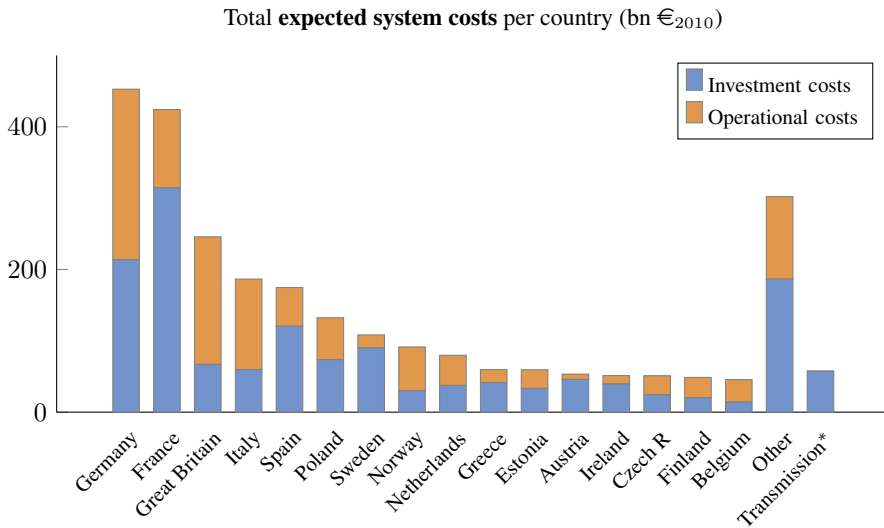


Figure 9.2: Breakdown of total expected, discounted system costs per country, generated by the stochastic programming (SP) approach. (*) Note that transmission investment costs have been included as a separate category, as these investment costs are split between the countries sharing the transmission infrastructure.

reported on a five-year basis, where for instance the operational costs reported for 2020 comprise the costs of operating the system from 2020-2025. Furthermore, following the discussion above, investments are not allowed in investment stages right after a branching stage in the long-term scenario tree, with the result that investments are only allowed in 2020, 2030 and 2040.

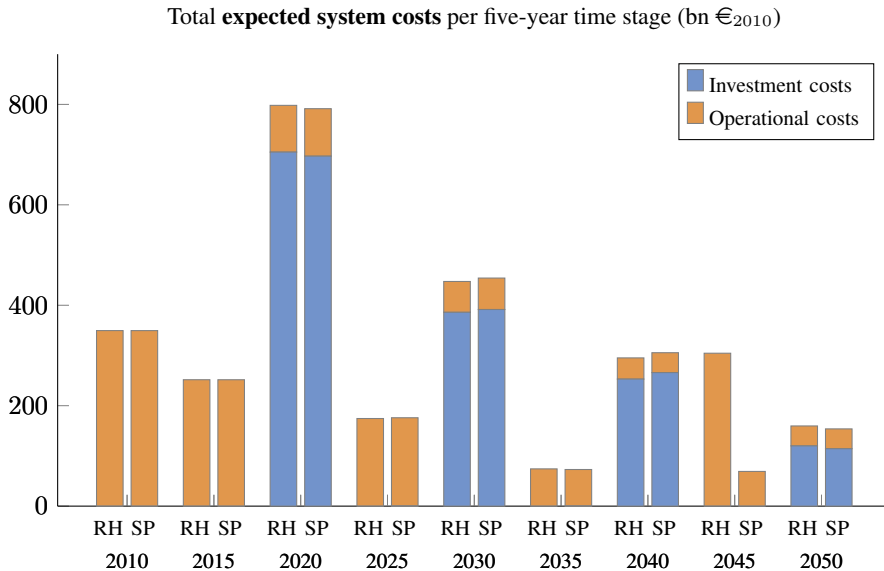


Figure 9.3: Breakdown of total expected, discounted system costs per five-year time stage. RH refers to the rolling horizon deterministic approach, while SP refers to the stochastic programming approach.

From Figure 9.3 slightly higher investment costs for the SP-approach relative to the RH-approach can be observed in the years 2030 and 2040, i.e. the investment stages where the second and third branching in the long-term scenario tree happen. This indicates that the SP-approach finds hedging strategies to be optimal in these stages. Similarly, indications of remedy investments in 2050 for the RH-approach can be observed. Another important observation from this chart is the high operational costs in 2045 in the RH-approach compared to the SP-approach. The mentioned observations indicate that hedging strategies are not very expensive, but that such strategies seem to vastly reduce the future expected operational costs of the system. Possible reasons for this result will be further analyzed in the paragraphs below.

Analysis of the expected costs of infrastructure investments

In the following paragraphs, the total expected, discounted costs related to infrastructure investments will be further analyzed. When studying hedging strategies in the context of uncertainty related to emission restrictions, it is natural to look at investments in generation technologies with high and low intensities of CO₂-emissions per unit of produced

electricity in a separate manner. The reason for this is that investments in low-CO₂ technologies should be considered as a hedging action against the possibility of more stringent emission restrictions in the future, while investments in high-CO₂ technologies should not. For this reason, a categorical distinction has been made between capacity investments in generation technologies with high and low CO₂-emission intensities, respectively. The intensities of CO₂-emissions per unit of electricity production for the different generation technologies are depicted in Figure 9.4.

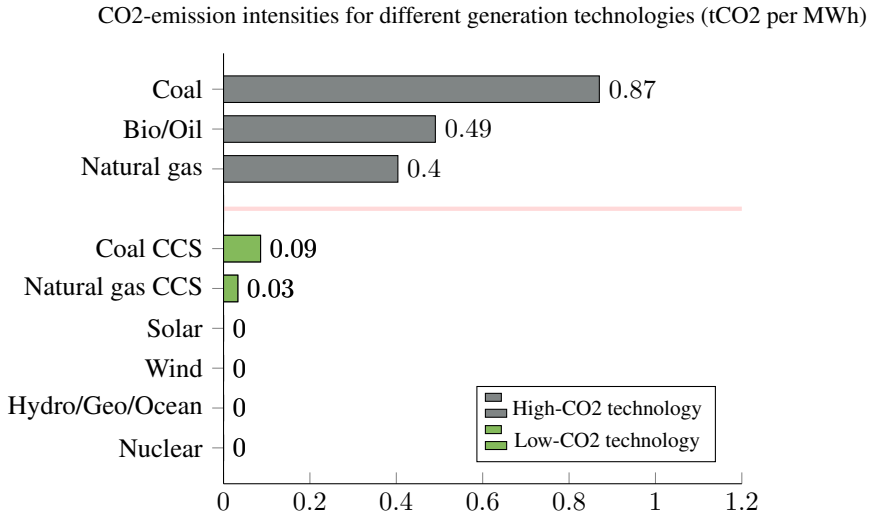


Figure 9.4: CO₂-emission intensities for different generation technologies. A distinction has been made between high and low CO₂-emission intensity technologies, as illustrated by the line in the chart.

In Figure 9.5, a breakdown of investment costs is presented per time stage where investments are made in the model. A distinction has been made between the SP- and the RH-approach, and the investment costs are split between the five different categories for investment costs mentioned above.

Figure 9.5 depicts some differences between the SP- and the RH-approach in terms of investment costs for the different infrastructure types. To make these differences more visible, a relative comparison has been made in Figure 9.6.

In Figure 9.6, the investment costs of the SP-approach relative to the RH-approach are presented. As a simple example, the investment costs of low-CO₂ generation investments in 2030 amount to €317.5 bn in the SP-approach and €311.3 bn in the RH-approach. This gives a relative investment cost in the SP-approach of $\frac{317.5-311.3}{311.3} = 2.0\%$, i.e. higher in the SP-approach than in the RH-approach. This means that in the SP-approach the model finds it optimal to spend 2.0% more on low-CO₂ generation technologies in 2030 compared to the RH-approach.

The figure provides further indications that the model chooses hedging investment decisions before long-term uncertainty is revealed. Recall that hedging actions are expected in 2020, 2030 and 2040 due to the branching stages of the long-term scenario tree for

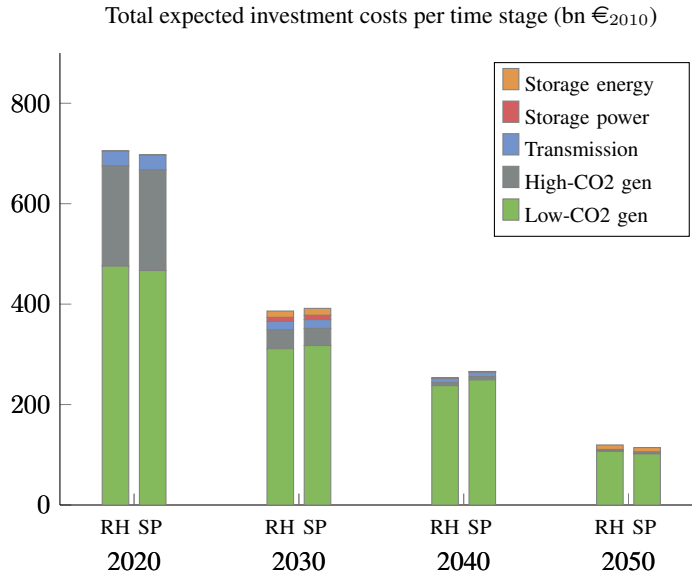


Figure 9.5: Comparison of investment costs for each investment stage for the SP- and RH-approach.

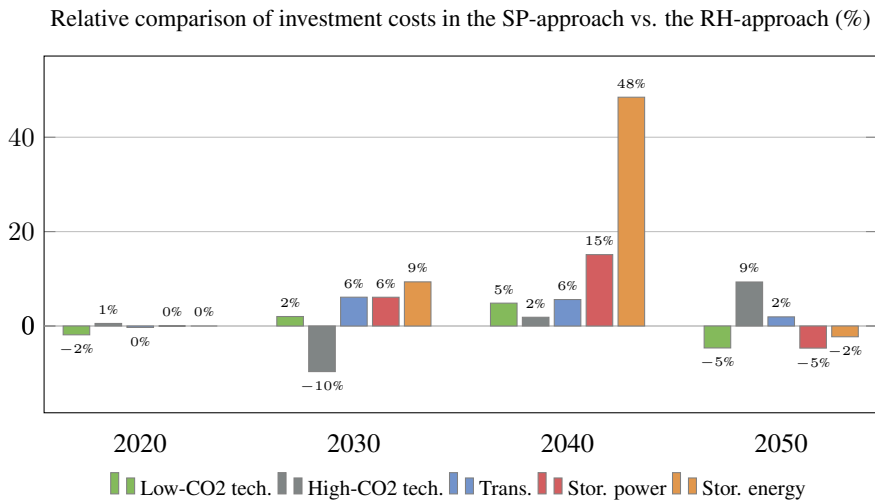


Figure 9.6: Relative comparison of investment costs in each investment stage for the SP- and RH-approach. Note that the large relative difference in storage energy investment costs in 2040 has to be seen in connection with the low absolute investment costs in storage energy in that year.

the 720_3_27 test instance, while remedy investments might occur in the last year when there is no uncertainty left to be revealed. Indeed, this expected behavior of the model seems to be correct. Although the results for 2020 is slightly ambiguous regarding the hedging behavior of the SP-approach, the results for 2030 and 2040 show clear indications of hedging. In both of these investment stages, the SP-approach chooses to invest more in low-CO₂ generation technologies compared to the RH-approach, as illustrated by the positive relative values. As expected, it also finds it optimal to invest less in high-CO₂ generation technologies in 2030 compared to the RH-approach, since investments in such technologies are not viewed as hedging investments in a context of uncertainty about emission restrictions. An explanation for the more surprising result that the SP-approach results in more high-CO₂ generation capacity in 2040 may be that more capacity is needed in general to limit future expected operational costs.

Furthermore, the SP-approach finds it optimal to invest more in both transmission and storage infrastructure compared to the RH-approach in 2030 and 2040. This is in line with the hypothesis that the SP-approach chooses hedging actions since the intermittency and uncontrollable nature of several renewable, low-CO₂ technologies requires transmission and storage infrastructure to ensure balance in the power system. In addition, remedy investments triggered by too low investments in low-CO₂ technologies in previous stages are observed in 2050 for the RH-approach. This can be seen from the fact that the RH-approach invests relatively more in low-CO₂ generation technologies and storages (i.e. the SP-approach invests relatively less) and relatively less in high-CO₂ generation technologies (i.e. the SP-approach invests relatively more).

Analysis of the expected costs of operating the system

In the following paragraphs, the total expected, discounted costs related to operations of the system will be further analyzed. Figure 9.7 presents a breakdown of operational costs per five-year time stage. The operational costs are split into the costs of power generation and the cost of lost load. The costs of power generation are made up of the variable costs from generation technologies requiring fuel inputs, such as natural gas, coal, bio-fuels, oil and nuclear. A distinction has also been made between the SP- and the RH-approach in the figure.

Two important conclusions can be drawn from studying Figure 9.7. First, the cost of lost load is comparatively equal for all five-year periods except from 2045, where it is orders of magnitude larger in the RH-approach. This explains parts of the reason why the SP-approach is superior to the RH-approach in the context of political uncertainty since this is evidence that the RH-approach is incapable of handling the political uncertainty in a proper manner.

The second observation made from Figure 9.7 is that the costs of power generation are slightly higher in the five-year operational periods from 2020 to 2030 in the SP-approach, while they are meaningfully lower in the five-year periods from 2035 to 2045. To make these differences more visible, a comparison of the costs of power generation for the SP-approach relative to the RH-approach has been made in Figure 9.8. The calculations of the values in the figure is similar to the procedure presented for the relative values in Figure 9.6.

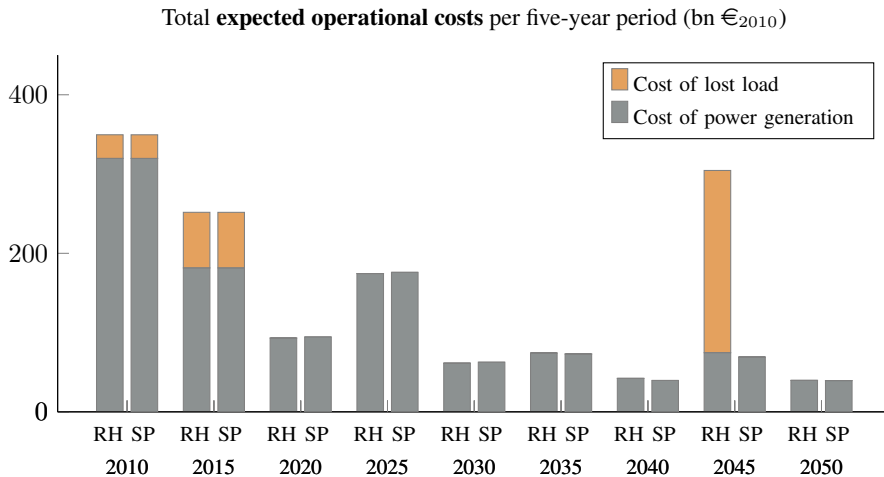


Figure 9.7: Comparison of operational costs for each five-year time period for the SP- and the RH-approach. The cost of lost load is comparative in all years but 2045, where it is drastically higher in the RH-approach.

The observation that the costs of power generation are slightly higher for the SP-approach in early years as compared to the RH-approach, indicates that the hedging behavior of the SP-

Based on the results presented above, it can be seen that the behavior of the SP-approach in early years generates more robust and cost-efficient solutions to future policy outcomes than the RH-approach. This is because the increased investment costs in the SP-approach is more than offset by the reductions achieved in future operational costs, as depicted in Figure 9.7 and 9.8. On the other hand, the increased operational costs in the RH-approach, both in terms of power generation costs and cost of lost load, can be explained by its overly optimistic and seemingly myopic approach to investments, lacking resilience and robustness to handle the different possible scenarios for emission restrictions that could be implemented in the future.

9.2 The effect of political uncertainty on infrastructure investments

In this section, the impact that long-term uncertainty in emission restrictions has on the optimality of investments in generation, transmission and storage infrastructure will be analyzed in detail. Note that in the analyses that will be presented in this section, it would not be reasonable to simply study the probability-weighted investment decisions, since the optimality of these decisions should be understood as conditional on a particular long-term scenario being realized. Hence, the number of distinguishable scenarios included in the analysis increases with each branching stage in the long-term scenario tree. Therefore, for 2020 there is only one distinguishable scenario to analyze, in 2030 there are three distin-

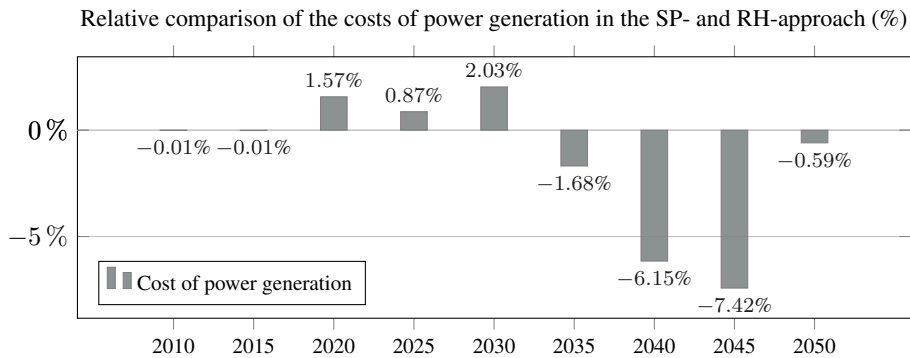


Figure 9.8: Relative comparison of the costs of power generation in each five-year period for the SP- and the RH-approach.

guishable scenarios (consisting of scenarios 1-9, 10-18 and 19-27 respectively), while in 2040 nine distinguishable scenarios have to be analyzed (consisting of scenarios 1-3, 4-6 and so on up to scenarios 25-27). Note that investment decisions are only analyzed for the investment stages corresponding to 2020, 2030 and 2040, as the investment decisions in 2050 are not made under uncertainty and that it would involve a cumbersome comparison of 27 distinguishable scenarios for both the SP- and the RH-approach.

9.2.1 Comparing investments in the SP-approach to the RH-approach

The comparisons of investment decisions in this section will be done for each investment stage, i.e. 2020, 2030 and 2040, in a separate manner. For each stage, two different analyses will be conducted. First, the absolute investment decisions for both the SP- and the RH-approach will be presented for all distinguishable long-term scenarios. Second, a relative comparison will be performed for the total accumulated infrastructure capacity installed at each investment stage. As a result, the first analysis will provide insights into the capacity additions in each investment stage, while the second analysis will provide a relative snapshot of the installed capacity at each stage, meaning that capacity retirements will also be accounted for in the second analysis.

2020-investments

The investment decisions for 2020 for different generation technologies are depicted in Figure 9.9. The figure validates the hedging actions of the SP-approach compared to the RH-approach, as more of the clean generation technologies wind and solar is installed. In addition, the SP-approach invests more in natural gas and less in coal compared to the RH-approach. This is an interesting observation that may explain the ambiguity alluded to in the 2020-numbers for relative investment costs in Figure 9.6. To understand this, a reference has to be made to Figure 9.4. Even though natural gas is categorized as a high-CO₂ generation technology, this figure shows that the CO₂-emission intensity of natural gas is less than half that of coal. Therefore, the observation that the SP-approach chooses to

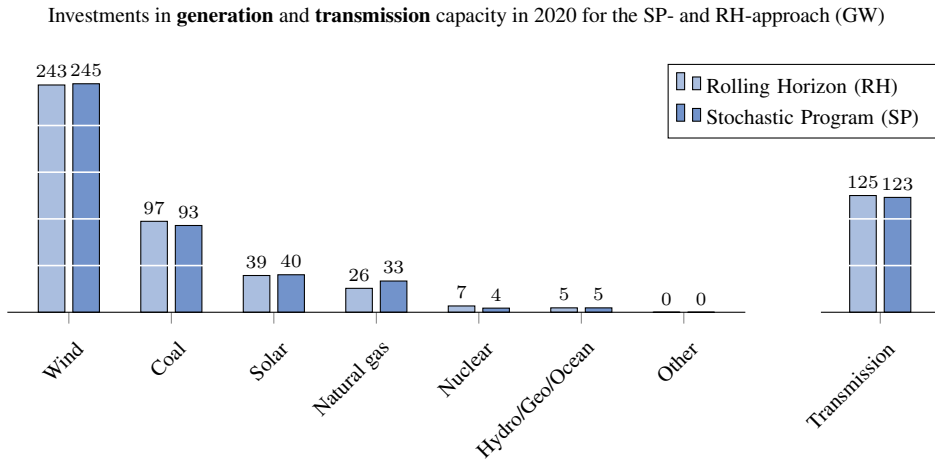


Figure 9.9: Investments in generation and transmission capacity in 2020 are compared for the SP- and the RH-approach.

invest relatively more in natural gas and relatively less in coal is in line with the hypothesis that the SP-approach invests in technologies with lower CO₂-emission intensities.

The total transmission investments in 2020 is also presented in Figure 9.9. This figure also confirms the hypothesis that the SP-approach chooses to invest more in transmission capacity with the target of introducing more flexibility in the power system and to balance fluctuations from intermittent, renewable generation. Note that no storage investments have been presented for 2020, simply because both approaches found it optimal to not invest in storage capacity in 2020. The reason for this may be that the expansion of intermittent, renewable generation has not come very far in 2020, making storage investments redundant that early in the planning horizon.

A relative comparison of the accumulated infrastructure capacities in 2020 for the SP- and the RH-approach is presented in Figure 9.10. The numbers in the figure present the relative differences in accumulated capacity for different technologies in the SP-approach compared to the RH-approach. As an example, the total optimal accumulated capacity for natural gas-fired generation in 2020 is 192 GW in the SP-approach and 184 GW in the RH-approach. This gives a relative difference in accumulated natural gas generation capacity of $\frac{192-184}{184} = 4.3\%$. This means that in the SP-approach the model finds it optimal to invest in such a manner that the accumulated natural gas generation capacity is 4.3% higher in 2020 compared to the RH-approach.

Figure 9.10 confirms the hedging behavior of the SP-approach in 2020 since accumulated capacities for both natural gas (which have a lower CO₂-emission intensity than e.g. coal), transmission, solar and wind are higher in the SP-case, while the capacity for coal is lower in the SP-case. The SP-approach also results in lower accumulated capacities for nuclear generation compared to the RH-approach despite the fact that nuclear is a low CO₂-emission intensity technology. Hence, it seems that the SP-approach favors investments in natural gas over nuclear. Both of the technologies are considered controllable generation sources and hence suited to complement power systems with high shares of

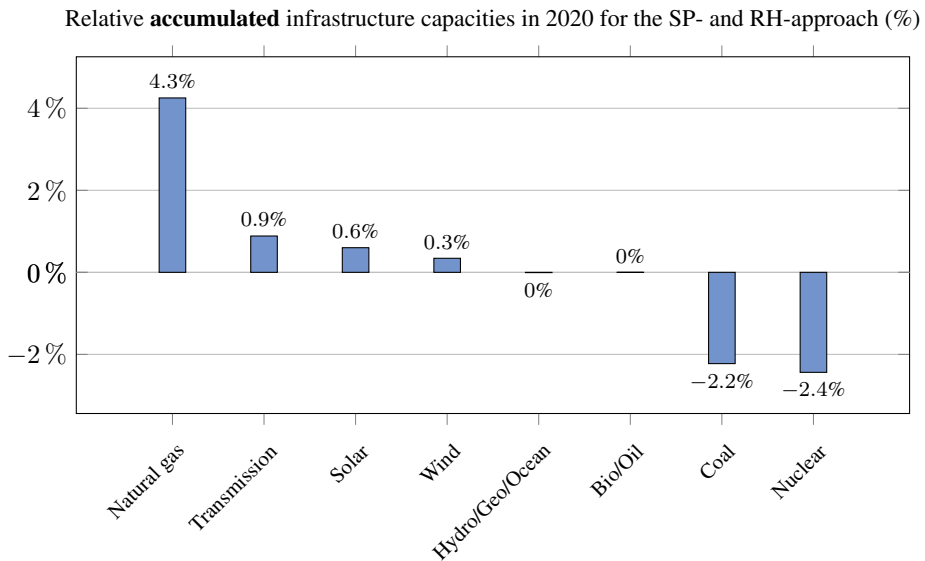


Figure 9.10: The figure shows the relative differences in accumulated capacity for different infrastructure technologies in 2020 in the SP-approach compared to the RH-approach.

intermittent renewable energy. However, the ramp-up characteristics of natural gas (i.e. the amount of time required to start up or increase production from the current production level) are significantly more flexible than for nuclear generation. This suggests that investments in natural gas provide more flexibility to the power system, which is preferable in the SP-approach due to the high accumulated capacities of intermittent, renewable generation capacity.

2030-investments

In Figure 9.11 the investment decisions for the different generation technologies in the investment stage corresponding to 2030 are presented. Since there are three distinguishable scenarios in 2030, a comparison between the SP- and the RH-approach has to be made for all three. That is, the dark blue bars for the SP-approach have to be compared to the light blue bars for the RH-approach, the dark green bars for the SP-approach have to be compared to the light green bars for the RH-approach, and so on. The results are somewhat ambiguous, however, hedging behavior is observed for solar investments in the first scenario and for coal generation with CCS-capabilities (i.e. a low-CO₂ generation technology) in all scenarios.

On the other hand, Figure 9.12 presents strong indications of hedging behavior for both transmission and battery storage investments. As discussed before, this is in line with a hedging strategy that invests in flexible solutions in order to balance possible future fluctuations in the power system from an increasing amount of renewable, low-CO₂ generation capacity.

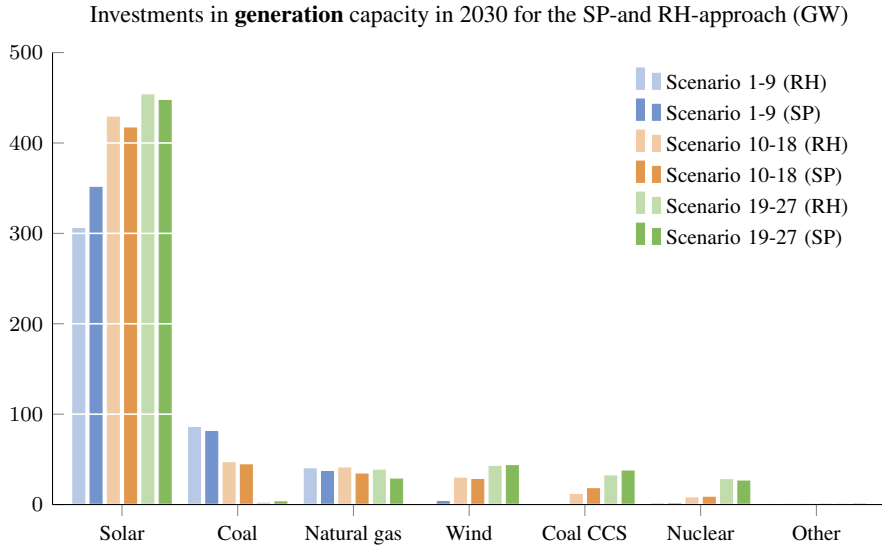


Figure 9.11: Investments in generation capacity in 2030 is compared for the SP- and the RH-approach. Since there are three distinguishable scenarios in the scenario tree in 2030, three different comparisons have to be made between the SP- and RH-approach. For each distinguishable scenario, a particular color has been chosen for eased comparison between the SP- and the RH-approach

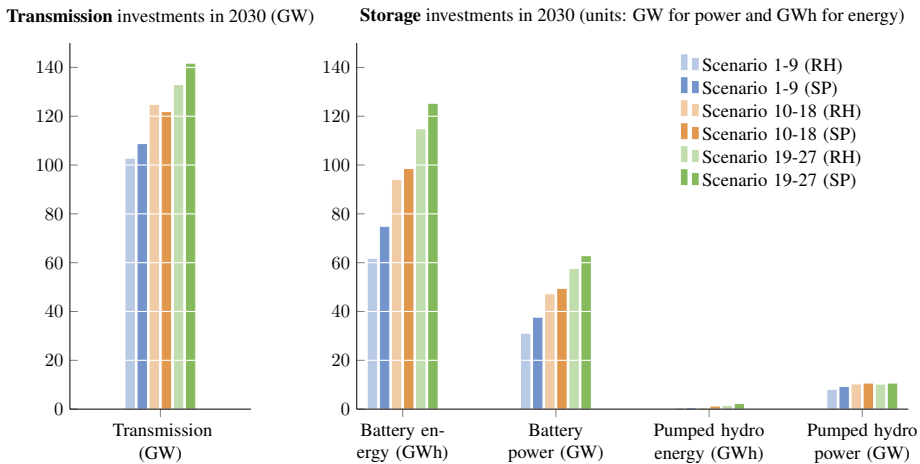


Figure 9.12: Investments in transmission and storage capacity in 2030 is compared for the SP- and the RH-approach. Since there are three distinguishable scenarios in the scenario tree in 2030, three different comparisons have to be made between the SP- and RH-approach. For each distinguishable scenario, a particular color has been chosen for eased comparison between the SP- and the RH-approach

Relative **accumulated** infrastructure capacities in 2030 for the SP- and RH-approach (%)

	Scenario 1-9	Scenario 10-18	Scenario 19-27
Coal CCS	>100 %	55.6 %	17.2 %
Batt. energy	21.4 %	4.8 %	9.1 %
Batt. power	21.4 %	4.8 %	9.1 %
Solar	10.6 %	-2.0 %	-0.9 %
Natural gas	5.6 %	1.3 %	-2.4 %
Transmission	2.6 %	-0.4 %	3.2 %
Wind	1.2 %	0.0 %	0.5 %
Pumped hydro energy	0.0 %	0.0 %	0.0 %
Pumped hydro power	2.0 %	0.6 %	0.7 %
Hydro/Geo/Ocean	0.0 %	0.0 %	0.1 %
Bio/Oil	0.0 %	0.0 %	0.0 %
Coal	-3.8 %	-3.5 %	-2.1 %
Nuclear	-3.8 %	-2.3 %	-4.3 %
Natural gas CCS	-21.3 %	-17.1 %	57.9 %

Figure 9.13: The table shows the relative differences in accumulated capacity for different infrastructure technologies in 2030 in the SP-approach compared to the RH-approach.

Figure 9.13 presents a relative comparison of accumulated infrastructure capacities in 2030 for the SP- and the RH-approach. This comparison for 2030 is analogous to the comparison presented for the 2020-capacities in Figure 9.10 in the sense that positive numbers mean higher investments in the SP-approach is found to be optimal. However, due to the large number of scenarios and infrastructure technologies, the comparison is presented in a tabular format. The results for all infrastructure types correspond very well with the hedging behavior hypothesis for the SP-approach, as this approach results in higher accumulated capacities in 2030 for both coal with CCS-capabilities, battery storage, natural gas, transmission infrastructure, wind capacity and pumped hydro storage in most scenarios, and for solar in one out of three scenarios. In addition, the SP-approach results in lower accumulated capacities for coal generation and nuclear.

2040-investments

In the investment stage corresponding to 2040, there are nine distinguishable scenarios, giving rise to nine different pairs of results for the SP- and the RH-approach to be analyzed. A selection of the results is presented in Figure 9.14, where generation investments for solar and wind capacity, transmission investments and battery energy storage investments for 2040 are presented. Similarly to the 2030-results, these charts have to be compared pairwise per color in order to see the differences between investment decisions in the SP- and the RH-approach. For completeness, the rest of the results can be found in the appendix.

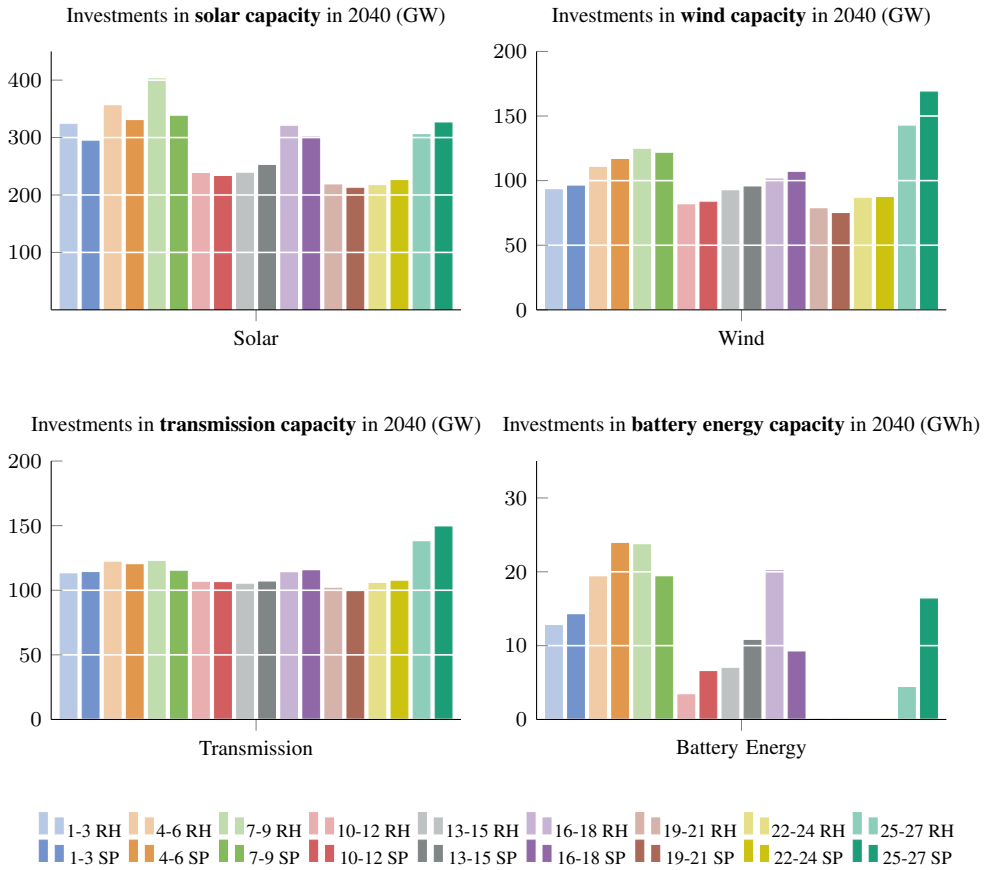


Figure 9.14: Investments in selected infrastructure types in 2040 is compared for the SP- and the RH-approach. Since there are nine distinguishable scenarios in the scenario tree in 2040, nine different comparisons have to be made between the SP- and RH-approach. For each distinguishable scenario, a particular color has been chosen for eased comparison between the SP- and the RH-approach. Note that results for the rest of the infrastructure types have been included in the appendix for completeness.

At first glance, the results seem quite ambiguous with little coherence. However, some insights in line with the hypothesis of hedging behavior for the SP-approach may still be extracted. First, investments in wind generation capacity are higher in the SP-approach compared to the RH-approach for most scenarios. This also applies to investments in battery energy investments. However, for many of the other infrastructure types, hedging behavior for the SP-approach is difficult to infer. An explanation for this may be that since the SP-approach has chosen to invest more heavily in both low-CO₂ generation technologies, transmission capacity and storage capacity in previous investment stages, the SP-approach may simply end up in a state where no more hedging investments are needed. That is, the SP-approach seems to be able to operate the power system in a robust and resilient manner during the rest of the planning horizon without investing a lot compared to the RH-approach. On the other hand, it may seem that the RH-approach has to embark on remedy investments already in 2040 to be able to comply with given operational requirements.

Figure 9.15 supports this explanation. That is, it shows that compared to the RH-approach, the SP-approach results in higher accumulated capacities in 2040 in most of the scenarios for most of the infrastructure types for which hedging investments should be expected, such as battery investments, coal with CCS-capabilities, natural gas, solar and wind capacity and transmission. Accumulated capacity for coal generation is also lower in the SP-approach.

Relative **accumulated** infrastructure capacities in 2040 for the SP- and RH-approach (%)

	Scenario 1-3	Scenario 4-6	Scenario 7-9	Scenario 10-12	Scenario 13-15	Scenario 16-18	Scenario 19-21	Scenario 22-24	Scenario 25-27
Battery energy	20 %	22 %	10 %	8 %	8 %	-6 %	9 %	9 %	19 %
Battery power	20 %	22 %	10 %	8 %	8 %	-6 %	9 %	9 %	19 %
Coal CCS	6 %	-1 %	5 %	8 %	4 %	7 %	0 %	7 %	-21 %
Natural gas	9 %	4 %	4 %	3 %	-1 %	2 %	1 %	-5 %	-3 %
Solar	2 %	3 %	-2 %	-2 %	0 %	-4 %	-1 %	0 %	2 %
Wind	2 %	3 %	0 %	0 %	1 %	1 %	0 %	1 %	6 %
Transmission	2 %	1 %	0 %	0 %	0 %	0 %	2 %	3 %	5 %
Nuclear	-9 %	-6 %	2 %	3 %	-1 %	-3 %	8 %	-6 %	13 %
Hydro/Geo/Ocean	0 %	0 %	0 %	0 %	0 %	0 %	0 %	0 %	0 %
Bio/Oil	0 %	0 %	0 %	0 %	0 %	0 %	0 %	0 %	0 %
Pumped hydro energy	0 %	0 %	0 %	0 %	0 %	0 %	0 %	0 %	0 %
Pumped hydro power	0 %	0 %	0 %	0 %	0 %	0 %	0 %	0 %	1 %
Coal	-4 %	-2 %	-5 %	-4 %	-1 %	-4 %	-4 %	-1 %	-3 %

Figure 9.15: The table shows the relative differences in accumulated capacity for different infrastructure technologies in 2040 in the SP-approach compared to the RH-approach. Positive values indicate that higher accumulated capacities were found to be optimal in the SP-approach compared to the RH-approach.

9.3 Summarizing the techno-economic analyses

In this chapter, a thorough analysis of the techno-economic implications of introducing long-term stochastic emission restrictions in the model has been conducted. The analysis has been performed with the underlying hypothesis that a treatment of long-term uncertainties in the model can give insights beyond the scope of a long-term deterministic approach. Therefore, a stochastic programming (SP) approach including both short-term operational uncertainty and long-term political uncertainty has been compared to a rolling horizon (RH) long-term deterministic approach where only short-term operational uncertainty has been included. Both total expected system costs and the optimality of investment decisions has been analyzed and compared for the two approaches, and some very interesting insights have been identified.

The analyses of total expected system costs have provided some notable results. First and foremost, VSS-calculations for several different test instances indicated significant values of modeling both long- and short-term uncertainty compared to short-term uncertainty only, ranging from 7.9% to 11.6% in the cases of 8 and 27 long-term scenarios. In addition, the calculations showed that the VSS was negligible for test instances with fewer long-term scenarios, indicating that a higher number of long-term scenarios is needed to capture the effect of modeling long-term uncertainty. Another interesting observation has been that the alternation between decisions and revelation of uncertainty in stochastic programs introduces a need to assume a time-lag from investment decision to the capacity is available, i.e. a lead-time for capacity expansions, in order to capture the value of modeling uncertainty. By neglecting lead-times overly optimistic and unrealistic results were found, as the model was given unrealistically much flexibility. This indicates that there may be a value to shortening lead-times for infrastructure investments from the time the investment decision is made. It also indicates that the value of infrastructure types with shorter lead-times may increase when long-term uncertainty is introduced in the model.

Further insights from the analysis include that compared to the RH-approach, the SP-approach seems to favor hedging actions in stages before long-term uncertainty is revealed. That is, it seems to spend larger amounts on investments in infrastructure capacity that are robust to handle possible different realizations of political uncertainty. On the other hand, the RH-approach seems to be forced to spend more on remedy investments later in the planning horizon due to an overly optimistic and seemingly myopic approach to investments early in the planning horizon. The hedging behavior of the SP-approach is observed before all uncertainty in the planning horizon is revealed, both in terms of increased investments in low-CO₂ generation technologies, transmission infrastructure and storage capacity. Note that investments in transmission and storage are viewed as hedging investments due to their ability to introduce operational flexibility and balance fluctuations in the system induced by an anticipated increase in the amount of unpredictable and intermittent renewable generation capacity. On the other hand, the RH-approach seems to increase investments in the same types of infrastructure later on in the planning horizon, underlining the overly optimistic approach to investments in the beginning. If in addition natural gas is viewed as a low-CO₂ generation technology compared to coal (considering the significantly lower emission intensity in natural gas) and a more flexible alternative to nuclear (considering the favorable ramp-up characteristics of natural gas for increased flexibility), the pattern of hedging investments early in the planning horizon for the SP-approach and

remedy investments for the RH-approach later in the planning horizon becomes even more evident.

The analyses show that the hedging behavior of the SP-approach is not overly expensive, particularly if the extra investment costs are compared to the future reductions in expected operational costs. That is, the investment decisions of the RH-approach results in drastically higher operational costs compared to the SP-approach. Further research efforts should verify this result for different values of lost load, as the costs of lost load make up a meaningful amount of the operational costs. However, the conclusion still stands – compared to the SP-approach the RH-approach to modeling the LSSCEPPS with uncertainty related to long-term emission restrictions seems to be incapable of handling the inherent uncertainty of the problem in a proper manner.

To summarize, the above analyses show that a treatment of long-term uncertainty indeed has given insights that the long-term deterministic approach was unable to identify, even though short-term operational uncertainty has been included in both approaches. Results from the analyses indicate that politicians can significantly reduce the expected costs of power system capacity expansion by reducing uncertainty about future energy policy in general and uncertainty about regulations for CO₂-emission restrictions in particular. In addition, the results suggest that energy policy should facilitate transmission and storage expansion in order to promote the progress of capacity expansion of renewable, typically intermittent generation capacity. In the meantime, before these uncertainties are resolved, the above results indicate that hedging investments as defined in this chapter is both favorable and valuable for the European power system.

Conclusion

In 2011 the European Council reconfirmed the EU's objective to reduce greenhouse gas emissions by more than 80 percent in 2050 compared to 1990-levels. Due to the large emission reduction potentials of the European power system, almost complete decarbonization of the sector is implied. This transition will take place in a period of significant expected changes in the power system. Due to the high-cost and irreversible nature of power system capacity investments, careful planning and quantitative models are needed to identify optimal capacity expansion pathways. Such models quickly become too complex to handle due to the broad scope and granular level of detail required, often resulting in deterministic approaches being applied.

This thesis presents and formulates the Long- and Short-term Stochastic Capacity Expansion Problem for the Power System (LSSCEPPS) in Europe. In this problem, long-term investment decisions are simultaneously co-optimized with short-term operational decisions to obtain least-cost and robust capacity expansion pathways for the European power system in the presence of both long- and short-term uncertainty. A thorough review of treatment of uncertainty in power system capacity expansion models is conducted as part of the thesis, finding that, at least to the best of the authors' knowledge, no optimization models including both long- and short-term uncertainty have been developed in previous research efforts.

To bridge this gap in the research literature, the EMPIRE model, a capacity expansion model for the European power system, is extended to include both long- and short-term uncertainty in this thesis. However, accounting for stochastics in two time-scales significantly increases the complexity of the model, making direct solution methods incapable of solving realistic problem instances. Hence, improved solution methods are needed, motivating the work in this thesis with developing a distributed progressive hedging algorithm to solve large instances of the EMPIRE model by decomposing the model by long-term scenarios.

The performance of this distributed progressive hedging algorithm is tested through a comprehensive computational study on a number of different test instances. The algorithm is proven to generate tight optimality gaps below 0.35 percent within a reasonable time for

all test instances studied in the thesis, underlining its stable convergence properties. It is also shown to be capable of solving problem instances with as much as 81 long-term scenarios, 720 short-term operational hours and 3 short-term scenarios (resulting in a problem instance with more than 1.2 billion variables and 1.7 billion constraints), obtaining an optimality gap of about 0.1 percent in 18 iterations after approximately 70 hours. This clearly illustrates the algorithm's ability to solve much larger instances than direct solution methods. The algorithm is also found to scale very well when additional long-term scenarios are included, as long as sufficient computational resources are available. This is demonstrated by the result that both the number of iterations and the elapsed time required to solve an instance is more or less constant for test instances with differing numbers of long-term scenarios. The main contributor to time-complexity is, therefore, found to be the size of the short-term operational input data, which is proven to significantly affect the elapsed time required to solve different test instances.

To verify the practical implications of including long-term uncertainty in power system capacity expansion models, an analysis of the techno-economic implications of introducing stochastic long-term emission limits is presented. VSS-calculations indicate significant values of using a long- and short-term stochastic approach compared to a long-term deterministic approach with short-term uncertainty only, ranging from 7.9 to 11.6 percent for the test instances with 8 or 27 long-term scenarios. In addition, the calculations show that the VSS is negligible for test instances with fewer long-term scenarios, indicating that a larger number of long-term scenarios is needed to illustrate the effect of modeling long-term uncertainty. The analyses also show that it is necessary to assume a lead-time from investment decision to the time the capacity is made available to capture the value of modeling uncertainty. This is due to the alternation between decisions and revelation of uncertainty characterizing stochastic programs. By neglecting lead-times, overly optimistic and unrealistic results are found, simply because the model is given unrealistic flexibility. These findings indicate that there may be a value of infrastructure types and generation technologies with shorter lead-times when long-term policy uncertainty is introduced in the model.

Further insights from the analyses indicate that compared to the long-term deterministic approach, the stochastic approach seems to favor hedging actions in stages before long-term uncertainty is revealed. That is, compared to the deterministic approach, the stochastic approach spends slightly more on robust infrastructure investments that exhibit the flexibility needed to handle several different possible emission scenarios. This includes higher investments in low-CO₂ generation, transmission, storage, and even natural gas power plants. This latter observation can be explained by the lower CO₂-emission intensity of natural gas compared to coal, and favorable ramp-up characteristics compared to both coal and nuclear power. Thus, the results indicate that natural gas may be a suitable complement to the anticipated increased shares of intermittent, renewable power supply in the future power system.

The results obtained also show that, compared to the long-term deterministic approach, the hedging behavior exhibited by the stochastic approach is comparatively inexpensive when measured against the vast reductions in future expected operational costs. This finding shows that politicians can significantly reduce the expected costs of power system capacity expansion by reducing uncertainty about future energy policy. The above results

are also clear evidence that a treatment of long-term uncertainty in capacity expansion models indeed provides insights beyond the scope of a long-term deterministic approach, as the latter approach seems to be incapable of handling the inherent uncertainty of the problem in a proper manner.

Further research

In this thesis, a substantial effort has been devoted to developing a proprietary library of code that implements a distributed progressive hedging algorithm aiming to solve instances of the EMPIRE model with a large number of long-term scenarios. The algorithm has been proven to scale well with increasing numbers of long-term scenarios, but the size of the short-term operational input data has been shown to vastly impact the elapsed time of the algorithm. Therefore, a natural next step for further research is to study methods for solving each subproblem of the distributed PHA in a shorter time. One such method could be to implement warm-start of the next iteration using the previously obtained solution. This is viable since only the objective function is changed between each iteration of the PHA, while the feasible area stays the same. Another strategy for improving the solution time could be to implement improved solution methods for each subproblem, for instance by using Benders decomposition as presented in chapter 4.

Another issue of the distributed progressive hedging algorithm relates to its synchronous implementation. The algorithm is solved synchronously in parallel, giving rise to significant challenges regarding resource allocation and interfering traffic, which has been shown to limit the algorithm's performance. A potential opportunity to remedy some of these effects is to understand how the progressive hedging algorithm can be implemented as an asynchronous parallel program, which might result in improved utilization of the aggregated computational resources on a computing cluster.

In the formulation of the EMPIRE model used in this thesis, a homogeneous lead-time of five years has been implemented for all types of investment decisions. This is a simplification since different infrastructure types require different amounts of time to be installed. Motivated by the results found in this thesis, indicating that reduced lead-times may reduce the costs of uncertainty in stochastic models, an analysis where different lead-times for each technology is implemented could be an exciting area of future research.

Finally, in the techno-economic analyses conducted, small increases in investment costs due to hedging behavior in the long-term stochastic approach were shown to reduce future expected operational costs drastically. A potential weakness with this observation is that a large portion of this increase comes from increases in the costs of lost load. As a result, further research efforts should verify the results obtained in this thesis by conducting sensitivity analyses for different values of lost load.

Bibliography

Abdolmohammadi, H. R., Kazemi, A., 2013. A benders decomposition approach for a combined heat and power economic dispatch. *Energy Conversion and Management* 71, 21 – 31.

URL <http://www.sciencedirect.com/science/article/pii/S0196890413001568>

Aertsens, J., Proost, S., Van Regemorter, D., 1999. Optimal investment strategy under uncertainty in the belgian energy system.

Akbari, T., Rahimikian, A., Kazemi, A., 2011. A multi-stage stochastic transmission expansion planning method. *Energy Conversion and Management* 52 (8), 2844 – 2853.

URL <http://www.sciencedirect.com/science/article/pii/S019689041100104X>

Archibald, T. W., Buchanan, C. S., McKinnon, K. I. M., Thomas, L. C., May 1999. Nested benders decomposition and dynamic programming for reservoir optimisation. *Journal of the Operational Research Society* 50 (5), 468–479.

URL <https://doi.org/10.1057/palgrave.jors.2600727>

Ben-Tal, A., Nemirovski, A., May 2002. Robust optimization – methodology and applications. *Mathematical Programming* 92 (3), 453–480.

URL <https://doi.org/10.1007/s101070100286>

Benders, J. F., Dec 1962. Partitioning procedures for solving mixed-variables programming problems. *Numerische Mathematik* 4 (1), 238–252.

URL <https://doi.org/10.1007/BF01386316>

Bertsimas, D., Brown, D. B., Caramanis, C., Aug. 2011. Theory and applications of robust optimization. *SIAM Rev.* 53 (3), 464–501.

URL <http://dx.doi.org/10.1137/080734510>

Birge, J. R., Oct. 1985. Decomposition and partitioning methods for multistage stochastic linear programs. *Oper. Res.* 33 (5), 989–1007.

URL <http://dx.doi.org/10.1287/opre.33.5.989>

-
- Birge, J. R., Louveaux, F., 2011. Introduction to Stochastic Programming, 2nd Edition. Springer Publishing Company, Incorporated.
- Bistline, J. E., Weyant, J. P., Nov 2013. Electric sector investments under technological and policy-related uncertainties: a stochastic programming approach. *Climatic Change* 121 (2), 143–160.
URL <https://doi.org/10.1007/s10584-013-0859-4>
- Boyd, S., Parikh, N., Chu, E., Peleato, B., Eckstein, J., Jan. 2011. Distributed optimization and statistical learning via the alternating direction method of multipliers. *Found. Trends Mach. Learn.* 3 (1), 1–122.
URL <http://dx.doi.org/10.1561/22000000016>
- Boßmann, T., 04 2015. The contribution of electricity consumers to peak shaving and the integration of renewable energy sources by means of demand response.
- Capros, P., Paroussos, L., Fragkos, P., Tsani, S., Boitier, B., Wagner, F., Busch, S., Resch, G., Blesl, M., Bollen, J., 2014. Description of models and scenarios used to assess european decarbonisation pathways.
URL https://ac.els-cdn.com/S2211467X13001065/1-s2.0-S2211467X13001065-main.pdf?_tid=0ecae3c0-cdd5-11e7-b27c-00000aab0f6c&acdnat=1511170242_ac4707a96700b86d799f8be55c23bb7f
- Castro, R., Faias, S., Esteves, J., 2016. The cost of electricity interruptions in portugal: Valuing lost load by applying the production-function approach. *Utilities Policy* 40, 48 – 57.
URL <http://www.sciencedirect.com/science/article/pii/S0957178716300972>
- Condevaux-Lanloy, C., Fragnière, E., Sep 2000. An approach to deal with uncertainty in energy and environmental planning: the markal case. *Environmental Modeling & Assessment* 5 (3), 145–155.
URL <https://doi.org/10.1023/A:1019061628063>
- Conejo, A., Castillo, E., Minguez, R., Garcia-Bertrand, R., 2006. Decomposition Techniques in Mathematical Programming: Engineering and Science Applications. Springer Berlin Heidelberg.
URL <https://books.google.no/books?id=gdJDAAAAQBAJ>
- Dantzig, G. B., 1955. Linear programming under uncertainty. *Management Science* 1 (3-4), 197–206.
URL <https://EconPapers.repec.org/RePEc:inm:ormnsc:v:1:y:1955:i:3-4:p:197-206>
- de Joode, J., Ozdemir, O., Veum, K., van der Welle, A., Miglavacca, G., Zani, A., L'Abbate, A., 2011. Trans-national infrastructure developments on the electricity and gas market. technical report.
URL <https://www.ecn.nl/publications/PdfFetch.aspx?nr=ECN-O--11-037>

-
- dos Santos, M. L., da Silva, E. L., Finardi, E. C., Gonçalves, R. E., 2009. Practical aspects in solving the medium-term operation planning problem of hydrothermal power systems by using the progressive hedging method. *International Journal of Electrical Power Energy Systems* 31 (9), 546 – 552, power Systems Computation Conference (PSCC) 2008.
URL <http://www.sciencedirect.com/science/article/pii/S0142061509000726>
- Dupačová, J., Consigli, G., Wallace, S. W., Dec 2000. Scenarios for multistage stochastic programs. *Annals of Operations Research* 100 (1), 25–53.
URL <https://doi.org/10.1023/A:1019206915174>
- Dupačová, J., 1995. Multistage stochastic programs: The state-of-the-art and selected bibliography. *Kybernetika* 31 (2), 151–174.
URL <http://eudml.org/doc/27579>
- EC, 2011. A roadmap for moving to a competitive low carbon economy in 2050.
URL <http://eur-lex.europa.eu/LexUriServ/LexUriServ.do?uri=COM:2011:0112:FIN:en:PDF>
- EU Reference Scenario, 2016. Eu reference scenario 2016.
URL https://ec.europa.eu/energy/sites/ener/files/documents/20160713%20draft_publication_REF2016_v13.pdf
- Fortes, P., Simões, S., Cleto, J., Seixas, J., 28-30 May 2008. Long-term energy scenarios under uncertainty. In: 5th International Conference on the European Electricity Market. Lisbon, Portugal.
URL <https://ieeexplore.ieee.org/stamp/stamp.jsp?tp=&arnumber=4579093>
- Fürsch, M., Nagl, S., Lindenberg, D., Mar 2014. Optimization of power plant investments under uncertain renewable energy deployment paths: a multistage stochastic programming approach. *Energy Systems* 5 (1), 85–121.
URL <https://doi.org/10.1007/s12667-013-0094-0>
- Fürsch, M., Hagspiel, S., Jagemann, C., Nagl, S., Lindenberg, D., Tröster, E., 2013. The role of grid extensions in a cost-efficient transformation of the european electricity system until 2050. *Applied Energy* 104, 642 – 652.
URL <http://www.sciencedirect.com/science/article/pii/S0306261912008537>
- G., F. L., Harold, A., 1981. Markal, a linear-programming model for energy systems analysis: Technical description of the bnl version. *International Journal of Energy Research* 5 (4), 353–375.
URL <https://onlinelibrary.wiley.com/doi/abs/10.1002/er.4440050406>
- Gabriel, S. A., Conejo, A. J., Fuller, J. D., Hobbs, B. F., Ruiz, C., 2013. *Complementarity Modeling in Energy Markets*, 2013th Edition. Springer.

-
- URL <https://EconPapers.repec.org/RePEc:spr:isorms:978-1-4419-6123-5>
- Gade, D., Hackebeit, G., Ryan, S. M., Watson, J.-P., Wets, R. J.-B., Woodruff, D. L., May 2016. Obtaining lower bounds from the progressive hedging algorithm for stochastic mixed-integer programs. *Mathematical Programming* 157 (1), 47–67.
URL <https://doi.org/10.1007/s10107-016-1000-z>
- Gardner, D. T., 1996. Flexibility in electric power planning: Coping with demand uncertainty. *Energy* 21 (12), 1207 – 1218.
URL <http://www.sciencedirect.com/science/article/pii/0360544296000618>
- Gassmann, H. I., Ziemba, W. T. (Eds.), 2013. *Stochastic Programming: Applications in Finance, Energy, Planning and Logistics*. World Scientific Publishing Co. Pte. Ltd.
URL <https://EconPapers.repec.org/RePEc:wsi:wsbook:8497>
- Gerbaulet, C., Lorenz, C., 2017. dynelmod: A dynamic investment and dispatch model for the future european electricity market. *Data Documentation, DIW 88*, Berlin.
URL <http://hdl.handle.net/10419/161634>
- Global Carbon Project, 2017. *Global carbon budget 2017*.
URL http://www.globalcarbonproject.org/carbonbudget/17/files/GCP_CarbonBudget_2017.pdf
- Gonçalves, R. E., Finardi, E. C., da Silva, E. L., 2012. Applying different decomposition schemes using the progressive hedging algorithm to the operation planning problem of a hydrothermal system. *Electric Power Systems Research* 83 (1), 19 – 27.
URL <http://www.sciencedirect.com/science/article/pii/S0378779611002227>
- Haller, M., Ludig, S., Bauer, N., 2012. Decarbonization scenarios for the eu and mena power system: Considering spatial distribution and short term dynamics of renewable generation.
URL https://ac.els-cdn.com/S0301421512003746/1-s2.0-S0301421512003746-main.pdf?_tid=a5031d8c-cddd-11e7-979a-00000aab0f01&acdnat=1511173930_cafa2f288c0a19c07a7dca2f21245cff
- Higle, J., Wallace, S., 7 2003. Sensitivity analysis and uncertainty in linear programming. *Interfaces* 33 (4), 53–60.
- Hobbs, B. F., 1995. Optimization methods for electric utility resource planning. *European Journal of Operational Research* 83 (1), 1 – 20.
URL <http://www.sciencedirect.com/science/article/pii/037722179400190N>
- Holz, F., von Hirschhausen, C., 2013. The infrastructure implications of the energy transformation in europe until 2050 — lessons from the emf28 modeling exercise.

Climate Change Economics 04 (supp01), 1340006.

URL <https://www.worldscientific.com/doi/abs/10.1142/S201000781340006X>

Hu, M.-C., Hobbs, B. F., 2010. Analysis of multi-pollutant policies for the u.s. power sector under technology and policy uncertainty using markal. Energy 35 (12), 5430 – 5442, the 3rd International Conference on Sustainable Energy and Environmental Protection, SEEP 2009.

URL <http://www.sciencedirect.com/science/article/pii/S0360544210003658>

Hübler, M., Löschel, A., 2013. The EU Decarbonisation Roadmap 2050—What way to walk? Energy Policy 55 (C), 190–207.

URL <https://ideas.repec.org/a/eee/enepol/v55y2013icp190-207.html>

Jaehnert, S., Wolfgang, O., Farahmand, H., Völler, S., Huertas-Hernando, D., 2013. Transmission expansion planning in northern europe in 2030—methodology and analyses. Energy Policy 61, 125 – 139.

URL <http://www.sciencedirect.com/science/article/pii/S0301421513005053>

Jägemann, C., Fürsch, M., Hagspiel, S., Nagl, S., 2013. Decarbonizing europe’s power sector by 2050 — analyzing the economic implications of alternative decarbonization pathways. Energy Economics 40 (Supplement C), 622 – 636.

URL <http://www.sciencedirect.com/science/article/pii/S0140988313001928>

Kann, A., Weyant, J. P., Jan 2000. Approaches for performing uncertainty analysis in large-scale energy/economic policy models. Environmental Modeling & Assessment 5 (1), 29–46.

URL <https://doi.org/10.1023/A:1019041023520>

Kanudia, A., Loulou, R., 1998. Robust responses to climate change via stochastic markal: The case of québec. European Journal of Operational Research 106 (1), 15 – 30.

URL <http://www.sciencedirect.com/science/article/pii/S0377221798003567>

Kaut, M., Midthun, K. T., Werner, A. S., Tomasgard, A., Hellemo, L., Fodstad, M., 2014. Multi-horizon stochastic programming. Computational Management Science Online first.

Kaut, M., Wallace, S. W., 2003. Evaluation of scenario-generation methods for stochastic programming. Humboldt-Universität zu Berlin, Mathematisch-Naturwissenschaftliche Fakultät II, Institut für Mathematik.

King, A., Wallace, S., 2012. Modeling with Stochastic Programming. Springer Series in Operations Research and Financial Engineering. Springer New York.

URL <https://books.google.no/books?id=L7eItgAACAAJ>

-
- Kiula, O., Rutherford, T. F., 2014. Economic modeling approaches: optimization versus equilibrium. Tech. rep.
- Krishnan, V., Ho, J., F. Hobbs, B., Liu, A., Mccalley, J., Shahidehpour, M., Zheng, Q., 08 2015. Co-optimization of electricity transmission and generation resources for planning and policy analysis: review of concepts and modeling approaches.
- Laia, R., Pousinho, H., Melício, R., Mendes, V., 2014. Stochastic emission constraints on unit commitment. *Procedia Technology* 17, 437 – 444, conference on Electronics, Telecommunications and Computers – CETC 2013.
URL <http://www.sciencedirect.com/science/article/pii/S2212017314004885>
- Listes, O., Dekker, R., May 2002. A scenario aggregation based approach for determining a robust airline fleet composition. *Econometric Institute Research Papers EI 2002-17*, Erasmus University Rotterdam, Erasmus School of Economics (ESE), Econometric Institute.
URL <https://ideas.repec.org/p/ems/eureir/570.html>
- London Economics, 2013. The value of lost load (voll) for electricity in great britain.
URL https://www.gov.uk/government/uploads/system/uploads/attachment_data/file/224028/value_lost_load_electricity_gb.pdf
- Loulou, R., Feb 2008. Etsap-tiam: the times integrated assessment model. part ii: mathematical formulation. *Computational Management Science* 5 (1), 41–66.
URL <https://doi.org/10.1007/s10287-007-0045-0>
- Loulou, R., Labriet, M., Feb 2008. Etsap-tiam: the times integrated assessment model part i: Model structure. *Computational Management Science* 5 (1), 7–40.
URL <https://doi.org/10.1007/s10287-007-0046-z>
- Maggioni, F., Allevi, E., Bertocchi, M., 01 2012. The value of information in multistage linear stochastic programming.
- Messner, S., Golodnikov, A., Gritsevskii, A., 1996. A stochastic version of the dynamic linear programming model message iii. *Energy* 21 (9), 775 – 784.
URL <http://www.sciencedirect.com/science/article/pii/0360544296000254>
- Messner, S., Strubegger, M., July 1995. User's guide for message iii. Iiasa working paper, IIASA, Laxenburg, Austria.
URL <http://pure.iiasa.ac.at/id/eprint/4527/>
- Mikkelsen, M. E., Reiten, A., 2017. A stochastic programming model for the european power system with short- and long term uncertainty, project report.
- Mirkhani, S., Saboohi, Y., 2012. Stochastic modeling of the energy supply system with uncertain fuel price – a case of emerging technologies for distributed power generation.

-
- Applied Energy 93 (Supplement C), 668 – 674, (1) Green Energy; (2) Special Section from papers presented at the 2nd International Energy 2030 Conf.
URL <http://www.sciencedirect.com/science/article/pii/S0306261912000049>
- Morgan, M. G., Henrion, M., 1990. *Uncertainty: A Guide to Dealing with Uncertainty in Quantitative Risk and Policy Analysis*. Cambridge University Press.
- Mulvey, J. M., Vladimirou, H., Dec 1991. Applying the progressive hedging algorithm to stochastic generalized networks. *Annals of Operations Research* 31 (1), 399–424.
URL <https://doi.org/10.1007/BF02204860>
- Murphy, J., Dec. 2013. *Benders, Nested Benders and Stochastic Programming: An Intuitive Introduction*. ArXiv e-prints.
- Nagl, S., Fursch, M., Lindenberg, D., 2013. The Costs of Electricity Systems with a High Share of Fluctuating Renewables: A Stochastic Investment and Dispatch Optimization Model for Europe. *The Energy Journal* 0 (Number 4).
URL <https://ideas.repec.org/a/aen/journal/ej34-4-08.html>
- Nahmmacher, P., Schmid, E., Knopf, B., 2014. *Documentation of limes-eu - a long-term electricity system model for europe*.
URL <https://pdfs.semanticscholar.org/477c/2ae7999e41d2bfedb61cd0a0cf1d95a09c52.pdf>
- Pacheco, P., 2011. *An Introduction to Parallel Programming*, 1st Edition. Morgan Kaufmann Publishers Inc., San Francisco, CA, USA.
- Pina, A., Silva, C., Ferrão, P., September 2011. Modeling hourly electricity dynamics for policy making in long-term scenarios. *Energy Policy* 39 (9), 4692–4702.
URL <https://ideas.repec.org/a/eee/enepol/v39y2011i9p4692-4702.html>
- Pindyck, R., Rubinfeld, D., 2013. *Microeconomics*, Global Edition. 8th ed. Essex: Pearson Education Ltd.
- Powell, W. B., George, A., Simão, H., Scott, W., Lamont, A., Stewart, J., 2012. Smart: A stochastic multiscale model for the analysis of energy resources, technology, and policy. *INFORMS Journal on Computing* 24 (4), 665–682.
URL <https://EconPapers.repec.org/RePEc:inm:orijoc:v:24:y:2012:i:4:p:665-682>
- Prékopa, A., 2003. Probabilistic programming. In: *Stochastic Programming*. Vol. 10 of *Handbooks in Operations Research and Management Science*. Elsevier, pp. 267 – 351.
URL <http://www.sciencedirect.com/science/article/pii/S0927050703100059>
- Reinelt, P. S., Keith, D. W., 2007. Carbon capture retrofits and the cost of regulatory uncertainty. *The Energy Journal* 28 (4), 101–127.
URL <http://www.jstor.org/stable/41323123>
-

-
- Richter, J., 2011. Dimension – a dispatch and investment model for european electricity markets.
URL http://www.ewi.uni-koeln.de/fileadmin/user_upload/Publikationen/Working_Paper/EWI_WP_11-03_DIMENSION.pdf
- Rockafellar, R. T., Wets, R. J.-B., Feb. 1991. Scenarios and policy aggregation in optimization under uncertainty. *Math. Oper. Res.* 16 (1), 119–147.
URL <http://dx.doi.org/10.1287/moor.16.1.119>
- Ryan, S. M., McCalley, J. D., Woodruff, D. L., 2011. Long term resource planning for electric power systems under uncertainty.
- Sadeghian, H., Ardehali, M., 2016. A novel approach for optimal economic dispatch scheduling of integrated combined heat and power systems for maximum economic profit and minimum environmental emissions based on benders decomposition. *Energy* 102, 10 – 23.
URL <http://www.sciencedirect.com/science/article/pii/S0360544216300871>
- Sagastizábal, C., Aug 2012. Divide to conquer: decomposition methods for energy optimization. *Mathematical Programming* 134 (1), 187–222.
URL <https://doi.org/10.1007/s10107-012-0570-7>
- Sanstad, A. H., Howarth, R. B., 1994. ‘normal’ markets, market imperfections and energy efficiency. *Energy Policy* 22 (10), 811 – 818, markets for energy efficiency.
URL <http://www.sciencedirect.com/science/article/pii/S0301421594901392>
- Schmid, E., Knopf, B., 2014. Quantifying the long-term economic benefits of european electricity system integration. FEEM Working Paper.
URL <http://dx.doi.org/10.2139/ssrn.2384544>
- Schwenen, S., 2014. Market design and supply security in imperfect power markets. *Energy Economics* 43 (Supplement C), 256 – 263.
URL <http://www.sciencedirect.com/science/article/pii/S0140988314000395>
- Seljom, P., Tomasgard, A., 2015. Short-term uncertainty in long-term energy system models — a case study of wind power in denmark. *Energy Economics* 49 (Supplement C), 157 – 167.
URL <http://www.sciencedirect.com/science/article/pii/S0140988315000419>
- Siddiqi, S. N., Baughman, M. L., Nov 1995. Value-based transmission planning and the effects of network models. *IEEE Transactions on Power Systems* 10 (4), 1835–1842.
- Sioshansi, R., Short, W., May 2009. Evaluating the impacts of real-time pricing on the usage of wind generation. *IEEE Transactions on Power Systems* 24 (2), 516–524.

-
- Skar, C., Doorman, G., Tomasgard, A., Aug 2014. Large-scale power system planning using enhanced benders decomposition. In: 2014 Power Systems Computation Conference. pp. 1–7.
- Skar, C., Doorman, G. L., Pérez-Valdés, G. A., Tomasgard, A., 2016. A multi-horizon stochastic programming model for the european power system. CenSES Working paper 2016 (2).
- Spiecker, S., Weber, C., 2014. The future of the european electricity system and the impact of fluctuating renewable energy – a scenario analysis. *Energy Policy* 65, 185 – 197.
URL <http://www.sciencedirect.com/science/article/pii/S0301421513010549>
- Sun, N., Ellersdorfer, I., Swider, D. J., April 2008. Model-based long-term electricity generation system planning under uncertainty, 1298–1304.
- Swider, D., Weber, C., 2007. The costs of wind’s intermittency in germany: application of a stochastic electricity market model.
URL <http://onlinelibrary.wiley.com/doi/10.1002/etep.125/epdf>
- Trutnevyte, E., 2013. Expanse methodology for evaluating the economic potential of renewable energy from an energy mix perspective. *Applied Energy* 111, 593 – 601.
URL <http://www.sciencedirect.com/science/article/pii/S0306261913003875>
- UNFCCC, 2015. The paris agreement on climate change.
URL <http://unfccc.int/resource/docs/2015/cop21/eng/l09r01.pdf>
- Usher, W., Strachan, N., 2012. Critical mid-term uncertainties in long-term decarbonisation pathways. *Energy Policy* 41 (Supplement C), 433 – 444, modeling Transport (Energy) Demand and Policies.
URL <http://www.sciencedirect.com/science/article/pii/S0301421511008810>
- Wallace, S. W., Fleten, S.-E., 2003. Stochastic programming models in energy. In: *Stochastic Programming. Vol. 10 of Handbooks in Operations Research and Management Science*. Elsevier, pp. 637 – 677.
URL <http://www.sciencedirect.com/science/article/pii/S0927050703100102>
- Watson, J.-P., Woodruff, D., R Strip, D., 01 2007. Progressive hedging innovations for a stochastic spare parts support enterprise problem.
- Watson, J.-P., Woodruff, D. L., Nov 2011. Progressive hedging innovations for a class of stochastic mixed-integer resource allocation problems. *Computational Management Science* 8 (4), 355–370.
URL <https://doi.org/10.1007/s10287-010-0125-4>
-

-
- Weitzman, M. L., 2009. On modeling and interpreting the economics of catastrophic climate change. *The Review of Economics and Statistics* 91 (1), 1–19.
URL <https://doi.org/10.1162/rest.91.1.1>
- Whittingham, M., 05 2012. History, evolution, and future status of energy storage 100, 1518–1534.
- Wolfgang, O., Haugstad, A., Mo, B., Gjelsvik, A., Wangensteen, I., Doorman, G., 2009. Hydro reservoir handling in norway before and after deregulation. *Energy* 34 (10), 1642 – 1651, 11th Conference on Process Integration, Modelling and Optimisation for Energy Saving and Pollution Reduction.
URL <http://www.sciencedirect.com/science/article/pii/S0360544209003119>
- World Nuclear Association, 2017. Nuclear power in germany.
URL <http://www.world-nuclear.org/information-library/country-profiles/countries-g-n/germany.aspx>
- Zehtabian, S., Bastin, F., 2016. Penalty parameter update strategies in progressive hedging algorithm. Tech. Rep. CIRRELT-2016-12, CIRRELT, Montreal, QC, Canada.
- ZEP, 2013. Co2 capture and storage: Recommendations for transitional measures to drive deployment in europe.
URL <http://www.zeroemissionsplatform.eu/library/publication/240-me2.html>
- Zhao, D., Chen, H., Li, X., Ma, X., 2018. Air pollution and its influential factors in china's hot spots. *Journal of Cleaner Production* 185, 619 – 627.
URL <http://www.sciencedirect.com/science/article/pii/S0959652618305006>

Appendix

Scenario trees

Table 10.1: Scenario tree with policy uncertainty for 4 long-term scenarios, restricting the total absolute amount of allowed CO₂-emissions across Europe per five-year time-stage. Units are given in MT CO₂/year.

Scenario	2010	2015	2020	2025	2030	2035	2040	2045	2050	Probability
1	1300	1138	975	975	975	975	975	975	975	0.090
2	1300	1138	975	975	975	813	650	488	325	0.210
3	1300	1138	975	813	650	650	650	650	650	0.210
4	1300	1138	975	813	650	488	325	163	0	0.490

Table 10.2: Scenario tree with policy uncertainty for 8 long-term scenarios, restricting the total absolute amount of allowed CO₂-emissions across Europe per five-year time-stage. Units are given in MT CO₂/year.

Scenario	2010	2015	2020	2025	2030	2035	2040	2045	2050	Probability
1	1300	1138	975	975	975	975	975	975	975	0.027
2	1300	1138	975	975	975	975	813	650	650	0.063
3	1300	1138	975	975	975	813	650	650	650	0.063
4	1300	1138	975	975	975	813	650	488	325	0.063
5	1300	1138	975	813	650	650	650	650	650	0.147
6	1300	1138	975	813	650	650	650	488	325	0.147
7	1300	1138	975	813	650	488	325	325	325	0.147
8	1300	1138	975	813	650	488	325	163	0	0.343

Table 10.3: Scenario tree with policy uncertainty for 81 long-term scenarios (part 1/2), restricting the total absolute amount of allowed CO₂-emissions across Europe per five-year time-stage. Units are given in MT CO₂/year.

Scenario	2010	2015	2020	2025	2030	2035	2040	2045	2050	Probability
1	1300	1138	975	1029	1083	1138	1192	1246	1300	0.0001
2	1300	1138	975	1029	1083	1138	1192	1246	1192	0.0002
3	1300	1138	975	1029	1083	1138	1192	1246	1083	0.0007
4	1300	1138	975	1029	1083	1138	1192	1138	1192	0.0002
5	1300	1138	975	1029	1083	1138	1192	1138	1083	0.0004
6	1300	1138	975	1029	1083	1138	1192	1138	975	0.0014
7	1300	1138	975	1029	1083	1138	1192	1029	1083	0.0007
8	1300	1138	975	1029	1083	1138	1192	1029	975	0.0014
9	1300	1138	975	1029	1083	1138	1192	1029	867	0.0049
10	1300	1138	975	1029	1083	1029	975	1029	1083	0.0002
11	1300	1138	975	1029	1083	1029	975	1029	975	0.0004
12	1300	1138	975	1029	1083	1029	975	1029	867	0.0014
13	1300	1138	975	1029	1083	1029	975	921	975	0.0004
14	1300	1138	975	1029	1083	1029	975	921	867	0.0008
15	1300	1138	975	1029	1083	1029	975	921	758	0.0028
16	1300	1138	975	1029	1083	1029	975	813	867	0.0014
17	1300	1138	975	1029	1083	1029	975	813	758	0.0028
18	1300	1138	975	1029	1083	1029	975	813	650	0.0098
19	1300	1138	975	1029	1083	921	758	813	867	0.0007
20	1300	1138	975	1029	1083	921	758	813	758	0.0014
21	1300	1138	975	1029	1083	921	758	813	650	0.0049
22	1300	1138	975	1029	1083	921	758	704	758	0.0014
23	1300	1138	975	1029	1083	921	758	704	650	0.0028
24	1300	1138	975	1029	1083	921	758	704	542	0.0098
25	1300	1138	975	1029	1083	921	758	596	650	0.0049
26	1300	1138	975	1029	1083	921	758	596	542	0.0098
27	1300	1138	975	1029	1083	921	758	596	433	0.0343
28	1300	1138	975	921	867	921	975	1029	1083	0.0002
29	1300	1138	975	921	867	921	975	1029	975	0.0004
30	1300	1138	975	921	867	921	975	1029	867	0.0014
31	1300	1138	975	921	867	921	975	921	975	0.0004
32	1300	1138	975	921	867	921	975	921	867	0.0008
33	1300	1138	975	921	867	921	975	921	758	0.0028
34	1300	1138	975	921	867	921	975	813	867	0.0014
35	1300	1138	975	921	867	921	975	813	758	0.0028
36	1300	1138	975	921	867	921	975	813	650	0.0098
37	1300	1138	975	921	867	813	758	813	867	0.0004
38	1300	1138	975	921	867	813	758	813	758	0.0008
39	1300	1138	975	921	867	813	758	813	650	0.0028
40	1300	1138	975	921	867	813	758	704	758	0.0008

Table 10.4: Scenario tree with policy uncertainty for 81 long-term scenarios (part 2/2), restricting the total absolute amount of allowed CO₂-emissions across Europe per five-year time-stage. Units are given in MT CO₂/year.

Scenario	2010	2015	2020	2025	2030	2035	2040	2045	2050	Probability
41	1300	1138	975	921	867	813	758	704	650	0.0016
42	1300	1138	975	921	867	813	758	704	542	0.0056
43	1300	1138	975	921	867	813	758	596	650	0.0028
44	1300	1138	975	921	867	813	758	596	542	0.0056
45	1300	1138	975	921	867	813	758	596	433	0.0196
46	1300	1138	975	921	867	704	542	596	650	0.0014
47	1300	1138	975	921	867	704	542	596	542	0.0028
48	1300	1138	975	921	867	704	542	596	433	0.0098
49	1300	1138	975	921	867	704	542	488	542	0.0028
50	1300	1138	975	921	867	704	542	488	433	0.0056
51	1300	1138	975	921	867	704	542	488	325	0.0196
52	1300	1138	975	921	867	704	542	379	433	0.0098
53	1300	1138	975	921	867	704	542	379	325	0.0196
54	1300	1138	975	921	867	704	542	379	217	0.0686
55	1300	1138	975	813	650	704	758	813	867	0.0007
56	1300	1138	975	813	650	704	758	813	758	0.0014
57	1300	1138	975	813	650	704	758	813	650	0.0049
58	1300	1138	975	813	650	704	758	704	758	0.0014
59	1300	1138	975	813	650	704	758	704	650	0.0028
60	1300	1138	975	813	650	704	758	704	542	0.0098
61	1300	1138	975	813	650	704	758	596	650	0.0049
62	1300	1138	975	813	650	704	758	596	542	0.0098
63	1300	1138	975	813	650	704	758	596	433	0.0343
64	1300	1138	975	813	650	596	542	596	650	0.0014
65	1300	1138	975	813	650	596	542	596	542	0.0028
66	1300	1138	975	813	650	596	542	596	433	0.0098
67	1300	1138	975	813	650	596	542	488	542	0.0028
68	1300	1138	975	813	650	596	542	488	433	0.0056
69	1300	1138	975	813	650	596	542	488	325	0.0196
70	1300	1138	975	813	650	596	542	379	433	0.0098
71	1300	1138	975	813	650	596	542	379	325	0.0196
72	1300	1138	975	813	650	596	542	379	217	0.0686
73	1300	1138	975	813	650	488	325	379	433	0.0049
74	1300	1138	975	813	650	488	325	379	325	0.0098
75	1300	1138	975	813	650	488	325	379	217	0.0343
76	1300	1138	975	813	650	488	325	271	325	0.0098
77	1300	1138	975	813	650	488	325	271	217	0.0196
78	1300	1138	975	813	650	488	325	271	108	0.0686
79	1300	1138	975	813	650	488	325	163	217	0.0343
80	1300	1138	975	813	650	488	325	163	108	0.0686
81	1300	1138	975	813	650	488	325	163	0	0.2401

Model input data

Table 10.5: Investment cost for generation technologies in €₂₀₁₀/kW (ZEP, 2013)

	2010	2015	2020	2025	2030	2035	2040	2045	2050
Lignite	1600	1600	1600	1600	1600	1600	1600	1600	1600
Lignite CCS	2600	2600	2600	2600	2600	2600	2600	2600	2600
Coal	1500	1500	1500	1500	1500	1500	1500	1500	1500
Coal CCS	2500	2500	2500	2500	2500	2500	2500	2500	2500
Gas CCS	1350	1350	1350	1350	1350	1350	1350	1350	1350
Gas OCGT	400	400	400	400	400	400	400	400	400
Gas CCGT	800	800	800	800	800	800	800	800	800
Gas CCS	1350	1350	1350	1350	1350	1350	1350	1350	1350
Bio 10 % cofiring	1600	1600	1600	1600	1600	1600	1600	1600	1600
Bio 10 % cofiring CCS	0	0	0	2600	2530	2470	2400	2330	2250
Nuclear	4500	4500	4500	4500	4500	4500	4500	4500	4500
Wave	6050	5669	5288	4906	4525	4144	3763	3381	3000
Geo	5500	5500	5500	5500	5500	5500	5500	5500	5500
Hydro regulated	3000	3000	3000	3000	3000	3000	3000	3000	3000
Hydro run-of-the-river	4000	4000	4000	4000	4000	4000	4000	4000	4000
Wind onshore	1200	1063	1033	1002	972	942	912	881	851
Wind offshore	4080	4080	3205	2770	2510	2375	2290	2222	2172
PV Solar	1900	998	760	540	325	295	285	260	232

Table 10.6: Investment cost for transmission infrastructure in €₂₀₁₀/MW/km (de Joode et al., 2011)

	2010	2015	2020	2025	2030	2035	2040	2045	2050
HVAC	719	719	662	662	604	604	604	604	604
HVDC	2769	2769	2769	2769	2160	2160	1551	1551	1551

Table 10.7: Investment costs for storage technologies in €₂₀₁₀/kW or €₂₀₁₀/kWh

	2010	2015	2020	2025	2030	2035	2040	2045	2050
Pumped hydro power (€ ₂₀₁₀ /kW)	1000	1000	1000	1000	1000	1000	1000	1000	1000
Pumped hydro energy (€ ₂₀₁₀ /kWh)	100	100	100	100	100	100	100	100	100
Battery energy (€ ₂₀₁₀ /kWh)	733	349	246	198	198	198	198	198	198
Battery power (€ ₂₀₁₀ /kW)	0	0	0	0	0	0	0	0	0

Table 10.8: Fixed operation and maintenance costs in €₂₀₁₀/kW/an (ZEP, 2013)

	2010	2015	2020	2025	2030	2035	2040	2045	2050
Lignite existing	32	32	32	32	32	32	32	32	32
Lignite	32	32	32	32	32	32	32	32	32
Lignite CCS	80	80	80	80	80	80	80	80	80
Coal existing	31	31	31	31	31	31	31	31	31
Coal	31	31	31	31	31	31	31	31	31
Coal CCS	78	78	78	78	78	78	78	78	78
Gas existing	20	20	20	20	20	20	20	20	20
Gas OCGT	20	20	20	20	20	20	20	20	20
Gas CCGT	30	30	30	30	30	30	30	30	30
Gas CCS	78	78	78	78	78	78	78	78	78
Oil existing	20	20	20	20	20	20	20	20	20
Bio existing	48	47	46	45	44	43	42	41	40
Bio 10 % cofiring	32	32	32	32	32	32	32	32	32
Bio 10 % cofiring CCS	0	0	0	51	50	49	47	46	45
Nuclear	134	131	127	123	120	116	112	108	105
Wave	154	154	154	154	154	154	154	154	154
Geo	92	92	92	92	92	92	92	92	92
Hydro regulated	125	125	125	125	125	125	125	125	125
Hydro run-of-the-river	125	125	125	125	125	125	125	125	125
Wind onshore	54	54	53	52	51	50	49	48	47
Wind offshore	138	133	128	122	117	112	107	102	96
PV Solar	20	20	19	17	16	14	13	11	10

Table 10.9: Generator efficiency for thermal technologies in percent (ZEP, 2013)

	2010	2015	2020	2025	2030	2035	2040	2045	2050
Lignite existing	35	35	36	36	36	36	36	37	37
Lignite	43	44	45	45	46	47	48	48	49
Lignite CCS	31	31	31	31	31	31	31	31	31
Coal existing	37	38	38	38	38	38	39	39	39
Coal	45	46	46	47	47	48	48	49	49
Coal CCS	33	33	33	33	33	33	33	33	33
Gas existing	48	49	50	51	52	52	53	54	55
Gas OCGT	40	40	41	41	41	41	42	42	42
Gas CCGT	60	60	60	60	61	63	64	65	66
Gas CCS	48	48	48	48	48	48	48	48	48
Oil existing	38	38	38	38	38	38	38	38	38
Bio existing	35	35	35	35	35	35	35	35	35
Bio 10 % cofiring	45	46	46	47	47	48	48	49	49
Bio 10 % cofiring CCS adv	0	0	0	39	40	41	41	42	43
Nuclear	36	36	36	36	37	37	37	37	37

Table 10.10: Variable operation and maintenance (O&M) costs in $\text{€}_{2010}/MWh$. The variable for oil, bio, hydro, wind and solar are added to the fixed O&M costs and reported in Table 10.8 (ZEP, 2013)

	2010	2015	2020	2025	2030	2035	2040	2045	2050
Lignite existing	0.48	0.48	0.48	0.48	0.48	0.48	0.48	0.48	0.48
Lignite	0.48	0.48	0.48	0.48	0.48	0.48	0.48	0.48	0.48
Lignite CCS	1.18	1.18	1.18	1.18	1.18	1.18	1.18	1.18	1.18
Coal existing	0.46	0.46	0.46	0.46	0.46	0.46	0.46	0.46	0.46
Coal	0.46	0.46	0.46	0.46	0.46	0.46	0.46	0.46	0.46
Coal CCS	1.16	1.16	1.16	1.16	1.16	1.16	1.16	1.16	1.16
Gas existing	0.45	0.45	0.45	0.45	0.45	0.45	0.45	0.45	0.45
Gas OCGT	0.45	0.45	0.45	0.45	0.45	0.45	0.45	0.45	0.45
Gas CCGT	0.45	0.45	0.45	0.45	0.45	0.45	0.45	0.45	0.45
Gas CCS	1.16	1.16	1.16	1.16	1.16	1.16	1.16	1.16	1.16
Bio 10 % cofiring	0.48	0.48	0.48	0.48	0.48	0.48	0.48	0.48	0.48
Bio 10 % cofiring CCS adv	0	0	0	3.28	3.28	3.28	3.28	3.28	3.28
Nuclear	1.8	1.75	1.7	1.65	1.6	1.55	1.5	1.45	1.4

Table 10.11: Transport and storage costs assumed for carbon capture and storage technologies, given in e_{2010}/tCO_2 .

	2025	2030	2035	2040	2045	2050
CCS T&S cost	20	20	20	20	20	20

Table 10.12: Derived short-run marginal costs for the various technologies in $\text{€}_{2010}/MWh$. Omitted technologies have SRCM less than 1 e/MWh . Based on procedure described in Skar et al. (2016).

	2010	2015	2020	2025	2030	2035	2040	2045	2050
Lignite existing	15	15	15	15	15	15	15	15	15
Lignite	12	12	12	12	12	12	12	12	12
Lignite CCS	0	0	0	35	34	33	32	32	31
Coal existing	27	19	23	27	33	34	36	37	37
Coal	23	16	19	23	27	28	29	29	30
Coal CCS	0	0	0	46	50	50	51	51	51
Gas existing	50	48	59	62	67	70	71	71	71
Gas OCGT	60	58	72	77	84	89	91	92	93
Gas CCGT	40	39	49	53	56	59	60	60	60
Gas CCS	0	0	0	69	72	74	74	74	73
Oil existing	100	77	120	136	150	156	165	169	173
Bio existing	70	77	85	93	102	113	124	136	150
Bio 10 % cofiring	26	20	24	27	32	33	35	36	38
Nuclear	12	12	12	12	12	12	13	13	13

Table 10.13: Initial capacities for the ten countries with the highest installed capacity in 2010, as assumed in the EMPIRE model. The other countries are aggregated. Numbers are given in GW. Data based on Skar et al. (2016)

	Bio/Oil	Coal	Coal CCS	Natural gas	Natural gas CCS	Hydro/Geo/Ocean	Nuclear	Solar	Wind
Other	13	46	0	48	0	47	23	13	23
Germany	11	46	0	29	0	4	11	40	45
France	10	3	0	11	0	21	63	7	10
Italy	4	9	0	55	0	15	0	19	9
Great Brit.	2	18	0	29	0	2	9	9	14
Spain	4	10	0	33	0	16	8	5	23
Sweden	6	0	0	1	0	16	10	0	6
Poland	1	26	0	1	0	1	0	0	5
Norway	0	0	0	2	0	30	0	0	1
Netherlands	0	6	0	20	0	0	0	1	3
Romania	0	5	0	4	0	6	1	1	3
Total	52	169	0	232	0	159	125	95	142

Investments in 2040

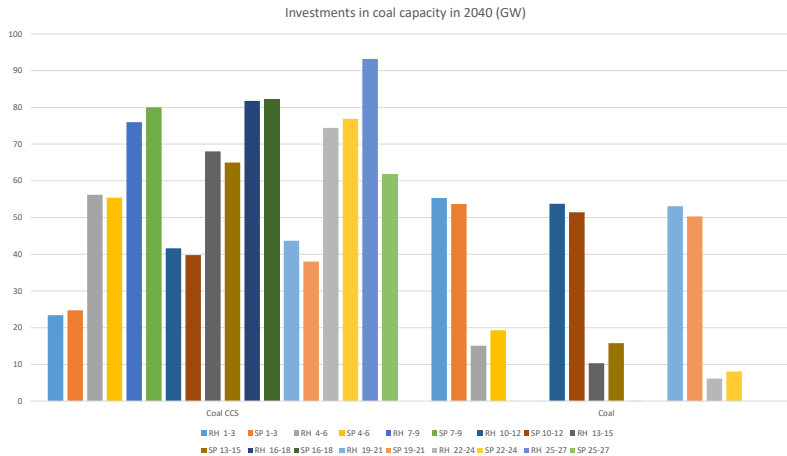


Figure 10.1: Investments in coal capacity in 2040 (GW) in the stochastic- and rolling horizon deterministic approach

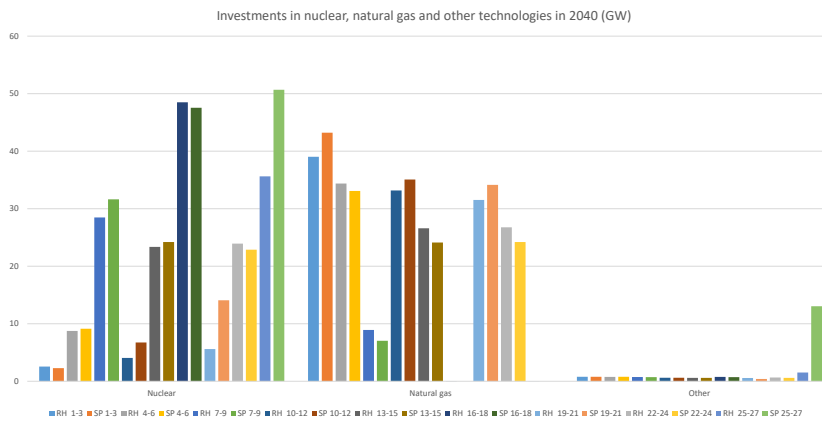


Figure 10.2: Nuclear, natural gas and other technology investments in 2040 in the stochastic- and rolling horizon deterministic approach

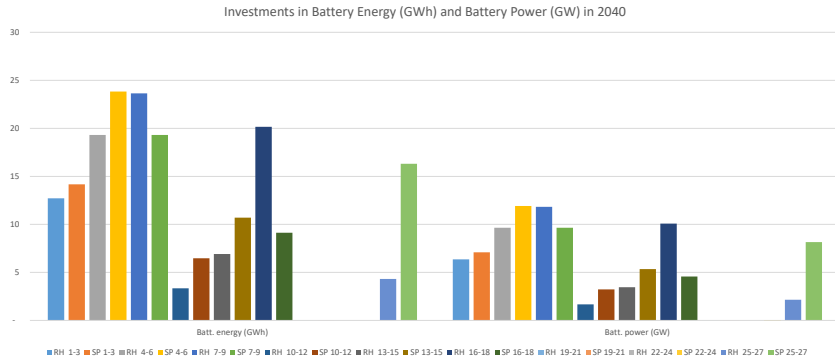


Figure 10.3: Investments in battery energy (GWh) and battery power (GW) in 2040 in the stochastic- and rolling horizon deterministic approach

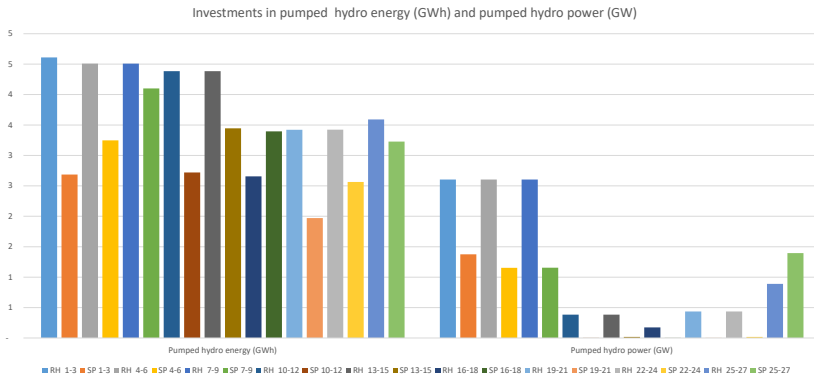


Figure 10.4: Investments in battery energy (GWh) and battery power (GW) in 2040 in the stochastic- and rolling horizon deterministic approach